The influence of hemispheric asymmetry and realistic basic states on tropical stationary waves in a shallow water model

Ian Kraucunas

A dissertation submitted in partial fulfillment
of the requirements for the degree of

Doctor of Philosophy

University of Washington

2005

Program Authorized to Offer Degree:
Department of Atmospheric Sciences

University of Washington
Graduate School

This is to certify that I have examined this copy of the doctoral dissertation by

Ian Kraucunas

and have found that it is complete and satisfactory in all respects,
and that any and all revisions required by the final
examining committee have been made.

Chair of Supervisory Committee:

Dennis L. Hartmann

Reading Committee:

Dennis L. Hartmann

John M. Wallace

David S. Battisti

Date: 9/13/2005

In presenting this dissertation in partial fulfillment of the requirements for the doctoral degree at the University of Washington, I agree that the Library shall make its copies freely available for inspection. I further agree that extensive copying of the dissertation is allowable only for scholarly purposes, consistent with "fair use" as prescribed in the U.S. Copyright Law. Requests for copying or reproduction of this dissertation may be referred to Proquest Information and Learning, 300 North Zeeb Road, Ann Arbor, MI 48106-1346, to whom the author has granted "the right to reproduce and sell (a) copies of the manuscript in microform and/or (b) printed copies of the manuscript made from microform."

Signature 

Date 9/14/05

University of Washington

Abstract

The influence of hemispheric asymmetry and realistic basic states on tropical stationary waves in a shallow water model

Ian Kraucunas

Chair of the Supervisory Committee:
Professor Dennis L. Hartmann
Department of Atmospheric Sciences

A shallow water model is used to study the stationary waves in the tropical upper troposphere. Realistic zonal-mean winds are generated by imposing a zonally-symmetric topography distribution underneath a thin fluid layer and relaxing the fluid towards its global-mean depth. Basic states with zero mean meridional flow are also constructed by balancing the height field with the equilibrium zonal-mean zonal winds. Both hemispherically-symmetric (equinoctial) and hemispherically-asymmetric (solstitial) basic states are considered. Stationary waves are generated by adding a mass source-sink distribution along or near the equator.

Westerly zonal-mean flow in the subtropics amplifies the stationary wave response to tropical eddy forcing and shifts the eddy height and vorticity maxima to the east, bringing the simulated eddies into better agreement with the observed seasonally-varying eddy circulations in the tropical upper troposphere. Moving the wave forcing off the equator amplifies the response in the forced hemisphere, but the response in the opposite hemisphere decreases only slightly because the eddy divergent winds act over a wide latitudinal range. The zonal-mean circulation in the solstitial basic state enhances

the eddy response in the winter hemisphere and limits the response in the summer hemisphere. Hemispheric asymmetry in either the eddy forcing or the basic state also leads to cross-equatorial eddy momentum fluxes. Linear experiments exhibit stronger subtropical anomalies, weaker variations along the equator, and less hemispheric symmetry than nonlinear integrations.

When the eddy forcing is located in the summer hemisphere of the solstitial basic state, the mean meridional winds enhance the propagation of wave activity across the equator, leading to stronger cross-equatorial eddy momentum fluxes and an eddy response with similar amplitudes in both hemispheres. Hence, the anti-correlation between the mean meridional flow and eddy momentum fluxes over the equator and the striking hemispheric symmetry of the tropical stationary waves over the course of the seasonal cycle can both be attributed to the tendency for the maximum eddy and zonal-mean diabatic forcing to occur in the same latitude band. The influence of the mean meridional flow on eddy momentum fluxes at low latitudes is also demonstrated in a simple linear barotropic model.

TABLE OF CONTENTS

LIST OF FIGURES

Figure Number Page

1. Introduction and background

The time-mean circulation of the tropical upper troposphere includes easterly zonal-mean zonal winds, a robust mean meridional circulation, and persistent zonal asymmetries, all of which vary substantially with the seasonal cycle. Observational studies indicate that the seasonally-varying quasi-stationary waves in the tropical upper troposphere are relatively symmetric about the equator, even when the zonally-averaged flow and eddy forcing are both centered in one hemisphere, and that the mean meridional winds and eddy momentum fluxes at low latitudes are strongly anti-correlated over the course of the seasonal cycle (Dima et al 2005). Another interesting feature of the stationary waves in the tropical band is that the largest eddy geopotential height and streamfunction anomalies tend to be located directly poleward of the strongest diabatic heating, rather than being displaced toward the west (see, e.g., Hendon 1986). The purpose of this dissertation is to explain these relationships using the simplest possible model capable of simultaneously simulating Earth-like basic state and the dominant wave motions in the tropical upper troposphere: the shallow water model.

The zonally-averaged circulation is usually described, and has been successfully modeled, as the nonlinear, inviscid, axisymmetric response to the latitudinal gradient in diabatic heating (e.g. Held and Hou 1980). The most widely cited models of tropical stationary waves, on the hand, are based on the linear, viscous, first-baroclinic-mode response to horizontal variations in eddy divergence or diabatic forcing (e.g. Gill 1980). Subsequent experiments with increasingly sophisticated models have demonstrated that the global three-dimensional stationary wave field can be reproduced reasonably well by specifying the zonal-mean flow and including the time-averaged, zonally-asymmetric forcing associated with tropical convection, midlatitude transient eddies, and topography (e.g. Wang and Ting 1999). However, a relative dearth of intermediate-complexity models and a tendency to focus on the midlatitude response to tropical forcing have led to

gaps in our understanding of the fundamental relationship between the zonally-averaged circulation, the horizontal distribution of diabatic forcing, and the quasi-stationary eddy circulations in the tropical band. The remainder of this chapter describes observational studies and previous modeling experiments that have examined the steady eddy circulations in the tropical upper troposphere.

The simplest system capable of resolving the important large-scale wave modes in the tropical upper troposphere are the shallow water equations, which are discussed in more detail below and in Chapter 2. Previous experiments with shallow water models have been hampered by the inability to simultaneously simulate Earth-like zonal-mean winds and tropical stationary waves without linearizing the problem or using unrealistically large fluid depths in the tropics, both of which limit the fidelity of the wave response. In Chapter 3, a novel technique is introduced for generating realistic zonally-symmetric basic states in the shallow water system without distorting tropical wave dynamics. This technique is used to generate a hemispherically-symmetric, or "equinoctial" basic state, and a hemispherically-asymmetric, or "solstitial" basic state. A balancing procedure is also used to generate "no Hadley" basic states with identical zonal-mean zonal winds but zero mean meridional flow.

The equilibrium response of the shallow water model to steady tropical eddy forcing is explored in Chapters 4-6. Chapter 4 describes the stationary wave response to forcing on or near the equator in a resting basic state, compares these results with the eddy structures obtained by previous authors, and evaluates how nonlinearity and hemispheric asymmetry affect the equilibrium solution. Chapter 5 evaluates the changes induced in the stationary wave response when the Earth-like basic states introduced in Chapter 3 are used in lieu of a resting basic state. Chapter 6 focuses on the zonally-averaged response of the shallow water model to tropical eddy forcing, including both the

eddy momentum fluxes associated with the tropical stationary wave circulations and the changes these fluxes induce in the zonal-mean climate, and also examines the relationship between the eddy momentum fluxes and the mean meridional flow using an analytic linear barotropic model.

The results of the experiments described in Chapters 4-6 indicate that westerly zonal-mean zonal flow in the subtropics is responsible for amplifying the steady eddy response to tropical wave forcing and shifting the centers of the eddy height and circulation anomalies in each hemisphere poleward and eastward, relative to their positions in simulations with a resting basic state. When either the eddy forcing or the basic state is hemispherically-asymmetric, the eddy response develops considerable hemispheric asymmetry, including cross-equatorial fluxes of eddy momentum, but the stationary wave response persists in both hemispheres because the eddy divergent winds force vorticity anomalies that extend over a broad latitudinal scale. On the other hand, when the eddy forcing and the zonal-mean divergence are both centered on the same side of the equator, on the other hand, the cross-equatorial mean meridional flow enhances the propagation of wave activity across the equator, resulting in strong cross-equatorial eddy momentum fluxes and a similar stationary wave response in both hemispheres.

The main conclusion that can be drawn from these experiments is that the pronounced hemispheric symmetry of the observed tropical stationary waves that prevails throughout the seasonal cycle and the anti-correlation between the mean meridional winds and eddy momentum fluxes at low latitudes may both be attributed to the tendency for the maximum eddy and zonal-mean diabatic forcing to be located in the same latitude band. The importance of westerly subtropical zonal-mean zonal winds and nonlinearity in shaping the low-latitude response to tropical eddy forcing is another major theme of this work. These conclusions are discussed in more detail in Chapter 7.

1.1 Tropical stationary waves

Dima et al (2005) and Dima (2005) have recently provided a comprehensive climatology of the seasonal cycle of the quasi-stationary waves in the tropical upper troposphere. Of particular interest for this study are the surprising amount of hemispheric symmetry in the eddy structures throughout the year and the anti-correlation between the mean meridional flow and the meridional fluxes of zonal angular momentum at low latitudes. Eddy momentum fluxes directed opposite the mean meridional flow near the equator have also been noted in an idealized general circulation model and its linear counterpart by Kraucunas (2001) and Kraucunas and Hartmann (2005), who demonstrated that the convergence of eddy momentum fluxes associated with tropical stationary waves will rapidly induce equatorial superrotation in an idealized general circulation model with a hemispherically-symmetric basic state, but not in a solstitial basic state that includes strong cross-equatorial mean meridional flow. Hence, the interaction between the mean meridional circulation and eddy momentum fluxes at low latitudes appears to represent an important, and heretofore largely unrecognized, aspect of the tropical upper-tropospheric circulation.

Watterson and Schneider (1987) have demonstrated that cross-equatorial mean meridional flow also enhances the propagation of wave activity across regions with easterly mean flow, where Rossby waves are normally evanescent. This effect could potentially promote hemispheric symmetry in the stationary wave response and cross-equatorial eddy momentum fluxes, although Watterson and Schneider did not focus on these attributes in their study. Kang and Held (1986) and Sardeshmukh and Hoskins (1988) showed that the advection of vorticity by the eddy divergent winds implied by tropical eddy divergence anomalies also tends to promote a strong stationary wave response on both sides of the equator, an effect that has been confirmed by subsequent authors in a variety of models (e.g. Jin and Hoskins 1995). More recently, Wang and

Ting (1999) and Ting et al (2001) have shown that the seasonal cycle in the amplitude of tropical stationary waves depends mostly on the seasonal variations in tropical heating, while the seasonal cycle in tropical stationary wave structure depends mostly on the seasonal variations in the basic state circulation, except during Northern summer.

Another notable aspect of the quasi-stationary eddy circulations in the tropical upper troposphere is the tendency for the eddy streamfunction and height anomalies in the subtropics and the eddy zonal winds along the equator to be roughly collocated in longitude with the maximum diabatic forcing (see, e.g., Murakami and Wang 1991). Hendon (1986) argues that nonlinearity, specifically the nonlinear forcing of rotational flow via vortex stretching, is responsible for the eastward displacement of the subtropical anticyclones, relative to their positions in linear models. Support for this hypothesis is also found in linear stationary wave models (Webster 1982; Ting and Sardeshmukh 1993), which tend to produce circulation anomalies centered to the west of the strongest tropical eddy forcing. The vorticity balance in the tropical upper troposphere (Sardeshmukh and Held 1984; Sardeshmukh and Hoskins 1985) also indicates that nonlinear advection is required to reproduce the observed stationary wave structure, which again suggests that the planetary-scale flow in the upper troposphere is inherently nonlinear (and inviscid).

Other authors offer alternative explanations for the longitudinal position of the subtropical anticyclones. Ting and Held (1990) found that nonlinearity acts to shift the centers of the subtropical anticyclones slightly to the east, regardless of the zonal-mean basic state of the model, but argued that tropical transient eddies (possibly extratropical transients reaching the tropics but most likely the temporal variations in tropical convection) are actually responsible for most of the eastward shift. Jin and Hoskins (1995) note that subtropical convergence anomalies induced by tropical forcing can also

modify the subtropical response to tropical forcing. Horizontal variations in the divergence field have also been noted in other studies (Webster 1982; Lau and Lim 1982; Rodwell and Hoskins 1996), but neither their origin nor their influence on the mean rotational response has been evaluated in detail.

The basic state flow is also undoubtedly important in determining the structure and amplitude of the stationary wave circulations induced by tropical eddy forcing. Jin and Hoskins (1995) noted that realistic zonal-mean zonal winds shift the anticyclones to the east, relative to their position in a resting basic state. An inspection of the horizontal circulation features in other experiments with idealized eddy forcing in realistic basic states (e.g. Kasahara and Silva Dias 1986) also reveals a tendency for the eddy forcing and substropical response to be collocated, particularly in models where nonlinearity is present or parameterized using GCM output. Wang and Ting (1999) and Ting et al (2001) used such a technique to show that the seasonal variations in the zonal-mean basic state are critical for resolving the structure of the observed stationary wave circulations. However, at this point it is unclear which factors are most important in centering the subtropical response at the same longitude as the tropical eddy forcing.

1.2 Stationary wave models

The non-divergent barotropic vorticity equation provides the simplest framework for studying the propagation of wave activity through the extratropical upper troposphere, and has been used extensively to isolate both the teleconnections associated with low-latitude forcing (e.g. Sardesmukh and Hoskins 1988) and the horizontal dispersion of midlatitude wavetrains (e.g. Watterson and Schneider 1987). Purely barotropic models are of little value in studying the tropical stationary wave response, however, because they do not resolve divergent circulations, such as the equatorial Kelvin wave. Barotropic

models also imply an infinite layer depth, which distorts the propagation of equatorial Rossby waves, as discussed in Chapter 2.

The simplest framework capable of resolving the important large-scale, low-frequency horizontal wave modes in the tropical atmosphere are the shallow water equations. Shallow water models, also called free surface or divergent barotropic models, can thus be used to isolate the dynamics of a particular baroclinic mode or isentropic layer, assuming that the effects of vertical motions can be neglected or parameterized. Stationary waves can be induced in the shallow water system by introducing horizontal variations in topography, a technique usually reserved for simulating the response to midlatitude topography, or by specifying a mass source-sink distribution, which induces a horizontal pattern of divergence and convergence anomalies in the same manner than horizontal variations in diabatic heating induce divergence and convergence anomalies in the real atmosphere. To achieve steady-state solutions, some form of damping is also required. The shallow water equations are discussed in more detail in Chapter 2.

Matsuno (1966) and Gill (1980) were the first to use the shallow water equations to study the response to steady eddy forcing near the equator. Both authors examined the linear response to idealized forcing on an equatorial beta-plane with a resting basic state and relatively strong frictional and thermal damping, and interpreted the resulting eddy circulation structures in terms of the horizontal propagation of forced tropical wave modes. Gill (1980) noted that vorticity generation in the mass source region is balanced by the meridional advection of planetary vorticity associated with the eddy meridional winds, so away from the equator the strongest height and vorticity anomalies in the equilibrium solution are centered to the west of the mass forcing. Both authors also noted that the eddy circulations induced by tropical eddy forcing are strongest near the equator

because the poleward increase of the Coriolis force tends to trap the dominant wave motions in the tropical band, namely the equatorial Rossby and Kelvin waves.

Spherical geometry (Gill 1982), nonlinearity (Van Tuyl 1984; Gill and Phlips 1986), and horizontally-uniform zonal winds (Lau and Lim 1982; Lim and Chang 1983; Phlips and Gill 1987) were subsequently found to induce small but interesting changes in the response to steady, idealized eddy forcing at low latitudes. Lau and Lim (1984) considered the combined effects of spherical geometry, nonlinearity, and realistic zonal-mean winds, and demonstrated that an extratropical wavetrain develops when the zonal-mean winds are westerly and the layer depth is sufficiently large. However, subsequent experiments with shallow water models have been restricted to studies of the response to midlatitude topographic forcing (e.g. Schneider and Watterson 1985; Brunet and Hayes 1996; Esler et al 2000) or the evolution of transient disturbances in the tropics (e.g. Webster and Chang 1988; Nieto Ferreira and Schubert 1999). One reason for this decline in the usage of shallow water models is undoubtedly the success of baroclinic and (nondivergent) barotropic models in reproducing the global stationary wave pattern, as discussed below. However, another major reason why shallow water models have not been used more extensively to study tropical stationary waves is because the three methods commonly used to impose realistic basic states in the shallow water system all have significant shortcomings. These techniques, and their shortcoming, are described in more detail in Chapter 2.

Beginning with Hoskins and Karoly (1981), the global stationary wave response to tropical and subtropical eddy forcing has been studied using linearized three-dimensional primitive equations models forced with persistent low-latitude heating anomalies. Webster (1982) used a two-level linear model to study the horizontal response to eddy forcing centered at a variety of latitudes. Nigam et al (1986, 1988) and Ting

(1994) expanded the technique to include the forcing associated with midlatitude topography and also the transient eddy fluxes and "stationary nonlinearity" derived from general circulation models (GCMs). Wang and Ting (1999) forced a linear baroclinic model with observationally-derived forcing. Held et al (2002) provide an extensive review of the evolution linear baroclinic stationary wave models, which are particularly useful for determining the relative influence of different types of stationary wave forcing, i.e. tropical heating, topography, and transient eddies, on the global stationary wave pattern. However, the absence of nonlinear terms in these models makes it difficult to determine the fidelity of the stationary wave response at low latitudes or to study wave-mean flow interactions.

An alternative approach, first introduced by Hoskins and Jin (1991), is to integrate a nonlinear primitive equations model forward from an initial, balanced basic state, terminating the integration before midlatitude baroclinic instabilities develop. Jin and Hoskins (1995) used this technique to study the steady, nonlinear response to an idealized tropical eddy heat source in both zonally-symmetric and zonally-asymmetric basic states. Rodwell and Hoskins (1995, 1996), performed similar experiments using both idealized diabatic forcing and realistic diabatic and orographic forcing to study the Asian summer monsoon and the influence of the monsoon on subtropical deserts. Hoskins et al (1999) also use a nonlinear, initial-value model to study the zonal-mean response to idealized tropical eddy forcing distributions. The advantage of the nonlinear, initial-value technique is that it does not require linearization to achieve a steady-state solution, and it also permits the evaluation of nonlinear terms by comparing the finite-amplitude response with the response to very small amplitude eddy forcing. However, some parameterization of surface exchange and radiative processes is still required, and

nonlinear vertical advection tends to make the analysis of the eddy response more difficult.

Ting and Yu (1998) and Ting et al (2001) compared linear steady-state baroclinic models with the nonlinear, initial-value technique. They concluded that the frictional drag in linear stationary wave models provides a crude but effective approximation of the influence of nonlinearity, which explains why linear baroclinic models are able to reproduce the observed global stationary wave pattern when forced with observationally- or GCM-derived eddy forcing. Ting and Held (1990) have also shown that frictional drag can roughly account for the damping effects of transient eddies. However, Nigam et al (1986) found that the strength of the tropical response in a linear stationary wave model is quite sensitive to the frictional damping strength. Kang and Held (1986), on the other hand, found that the stationary wave response in a barotropic model is relatively insensitive to the type of damping used. Hence, the relative importance of nonlinearity remains somewhat unclear, as does the fidelity of linear stationary wave models.

1.3 Chapter summary

- The observed stationary waves in the tropical upper troposphere tend to be collocated in longitude with the strongest eddy forcing and exhibit similar amplitudes in both hemispheres throughout the seasonal cycle; the eddy momentum fluxes associated with these waves tend to be directed opposite the prevailing mean meridional wind.
- A variety of models have been used to study the seasonally-varying steady eddy circulations in the upper troposphere, with varying success.
- The amplitude and horizontal structure of the stationary wave response have been shown to be sensitive to the location of the tropical eddy forcing, the zonal-mean zonal winds, the mean meridional circulation, and the inclusion of nonlinearity.

2. Model description

Shallow water models are often used to study the horizontal structure of an individual baroclinic mode or the dynamics of a particular isentropic layer in a continuously stratified atmosphere, as discussed in Chapter 1. The stationary wave response to horizontal variations in tropical convective heating can be modeled in the shallow water framework by introducing a fixed pattern of mass sources and sinks to generate eddy divergence and convergence anomalies, respectively, along with some form of damping to achieve a steady-state solution. The resulting circulation features bear a reasonable resemblance to the observed quasi-stationary waves at low latitudes because the shallow water system includes the terms necessary to resolve the dominant large-scale wave motions in the tropics, including the equatorial Kelvin and Rossby waves. Shallow water models are particularly well suited for studying the stationary waves in the tropical upper troposphere, where problems with improperly representing vertical heating functions, orography, and surface fluxes are less acute (e.g. Wu et al 2001).

This chapter describes the shallow water model used in subsequent chapters to generate zonally-symmetric basic states and study the response to tropical eddy forcing. The shallow water equations are introduced in section 2.1. The methods commonly used to force the shallow water system are examined in section 2.2, along with a discussion of the strengths and limitations of these techniques, including an explanation of why it has proven difficult to simultaneously simulate realistic zonal-mean flow and tropical stationary waves in the shallow water framework. Section 2.3 introduces the eddy vorticity balance and eddy zonal wind balance equations, which are used extensively to study the tropical stationary wave response in Chapters 4 and 5. A short chapter summary is provided in Section 2.5.

2.1 Shallow water equations

The following set of equations describes the evolution of an incompressible, homogeneous, hydrostatically balanced fluid on a spherical rotating planet with radius a, gravitational acceleration g, and planetary vorticity $f = 2\Omega \sin\theta$ (where Ω is the planetary rotation rate), under the influence of an arbitrary forcing F. The total height field H is the sum of the fluid depth h and surface topography h_s ($H = h + h_s$), and θ and λ denote latitude and longitude, respectively.

$$\frac{\partial u}{\partial t} = fv - \frac{u}{a\cos\theta}\frac{\partial u}{\partial \lambda} - \frac{v}{a}\frac{\partial u}{\partial \theta} + \frac{uv\tan\theta}{a} - \frac{g}{a\cos\theta}\frac{\partial H}{\partial \lambda} + F_u \tag{2.1}$$

$$\frac{\partial v}{\partial t} = -fu - \frac{u}{a\cos\theta}\frac{\partial v}{\partial \lambda} - \frac{v}{a}\frac{\partial v}{\partial \theta} - \frac{u^2\tan\theta}{a} - \frac{g}{a}\frac{\partial H}{\partial \theta} + F_v \tag{2.2}$$

$$\frac{\partial h}{\partial t} = -\frac{u}{a\cos\theta}\frac{\partial h}{\partial \lambda} - \frac{v}{a}\frac{\partial h}{\partial \theta} - \frac{h}{a\cos\theta}\frac{\partial u}{\partial \lambda} - \frac{h}{a}\frac{\partial v}{\partial \theta} + F_h \tag{2.3}$$

It is often convenient to express the shallow water equations in vorticity-divergence form, using the absolute vorticity $\zeta = f + \xi$ (where ξ is the relative vorticity) and kinetic energy per unit mass $K = (u^2 + v^2)/2$:

$$\frac{\partial \zeta}{\partial t} = \frac{\partial \xi}{\partial t} = -\zeta\delta - \frac{u}{a\cos\theta}\frac{\partial \xi}{\partial \lambda} - \frac{v}{a}\frac{\partial \zeta}{\partial \theta} + F_\zeta \tag{2.4}$$

$$\frac{\partial \delta}{\partial t} = -\frac{1}{a\cos\theta}\frac{\partial(\zeta v)}{\partial \lambda} - \frac{\partial(\zeta u)}{a\partial\theta} - \nabla^2(K + gH) + F_\delta \tag{2.5}$$

$$\frac{\partial h}{\partial t} = -h\delta - \frac{u}{a\cos\theta}\frac{\partial h}{\partial \lambda} - \frac{v}{a}\frac{\partial h}{\partial \theta} + F_h \tag{2.6}$$

In the absence of forcing, the shallow water equations conserve potential vorticity $(\eta = \zeta/h)$, potential enstrophy $(\eta^2/2)$, and total energy. Total energy conservation may be demonstrated by writing the potential energy and (mass-weighted) kinetic energy tendency equations in the following form:

$$\frac{\partial P}{\partial t} = \frac{\partial}{\partial t}\left\{ gh\left(h_s + \frac{1}{2}h \right) \right\} = -\nabla \cdot \left\{ \mathbf{v}gh\left(h_s + h \right) \right\} + gh\mathbf{v} \cdot \nabla \left\{ h\left(h_s + h \right) \right\} \tag{2.7}$$

$$\frac{\partial (hK)}{\partial t} = -\nabla \bullet \left(\mathbf{v}hK \right) - gh\mathbf{v} \bullet \nabla \left\{ h\left(h_s + h \right) \right\} \tag{2.8}$$

Here ∇ is the horizontal gradient operator and $\mathbf{v} = (u, v)$. The first terms on the RHS of (2.7)-(2.8) are equal to zero when integrated over the sphere, and the final terms represent the conversion between potential energy and kinetic energy. Note that the only place where topography enters (2.4)-(2.6) is through the Laplacian term in the divergence equation (or, in (2.1)-(2.3), through the horizontal derivatives of the total height field in the zonal and meridional momentum equations), and that total energy is conserved even when topography is present. These properties are crucial for the basic state generation method discussed in Chapter 3.

The numerical shallow water model used in the following chapters to generate realistic basic states and study the response to tropical eddy forcing is based on the Flexible Modeling System (FMS) shallow-water model developed at the Geophysical Fluid Dynamics Laboratory (GFDL, 2005). The model employs the vorticity-divergence form of the shallow water equations (2.4)-(2.6), with linear terms computed using a spectral transform method and nonlinear terms calculated on the corresponding Gaussian grid. Time differencing is treated semi-implicitly, with a Robert-Asselin time filter. All experiments are performed at T42 resolution with a timestep of 30 minutes and a weak ∇^8 hyper-diffusion that damps the smallest resolved features at a timescale of roughly 1 day, except for a limited number of experiments in Chapter 4 that are performed with stronger diffusion.

2.2 Forcing the shallow water system

In shallow water models, mass sources and sinks play a role analogous to diabatic forcing in a stratified atmosphere. For a layer intended to represent the tropical upper troposphere, mass sources correspond to diabatic heating because the divergence anomalies that they generate are analogous to the divergence anomalies associated with the outflow from tropical convection, while mass sinks correspond to areas dominated by radiative cooling. Mass forcing can be introduced by imposing a fixed source/sink Q, relaxing the fluid depth towards a reference height field h_{ref}, or both:

$$F_h = Q(\lambda,\theta) - k_h\left(h - h_{ref}(\lambda,\theta)\right) \tag{2.9}$$

k_h is usually referred to as the "thermal" damping strength because the height field in the shallow water system is analogous to the temperature or thickness fields in three-dimensional models.

Gent (1993) notes that when mass sources are present in the shallow water system, an additional term should be included in the momentum equations to represent the changes to momentum and kinetic energy associated with the added fluid. Unfortunately, it is impossible to simultaneously preserve momentum balance and energetic consistency. Gent recommends preserving energetic consistency by including the following forcing terms in the momentum equations:

$$\begin{aligned} F_u &= \ldots - uF_h / 2h \\ F_v &= \ldots - vF_h / 2h \end{aligned} \tag{2.10}$$

For a shallow water system intended to represent the upper troposphere, it is usually assumed that the mass source comes from a motionless lower layer, while the fluid removed by a mass sink deposits its energy and momentum in the lower layer, so these damping terms are usually only applied to regions where mass is being added to the

system (i.e. where $F_h > 0$). Using $-uF_h/h$ and $-vF_h/h$ instead of (2.10) preserves momentum balance instead of energetic consistency, and would also be an appropriate form if one were studying the horizontal circulation of the first baroclinic mode, which is assumed to have roughly equal and opposite circulations in the upper and lower levels. Analagous terms, with ξ and δ replacing u and v, would be used in (2.4)-(2.5). Gent (1993) also notes that harmonic diffusion is not negative definite in the shallow water system, although the higher-order diffusion is so weak in the present model that this deficiency is unlikely to cause any problems.

In addition to providing a convenient mechanism for forcing tropical stationary waves, mass forcing can be used to generate zonally-symmetric basic states in the shallow water system. To generate a general circulation resembling the zonally-averaged flow in the upper troposphere on Earth, mass can simply be added near the equator and removed in midlatitudes (e.g. Webster and Holton 1982; Chang and Webster 1990), or the fluid depth can be relaxed towards a zonally-invariant reference height distribution that is large near the equator and decreases towards the poles (e.g. Held and Phillips 1990, Shell and Held 2004). Both of these methods produce a mean meridional circulation analogous to the Hadley circulation, and the latitudinal gradient of the equilibrium height distribution gives rise to westerly midlatitude jet streams in the same manner that the equator-to-pole geopotential height distribution on Earth gives rise to the observed zonal-mean zonal winds.

Another method commonly used to impose realistic basic states in shallow water models is to specify the desired wind field and then use a balancing procedure to obtain the corresponding initial height distribution. Simple geostrophic balance can suffice under certain approximations, for instance the long-wave approximation (e.g. Lau and Lim 1983), but in general the nonlinear balance equation should be used:

$$g\nabla^2 h_{bal} = \frac{1}{a\cos\theta}\frac{\partial(\zeta v)}{\partial\lambda} - \frac{\partial(\zeta u\cos\theta)}{a\cos\theta\,\partial\theta} - \nabla^2 K \qquad (2.11)$$

Esler et al (2001) used (2.11) with v set to zero and the zonal winds (and vorticity) set equal to the zonal-mean flow from a previous experiment to generate balanced zonally-symmetric basic states. Note that this method will not produce a mean meridional circulation without additional zonal-mean forcing, and that perturbations induced by any applied eddy forcing must typically be damped towards the balanced basic state fields in order to produce steady solutions. A similar procedure will be used to produce basic states with zero mean meridional flow in Chapter 3. Equation (2.11) can also be used to create a zonally-varying initial state, which can then be allowed to evolve without gravitational instabilities developing (e.g. Neito Ferreira and Schubert 1999).

Basic states generated using either (2.9) or (2.11) suffer from a critical deficiency. In order to produce a basic state zonal wind distribution that resembles the observed flow in the upper troposphere, i.e. with weak easterly flow near the equator and westerly midlatitude jetstreams, the basic state height field must be quite large in the tropics, typically on the order of several kilometers. Unfortunately, a deep layer near the equator is inconsistent with the 15-250 m fluid depths implied by phase speed estimates for the first baroclinic mode in the tropical atmosphere ($c = \sqrt{gh_o} \approx 12-50\ m/s$; Wheeler et al 1999), or by the stability of an isentropic layer representing the outflow from the Hadley cell ($gh_o \sim 1000\ m^2 s^{-2}$; Held and Phillips 1990). Decreasing fluid depths away from the equator are also inconsistent with both the flat potential vorticity profile observed in the tropics and the increase in static stability with latitude. Hence, shallow water models with basic states constructed by using a mass source/sink distribution or a balancing procedure might be useful for studying the meridional propagation of extratropical waves, which are generally equivalent barotropic in structure, but will distort the response to zonally-asymmetric forcing in the tropics.

An alternative method that has been used to study the influence of different basic states on the response to tropical eddy forcing in the shallow water system is to linearize the equations of motion about zonally-symmetric (or zonally-asymmetric) height and wind fields (e.g. Zhang and Webster 1989). Although this technique is useful for gauging the qualitative sensitivity of the eddy response to different basic states and horizontal forcing patterns, the applicability of the results is questionable because both wave-wave and wave-mean flow interactions are precluded. It is also difficult to justify a linear approach in the tropics a priori because the eddy circulations at low latitudes are often comparable in intensity to the basic state flow. In addition, strong frictional drag is usually required to produce realistic-looking solutions in linear stationary wave models. Although Rayleigh friction has been shown to serve as a crude parameterization of the damping effects of nonlinear processes and transient eddies in multi-level models (see, e.g., Ting and Held 1990), vorticity budgets (e.g. Sardeshmukh and Held 1984) and axisymmetric models (e.g. Held and Hou 1980) suggest that the motions in the tropical upper troposphere are inherently inviscid and nonlinear, so ideally one would like to simulate both the basic state and stationary waves using a nonlinear system with relatively weak damping.

An additional concern arises if one wishes to simulate the global stationary wave pattern in the upper troposphere using a single-level model. As noted by Held and Phillips (1990), and also Shell and Held (2004), tropospheric isentropes have a positive latitudinal slope, so that an isentropic layer representing the outflow from the tropical Hadley cell will lie well above the tropopause in midlatitudes. However, this problem can be avoided if one focuses on the low-latitude stationary wave response. Shallow water models are also unable to simulate the effects of transient eddies associated with baroclinic instability. However, experiments with multi-level models (e.g. Ting and Held

1990) have indicated that the influence of transient eddies on low-latitude stationary waves can be approximated by including simple frictional damping.

In Chapter 3, a novel technique is used to create realistic basic states in the nonlinear shallow water system. Instead of large variations in fluid depth, topography is used to create the large equator-to-pole height gradients required to generate Earth-like zonal-mean zonal winds, thus avoiding unrealistic tropical wave speeds. A mean meridional circulation is generated by relaxing the fluid depth towards its initial, global-mean value. Balanced basic states are also constructed using (2.11) to isolate the influence of the mean meridional flow on the response to tropical eddy forcing. These basic states are then used to study the influence of non-zero basic states on the tropical stationary wave response to eddy forcing at or near the equator in Chapters 5 and 6.

2.3 Eddy vorticity balance

In order to identify the factors controlling the Rossby wave response to tropical eddy forcing and the changes induced by imposing hemispheric asymmetry and/or realistic basic states, it is useful to consider the eddy vorticity balance in the shallow water system, which may be written:

$$\frac{\partial \xi^*}{\partial t} = -\left(\zeta\delta\right)^* - \left(\mathbf{v}_i^* \cdot \nabla\zeta\right)^* - \left(\mathbf{v}_r^* \cdot \nabla\zeta\right)^* - \frac{[u]}{a\cos\theta}\frac{\partial \xi^*}{\partial \lambda} - \frac{[v]}{a}\frac{\partial \xi^*}{\partial \theta} + F_\zeta^* \approx 0 \qquad (2.12)$$

The subscripts r and i in (2.12) denote the rotational and irrotational (divergent) components of the equilibrium eddy circulation, respectively, while brackets and asterisks denote zonal-mean and zonally-asymmetric (eddy) quantities. The absolute vorticity ζ includes the planetary vorticity f, the eddy vorticity ξ^*, and the zonal-mean relative vorticity $[\xi]$, which is equal to the meridional derivative of the zonal-mean zonal wind field. Since the model is forced by adding mass sources and sinks in the height

tendency equation, the forcing term in (2.12) represents damping, which can take the form of linear frictional drag ($-k_f\xi^*$), horizontal diffusion ($-\nabla^8\xi^*$), and/or "vertical" momentum transfer ($-F_h\xi^*/2h$ or $-F_h\xi^*/h$).

Several authors (e.g. Sardeshmukh and Hoskins 1988) have noted that vorticity advection by the eddy divergent flow (i.e. the second term on the RHS of (2.12)) reinforces and expands the Rossby wave forcing associated with tropical divergence acting directly on the total vorticity field (first term on the RHS), which is often called vortex stretching. Hence, it is important to consider the divergent and rotational components of the eddy response separately. Separating the eddy circulation into rotational and divergent components also provides a convenient way to isolate and compare the Kelvin and Rossby wave components of the equilibrium stationary wave response, since Kelvin waves are purely divergent while Rossby waves are purely rotational. It is shown in Chapter 3 that the response to off-equatorial eddy forcing is strongly influenced by the different latitudinal structures of the divergent and rotational components of the response.

The advection of eddy vorticity by the (purely rotational) zonal-mean zonal winds and (purely divergent) mean meridional flow are also listed separately in (2.12) to facilitate the study of how realistic basic state winds modify the response to eddy forcing in Chapter 5. However, the zonally-averaged zonal and meridional winds also enter the vorticity balance through the zonal-mean divergence and zonal-mean vorticity in first three terms on the RHS of (2.12). To see this more clearly, the eddy vorticity balance equation can be further decomposed into linear and nonlinear terms:

$$\begin{aligned}\frac{\partial\xi^*}{\partial t} = &-\left(f+[\xi]\right)\delta^* - \xi^*[\delta] - \frac{v^*}{a}\frac{\partial\left(f+[\xi]\right)}{\partial\theta} - \frac{[u]}{a\cos\theta}\frac{\partial\xi^*}{\partial\lambda} - \frac{[v]}{a}\frac{\partial\xi^*}{\partial\theta} + F_\zeta^* \\ &-\left(\xi^*\delta^*\right)^* - \left(\frac{u^*}{a\cos\theta}\frac{\partial\xi^*}{\partial\lambda}\right)^* - \left(\frac{v^*}{a}\frac{\partial\xi^*}{\partial\theta}\right)^* \approx 0\end{aligned} \tag{2.13}$$

The nonlinear terms are located on the second line of (2.13), and the rotational and divergent eddy advection terms have been combined for simplicity. The zonal-mean divergence [δ] is equal to the meridional derivative of the mean meridional flow, just like the zonal-mean relative vorticity [ξ] is equal the meridional derivative of the zonal-mean zonal wind.

The first term on the RHS of (2.13) indicates that a positively sheared basic state zonal wind field will amplify the response to eddy forcing, an effect that has been noted by many authors (e.g. Chang and Webster 1989). The second term on the RHS of (2.13) indicates that the tropical Hadley circulation also amplifies vorticity anomalies in regions where the mean meridional flow is convergent, and damps vorticity anomalies in regions where the mean meridional winds diverge, an effect previously noted by Sardesmukh and Hoskins (1988). The tropical Hadley circulation has also been shown to enhance the propagation of wave activity in the direction of the mean meridional flow, and inhibit wave propagation in the opposite direction, by Watterson and Schneider (1988). This effect will also be investigated in Chapter 5 by comparing the eddy response in basic states with and without a Hadley circulation.

2.4 Chapter summary

- The shallow water equations have been presented and discussed, and the numerical model used to perform the experiments in the following chapters is introduced.
- Previous experiments using the shallow water system have relied on linearization or large fluid depths at the equator to generate realistic basic state circulations, but these techniques are limited in their ability to accurately resolve tropical wave dynamics.
- The eddy vorticity balance has been presented and discussed.

3. Earth-like zonally-symmetric basic states

Previous studies using the shallow water equations to investigate low-latitude stationary waves have been limited by the inability of the shallow water system to accurately represent tropical wave dynamics in the presence of a realistic zonal-mean flow. In this chapter, a novel technique is introduced for generating realistic basic states in the shallow water framework that does not require linearization or large fluid depths at the equator. This technique was inspired by Held and Phillips (1990), who used a hybrid model consisting of nonlinear momentum equations coupled to a linearized height equation with a shallow fluid depth to generate a realistic basic state. Both equinoctial and solstitial basic states can be generated using the topographic forcing procedure, and a balancing technique can also be used to generate corresponding basic states with zero mean meridional flow. The basic states described in this chapter will be used in Chapters 4 and 5 to study the influence of Earth-like basic states on the equilibrium response to tropical eddy forcing.

The chapter is organized as follows. Section 3.1 describes how Earth-like zonally-symmetric basic states can be generated in the shallow water system by specifying a zonally-invariant topography distribution that spans the entire globe. Section 3.2 presents the zonally-symmetric basic state solutions obtained by using this technique in the numerical model introduced in Chapter 2. Section 3.3 evaluates the sensitivity of the basic state solutions to the various forcing parameters. Section 3.4 provides a summary of important results.

3.1 A novel technique

Consider a thin fluid layer sitting on top of a zonally-symmetric topography distribution with the following form:

$$h_s = \mathrm{H_o}\left\{1-\left(\sin\theta-\sin\theta_\mathrm{o}\right)^2\right\} \tag{3.1}$$

Here $\mathrm{H_o}$ represents the maximum height of the topography and θ_o is the latitude at which this peak height occurs. The sine-squared latitudinal profile of the topography is similar to the reference geopotential profile used by Held and Phillips (1990) and the "radiative equilibrium" temperature profiles used by Held and Hou (1980), and it also resembles the observed geopotential height gradient in the upper troposphere. This similarity should not be surprising, since the topography field is being introduced to generate realistic zonal-mean zonal winds, and the zonal-mean zonal flow is determined by the equator-to-pole geopotential height gradient.

Specifying θ_o=0° produces a hemispherically-symmetric, or "equinoctial" basic state zonal wind distribution. Hemispherically-asymmetric, or solstitial, basic states are created when (3.1) is imposed with nonzero θ_o. The hemisphere containing the peak of the topography distribution, which corresponds to the "summer" hemisphere, has smaller meridional height gradients and weaker zonal-mean zonal winds, while the other ("winter") hemisphere has larger height gradients and hence stronger mean zonal flow.

To generate a mean meridional circulation, and prevent the fluid from simply "running down" the mountain, the fluid depth is relaxed towards its initial, global-mean value h_o:

$$F_h = -k_h\left(h-h_\mathrm{o}\right) \tag{3.2}$$

In most of the experiments below, the thermal damping strength is $k_h = \left(10\,\mathrm{days}\right)^{-1}$ and the global-mean fluid depth is $h_\mathrm{o} = 200\,\mathrm{m}$, although the sensitivity of the basic state fields to variations in these parameters is also discussed. Note that the equilibrium fluid depth will be lower than h_o near the equator and larger than h_o away from the equator, giving rise to a mean meridional flow analogous to the upper-tropospheric Hadley circulation. In

the solstitial integrations, the fluid lying between the equator and the peak of the topography will tend to move downhill. Thus, the maximum zonal-mean divergence will also reside in the summer hemisphere, and the Hadley circulation will include cross-equatorial mean meridional flow, just as in the tropical upper troposphere during solstitial seasons (see, e.g., Dima et al 2005).

Since the shallow water system does not support extratropical transient baroclinic eddies, frictional drag must be included in the zonal momentum equation in order to balance the Coriolis accelerations associated with the mean meridional circulation and permit an equilibrium solution. Here a linear drag is used for both the zonal and meridional velocities:

$$\begin{aligned} F_u &= -k_f u \\ F_v &= -k_f v \end{aligned} \tag{3.3}$$

In most of the experiments described below, the strength of the frictional drag is the same as the thermal damping strength, i.e. $k_h = k_f = (10\,\text{days})^{-1}$. Since the tropical upper troposphere is generally regarded as a region with weak frictional drag and long thermal damping timescales, ideally one would like to use even weaker damping parameters, along with smaller fluid depths. However, as discussed below, problems with large Froude numbers limit the minimum fluid depth that can be used, and some amount of damping is required to produce mean meridional winds similar to those observed in the upper troposphere. The effect of including a momentum source corresponding to (2.10) is discussed in each of the subsequent chapters, but is generally small. The horizontal diffusion in the model is also so weak that it can generally be ignored.

To study the influence of the mean meridional circulation on the response to tropical eddy forcing, zonally-symmetric basic states without a mean meridional circulation are also considered. These "no Hadley" basic states are generated by solving

the nonlinear balance equation (2.11) with the meridional winds set equal to zero and the zonal winds set equal to one of the equilibrium zonal wind fields generated using (3.1)-(3.3). The topography distribution is then set equal to the difference between the balanced height field and the equilibrium height field from the corresponding full basic state integration. Since the general circulation is usually very close to nonlinear balance, and the mean meridional winds are always much smaller than the mean zonal winds, this procedure yields topography and total height fields, and hence potential vorticity profiles, that are nearly identical to those produced using (3.1)-(3.3). For consistency, the wind and height field perturbations in the "no Hadley" experiments are relaxed towards their original values with the same damping strength as that used in the corresponding experiments with a full basic state, i.e. $k_h = k_f = (10\,\text{days})^{-1}$.

3.2 Numerical solutions

To produce Earth-like zonally-symmetric climates, the FMS model described in Chapter 2 was forced using (3.1)-(3.3) with $k_h = k_f = (10\,\text{days})^{-1}$, $H_0 = 1500$ m, and θ_0 set to either 0° or 5°N. The $\theta_0 = 0°$ case is referred to as the "equinoctial" basic state, while $\theta_0 = 5°$N corresponds to the "solstitial" basic state. In order to prevent negative fluid depths near the pole in the solstitial basic state, a constant-in-latitude offset of 200 m is added to the topography distribution in all runs; this offset does not affect the results. Integrations are initialized from a resting fluid with uniform depth $h_0 = 200$ m, and the zonally-symmetric topography is raised over the first 25 days of the integration. The equilibrium response is typically established in less than 50 days. The results presented below are from day 200.

Figure 1 shows the topography distributions and the equilibrium fluid depths, wind fields, and potential vorticity distributions for the equinoctial ($\theta_0 = 0°$, solid lines)

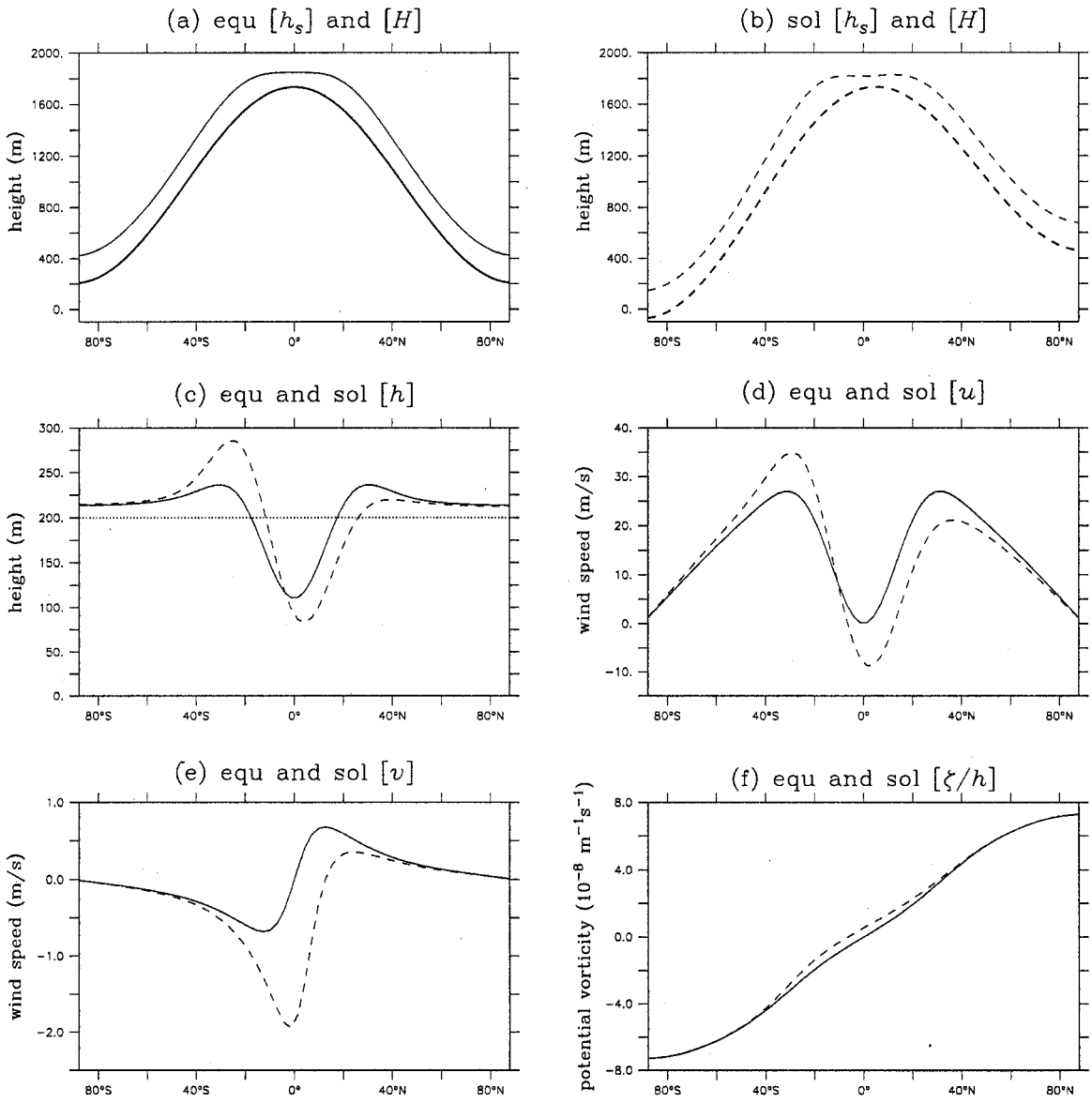

Figure 1. The (a-b) topography and total height, (c) fluid depth, (d) zonal winds, (e) meridional winds, and (f) potential vorticity in the zonally-symmetric equinoctial (solid) and solstitial (dashed) basic states. The dotted line in (c) represents the initial, global-mean fluid depth.

and solstitial (θ_o = 5°N, dashed lines) basic states. The dashed line in Figure 1c represents the global-mean fluid depth in both runs. The equilibrium fluid depth in both basic states is ~100 *m* near the equator, which is within the appropriate range for resolving equatorial waves discussed in Chapter 2. The fluid depth increases to ~250 m at ~15°N, which tends

to "flatten" the potential vorticity profile in the tropics (Figure 1f), and then gradually decreases to ~220 m at the poles. These depths are too small to permit extratropical wavetrains to develop in response to tropical forcing (c.f. Lau and Lim 1984). Presumably, one could attempt to simulate both tropical wave dynamics and the corresponding extratropical teleconnections by specifying a reference fluid depth that increases away from the equator, with an even steeper zonally-symmetric topography distribution to maintain the same total height gradient. However, since the focus of this dissertation is on the steady eddy circulations at low latitudes, only a globally-uniform reference height field is considered.

The zonal and meridional winds in the equinox basic state (solid lines in Figure 1d-e) bear a strong resemblance to the observed zonally-averaged circulation in the upper troposphere averaged over either the equinox months or the entire year (see, e.g., Dima et al 2004). The solstitial basic state (dashed) also provides a reasonable facsimile of the observed upper-tropospheric flow during Northern winter, with stronger zonal winds in the "winter" hemisphere, weaker zonal flow in the "summer" hemisphere, and a mean meridional circulation dominated by a single "Hadley cell" straddling the equator. The conservation of angular momentum following the cross-equatorial flow also gives rise to easterly zonal winds at the equator in the solstitial basic state, in accordance with observations and axisymmetric models (Lindzen and Hou 1988).

The equatorial no-Hadley and solstitial no-Hadley experiments have equilibrium zonal-mean height and wind fields that are identical to those shown in Figure 1(c-d), but the mean meridional flow is identically zero. Figure 2 shows the small differences between the topography distributions in the full and no-Hadley basic state integrations. These differences arise due to the omission of the mean meridional winds when using (2.11) to specify the total height field in the no-Hadley basic state, and they are very

small because the general circulation is typically very close to nonlinear balance and the mean zonal winds are typically much stronger than the mean meridional winds.

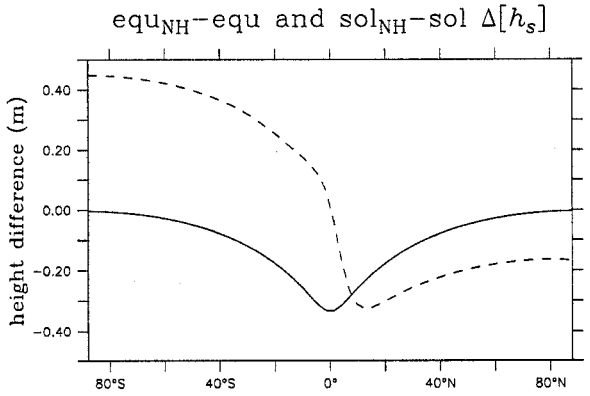

Figure 2. The difference between the topography fields in the (solid) equinoctial and equinoctial no-Hadley and (dashed) solstitial and solstitial no-Hadley basic states.

3.3 Sensitivity to damping

Figure 3 shows the sensitivity of the equinox basic state to variations in k_f and k_h. As k_f is decreased, the mean zonal winds follow an angular momentum conserving profile more closely in the tropics, leading to sharper and slightly stronger subtropical jets (cf. Held and Hou 1980). Decreasing k_f also weakens the mean meridional flow because the Coriolis acceleration is balanced primarily by frictional drag. Reducing k_h, on the other hand, weakens both the mean zonal winds and the mean meridional flow, because the thermal damping strength controls both the equilibrium fluid depth and the strength of the tropical mass source. The sensitivities of the equilibrium height distribution to reductions in k_f and k_h, shown in Figure 3b, are consistent with the corresponding changes in the zonal and meridional winds, with steeper meridional gradients but smaller departures from the initial fluid depth when k_f is reduced, and larger depth variations with weaker meridional gradients when k_h is reduced.

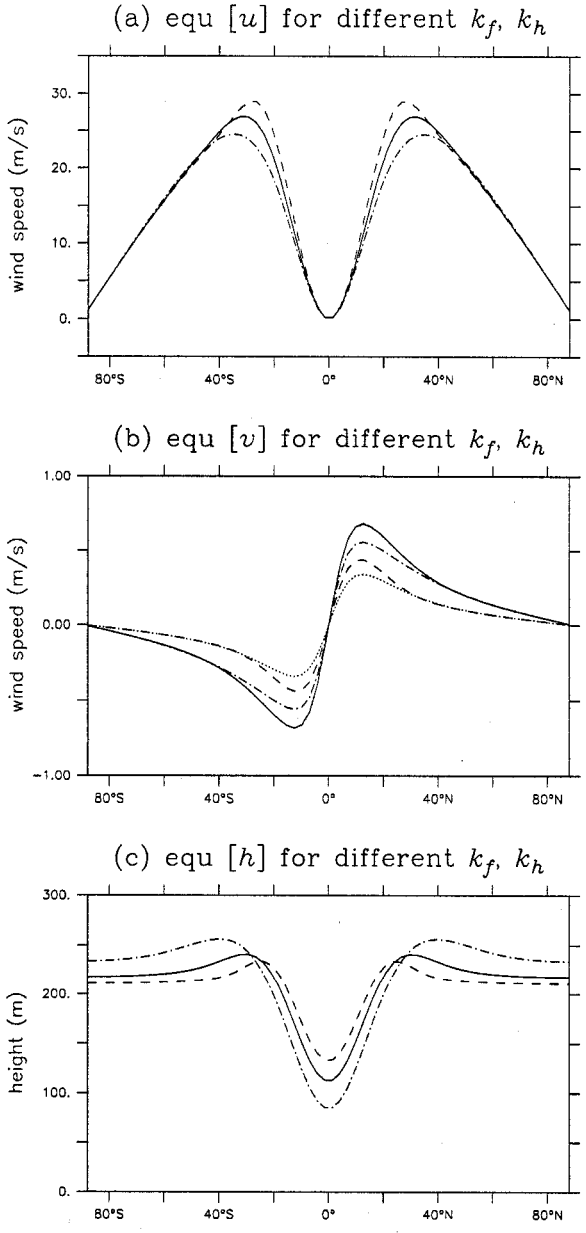

Figure 3. The (a) zonal wind, (b) meridional wind, and (c) fluid depth in equinoctial basic states constructed using $k_f = k_h = (20\,\text{days})^{-1}$ (solid) ; $k_f = (20\,\text{days})^{-1}$, $k_h = (10\,\text{days})^{-1}$ (dashed); $k_f = (10\,\text{days})^{-1}$, $k_h = (20\,\text{days})^{-1}$ (dotted); and $k_f = k_h = (20\,\text{days})^{-1}$ (dot-dash).

The mean zonal wind distribution and height field for $k_h = k_f = (20\,\text{days})^{-1}$ are nearly identical to those for $k_h = k_f = (10\,\text{days})^{-1}$, but the mean meridional flow is reduced by ~50%. These results are consistent with Held and Phillips (1990), who note that the mean zonal wind distribution in a similar but slightly simpler model depends on

the damping parameters and fluid depth only through the combination $h_o k_t k_f^{-1}$, while the mean meridional flow approaches a lower bound proportional to $k_t h_o^{-1}$ as $k_f \to 0$. The nonlinear terms in (2.1)-(2.3) preclude such clean analytical solutions, but the numerical results in Figure 3 indicate a similar sensitivity to the basic state forcing parameters.

The easterly winds and shallow layer depth near the equator in the solstitial basic state impose a practical lower bound on the thermal damping strength and global-mean fluid depth that can be used in the model, since flows with Froude numbers ($F = 2K / gh$) exceeding unity cause the numerical model to become unstable, and are not consistent with the observed atmospheric general circulation. The solstitial basic state becomes unstable when the thermal damping strength is reduced below $(20\,\text{days})^{-1}$, when the global-mean fluid depth is reduced below 55 m, or if the center of the topography distribution is moved beyond 10°N. These problems become even more acute when eddy forcing is added to the solstitial basic state in Chapter 5, because tropical eddy forcing leads to a localized trough and easterly eddy zonal wind anomalies at the equator.

One modification to the model would allow a thinner fluid layer and weaker damping parameters to be used, namely the energetically-consistent momentum source (2.10) suggested by Gent (1993) and discussed in Chapter 2. Figure 4 shows the change in the basic state solutions obtained when (2.10) is included with the zonally-symmetric forcing (3.1)-(3.3). The changes to the equinox basic state are very small because the zonally-symmetric mass source associated with thermal relaxation is centered at the equator, where the mean zonal winds are nearly zero, although slight reductions appear in the zonal and meridional velocities on either side of the equator. When the topography distribution is shifted off the equator, the addition of resting fluid north of the equator reduces the strength of the cross-equatorial flow by ~5% and the corresponding easterly zonal-mean zonal winds, which are also damped themselves, by ~30%.

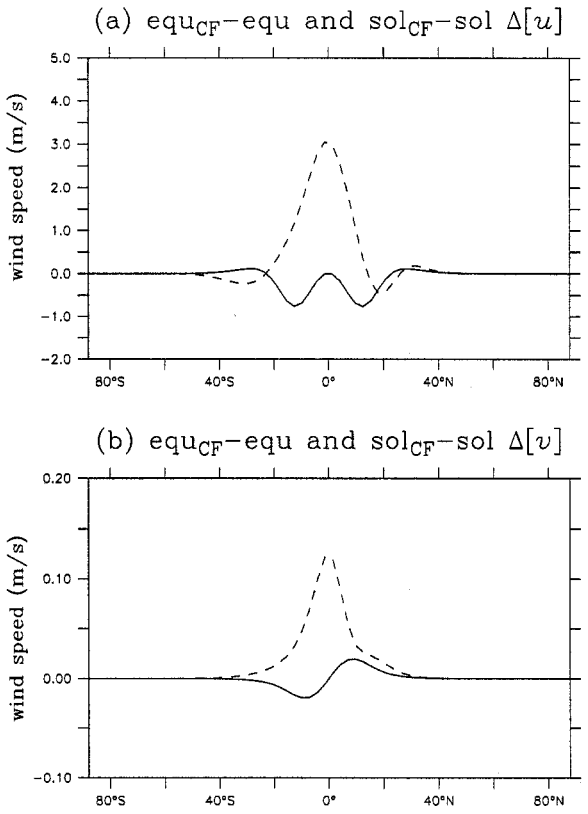

Figure 4. The change in the (a) zonal winds and (b) meridional winds in the equinoctial (solid) and solstitial (dashed) basic states resulting from the introduction of a momentum source proportional to the mass source as per (2.10)

3.4 Chapter summary

- Earth-like basic states are generated in the shallow water system by adding a large, zonally-invariant topography distribution that decreases smoothly from the tropics to the poles and relaxing the fluid towards its global-mean depth.
- Basic states with identical zonal-mean zonal winds, but zero mean meridional flow, are also generated by using the nonlinear balance equation.
- The basic states produced using this technique show a similar sensitivity to damping strength and mean fluid depth to those in Held and Phillips (1990).

4. Tropical stationary waves in a resting basic state

Before the influence of Earth-like basic states on the response to tropical eddy forcing is evaluated, it is instructive to investigate the response of the shallow water system to a low-latitude mass forcing in the simpler context of a resting basic state. In this chapter, the zonally-asymmetric response of the shallow water model described in Chapter 2 to a particular distribution of mass sources and sinks along the equator is described and compared with the equilibrium eddy circulations obtained by previous authors. The influence of nonlinearity and the effect of moving the eddy forcing off the equator are also discussed at length. It is found that hemispherically-asymmetric forcing leads to a much stronger response in the forced hemisphere, although the response in the opposite hemisphere does not decrease as much as might be expected, because the eddy divergent winds provide vorticity advection across a wide range of latitudes. It is also shown that nonlinear effects are quite important near the equator, especially when the forcing is hemispherically-asymmetric, and that increasing the strength of the damping does not account for neglecting nonlinearity.

Section 4.1 describes the eddy mass source-sink distribution using to force the model. Section 4.2 describes the zonally-asymmetric response of the model to finite-amplitude eddy forcing imposed both on and off the equator in a resting basic state, decomposes the response into divergent and rotational components, and analyzes the eddy vorticity balance in each experiment. Section 4.3 evaluates the nonlinear aspects of the response by comparing the finite-amplitude response with linear experiments, and also briefly discusses the sensitivity of the linear response to stronger damping. The final section of the chapter contains a summary of the most important findings from the preceding sections.

4.1 Eddy forcing description

To generate a stationary wave response in the shallow water model described in Chapter 2, the following zonally-asymmetric mass source-sink distribution is imposed in the height tendency equation:

$$Q^*(\lambda,\theta) = \mathrm{Q_e} \exp\left\{-\left(\frac{\lambda-\lambda_e}{\Delta\lambda}\right)^2 - \left(\frac{\theta-\theta_e}{\Delta\theta}\right)^2\right\} - \bar{Q}(\theta) \qquad (4.1)$$

The mass source is centered at the dateline (λ_e=180°) with a longitudinal scale of $\Delta\lambda$=30°, a latitudinal scale of $\Delta\theta$=5°, and an amplitude of $\mathrm{Q_e}$=100 *m/day*. These values are chosen to produce an eddy response that resembles the observed upper-tropospheric stationary waves forced by deep convection over the Pacific warm pool region. $\bar{Q}$ represents the zonal average of the forcing, which is removed in order to prevent the direct forcing a zonal-mean response; the use of a zonally-distributed mass sink to balance a concentrated mass source is also intended to replicate the conditions in the tropical upper troposphere, where concentrated regions of convection are balanced by broad areas of subsidence and radiative cooling.

To study the effects of hemispherically-asymmetric forcing, experiments are performed with the mass forcing pattern centered at both the equator (θ_e=0°) and at 10°N. The linear integrations discussed in Section 4.3 are performed by reducing the amplitude of the mass source by a factor of 1000, and then multiplying the equilibrium eddy response by the same factor; this procedure reduces the amplitude of nonlinear terms in the governing equations by a factor of 1×10^{-6}. The sensitivity of the response to different damping schemes, different fluid depths, the inclusion of a momentum source corresponding to the mass forcing is also considered in Section 4.4.

In this chapter, the model is initialized with a resting basic state constructed by specifying zero topography everywhere ($h_s \equiv 0$) and a fluid depth of 100 *m*, which

approximates the equilibrium depth near the equator in the realistic basic states (see Figure 1c). In all of the experiments described in this chapter and the following two chapters, the mass forcing is ramped up linearly over the first 25 days of each run, and the equilibrium response is typically established by day 75. Results shown below are from day 200. The zonal-mean component of the response, which is studied in the next chapter, is generally small due to the removal of the zonal mean forcing in (4.1), and has been removed from all of the figures in the next two chapters in order to focus on the steady eddy circulation.

4.2 Nonlinear response to eddy forcing

Figure 5 shows the equilibrium eddy responses obtained when the numerical shallow water model described in Chapter 2 is integrated with Q^* centered either on or off the equator in the resting basic state. The eddy height and wind anomalies in the hemispherically-symmetric solution (Figure 5a) are analogous to those found in the linear response to an isolated mass sink studied by Gill (1980). However, the broad compensating mass sink in (4.1), along with the relatively weak damping and periodic domain used in the model, engender an equilibrium solution that bears a closer resemblance to the response to periodic forcing obtained by Matsuno (1966). Note that at the equator, both the ridge in the height field and the dividing line between easterly and westerly flow are located slightly to the east of the maximum forcing, while the strongest eddy zonal winds and negative height anomalies are found to the west of the mass source. Away from the equator, the largest height perturbations are centered to the west of the forcing, and the eddy circulation is rather weak. This latitudinal structure is consistent with the increase in planetary vorticity with latitude, since the eddy winds must be stronger near the equator in order to remain in approximate geostrophic balance with the eddy height field.

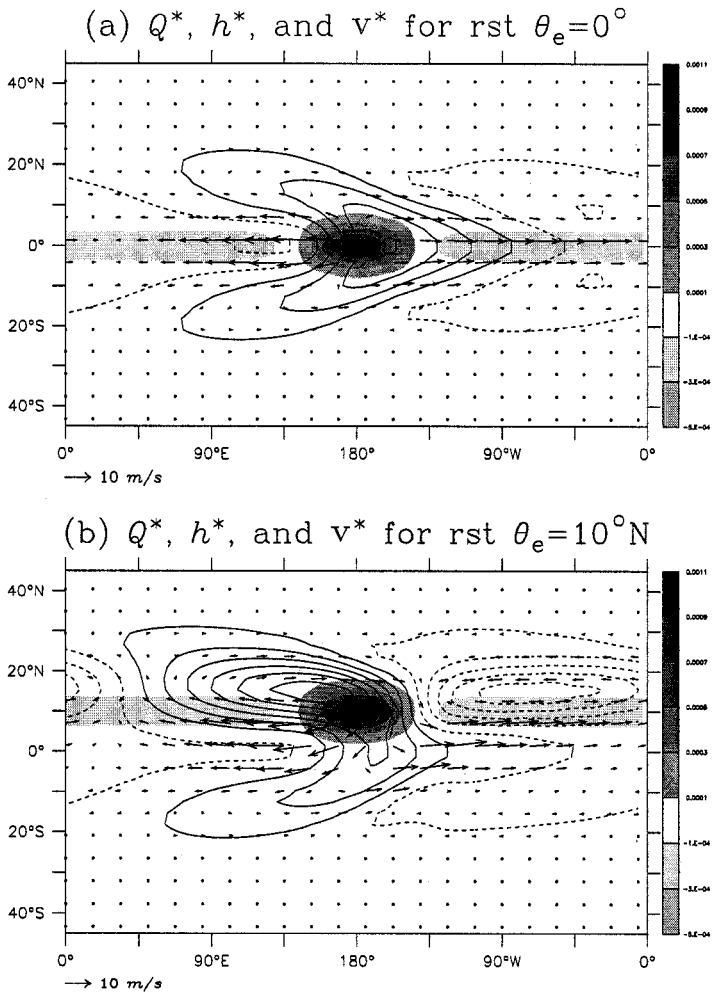

Figure 5. The mass source (shading), eddy height field (contours every 5 *m*), and eddy winds (vectors) in the (a) $\theta_e = 0°$ and (b) $\theta_e = 10°$N resting basic state experiments.

Moving the mass forcing off the equator (Figure 5b) leads to a significant amplification, and slight northward shift, in the eddy response in the forced hemisphere. The strongest eddy winds are still found near the equator, and the maximum wind speed is slightly larger than the maximum wind speed in the hemispherically-symmetric solution, even though the height variations along the equator are slightly weaker. Also note that the wind vectors immediately south and west of the mass source exhibit a northeast-southwest tilt, implying a northward flux of eddy momentum across the equator. Surprisingly, the eddy response in the Southern Hemisphere is comparable in intensity to the response in the hemispherically-symmetric case, despite the fact that the

eddy forcing resides entirely north of the equator. Dima et al (2005) obtained a similar response to off-equatorial forcing in a nonlinear shallow water model forced with an isolated mass source, and noted that the observed seasonally-varying stationary waves in the tropical upper troposphere also exhibit cross-equatorial eddy momentum fluxes and substantial hemispheric symmetry throughout the year.

Figure 6 shows the rotational and divergent components of the eddy response in the resting basic state experiment with eddy forcing at the equator; these two panels may also be thought of as the Rossby and Kelvin wave components of the total response. As in previous studies examining the response to tropical eddy forcing a resting basic state, the eddy vorticity field (contours in Figure 6b) is dominated by a pair of anticyclones straddling the equator to the west of the mass source. The strong easterly winds west of, and extending slightly over, the mass source in Figure 5a are associated primarily with the rotational flow around these anticyclones (vectors in Figure 6b). The rotational meridional winds are directed towards the equator in the mass source region and away from the equator across the entire mass sink region to complete the nondivergent circulation. The eddy divergence field (shading in Figure 6c) is virtually identical in structure to the mass forcing, which may be interpreted as the shallow water equivalent of the balance between eddy heating and vertical motion in the tropical atmosphere (see, e.g., Schumacher et al 2004). The divergent winds (vectors in Figure 5c) reinforce the rotational winds along the equator, but tend to offset the rotational flow in both hemispheres, which explains why the total wind field in Figure 5a is weak except near the equator.

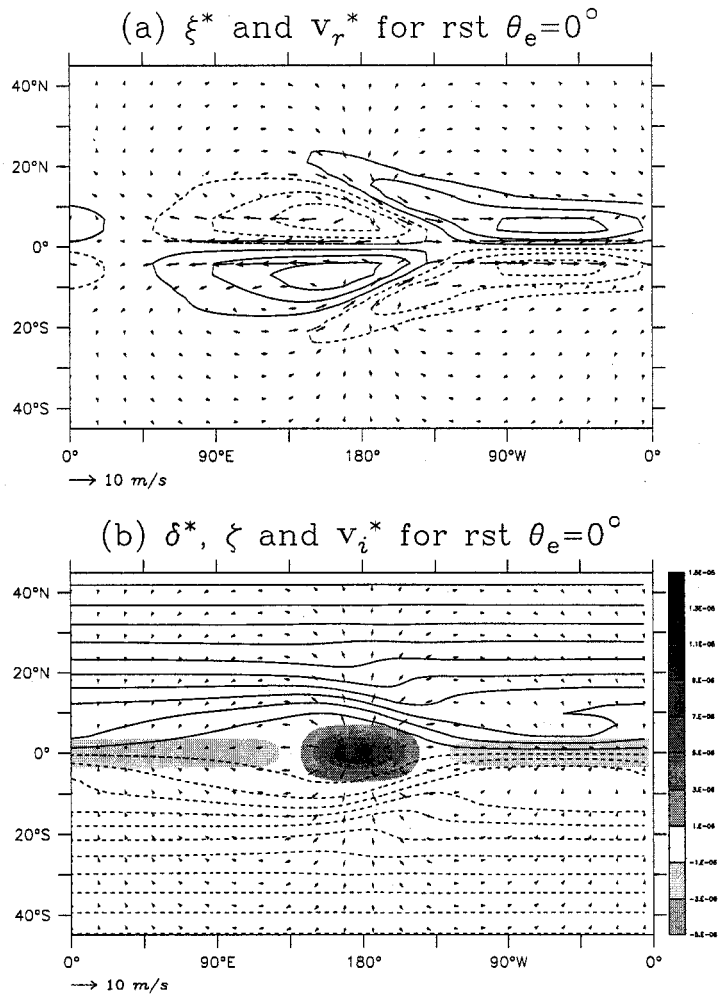

Figure 6. The (a) eddy vorticity (contours every 5×10^{-6} s^{-1}) and eddy rotational winds (vectors); and (b) eddy divergence (shading), total vorticity (contours every 1×10^{-5} s^{-1}), and eddy divergent winds (vectors) in the $\theta_e = 0°$ resting basic state experiment.

The divergent and rotational flow components in the experiment with eddy forcing centered north of the equator (Figure 7) indicates that the amplification of the Northern Hemisphere response in Figure 5b can be attributed mainly to the increase in the strength of the anticyclonic circulation in that hemisphere. The stronger eddy zonal winds along the equator can also be attributed to the stronger Rossby wave response in the Northern Hemisphere, since both the anticyclonic circulation in the Southern Hemisphere and the divergent Kelvin wave circulation along the equator are slightly weaker than the corresponding features in the hemispherically-symmetric case. Also note

that the eddy divergence remains collocated with the mass forcing, so that the eddy divergent winds in Figure 7b now include a northerly component at the equator. This subtle shift in the divergent wind field, coupled with the slight eastward displacement of the dividing line between easterly and westerly rotational flow observed in both experiments, is responsible for the tilt in the total eddy wind vectors along the equator noted in Figure 5b. We will discuss these tilts, and the eddy momentum fluxes they imply, in more detail in Chapter 5.

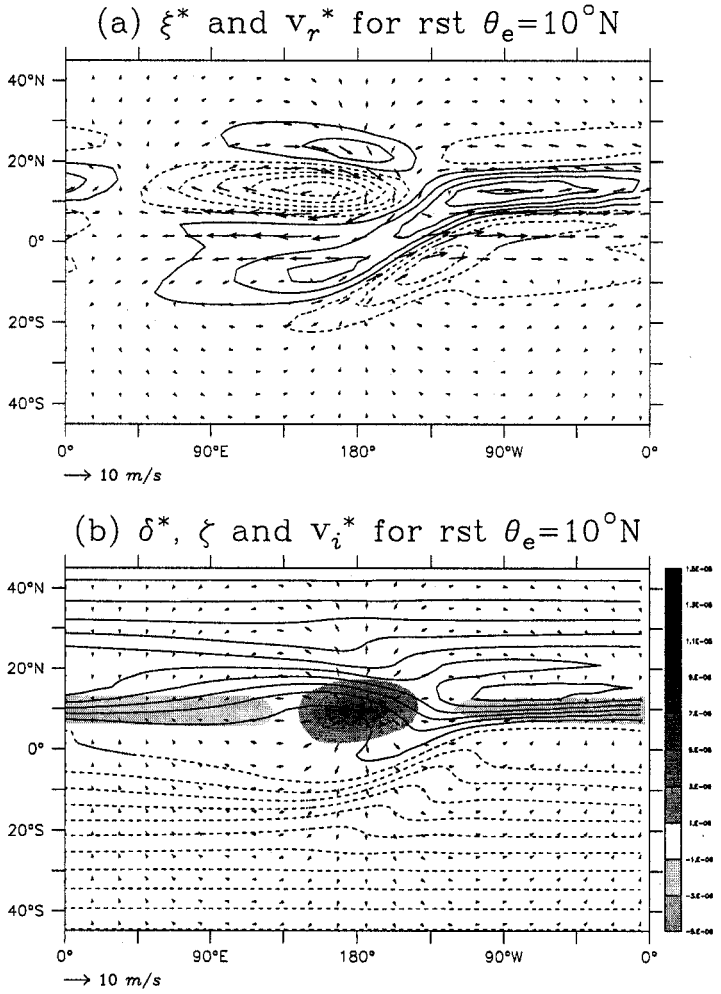

Figure 7. The (a) eddy vorticity (contours every 5×10^{-6} s^{-1}) and rotational winds (vectors); and (b) eddy divergence (shading), total vorticity (contours every 1×10^{-5} s^{-1}), and eddy divergent winds (vectors) in the θ_e = 10°N resting basic state experiment.

Figure 8 shows the components of the eddy vorticity balance (2.12) for the resting basic state experiment with eddy forcing centered at the equator (the terms involving the zonal-mean winds are negligible in the resting basic state). The dominant balance is between the generation of vorticity by divergent advection (Figure 8b) and the advection of vorticity by the rotational winds (Figure 8c), with vortex stretching (Figure 8a) and damping (Figure 8d) making only small contributions near the equator. The vortex stretching, which represents the direct generation of vorticity by eddy divergence, is weak because the finite anticyclonic vorticity anomalies that form near the mass source flatten the vorticity field; this "pool of zero absolute vorticity" (Hoskins et al 2000; see also Gill and Phlips 1986) can be seen at, and to the west of, the divergence anomaly in Figure 6b, and corresponds to the nonlinear $-\left(\xi^*\delta^*\right)^*$ term in (2.13). Also apparent in Figure 8 is a corresponding increase in the vorticity gradient and cyclonic vorticity generation in the mass sink region, which explains why the weak and diffuse convergence anomalies in the mass sink region give rise to cyclonic vorticity anomalies that are nearly as strong as their anticyclonic counterparts in Figure 6a. The small differences in structure between the eddy vorticity field in Figure 6a and the damping term in Figure 8d provide an indication of the influence of numerical diffusion in the model; the effect of stronger diffusion is examined in Section 4.4.

Advection by the divergent flow (Figure 8b) provides significant anticyclonic forcing across a broad region because the eddy divergent winds in Figure 6b are much broader in scale than the eddy divergence or eddy vorticity anomalies, and are generally oriented orthogonal to the total vorticity field (cf Figure 6b). An examination of the temporal evolution of this experiment (not shown) confirms that the anticyclonic circulation features increase in intensity until rotational advection (plus the weak damping term) balances the sum of the vortex stretching (which decreases over the

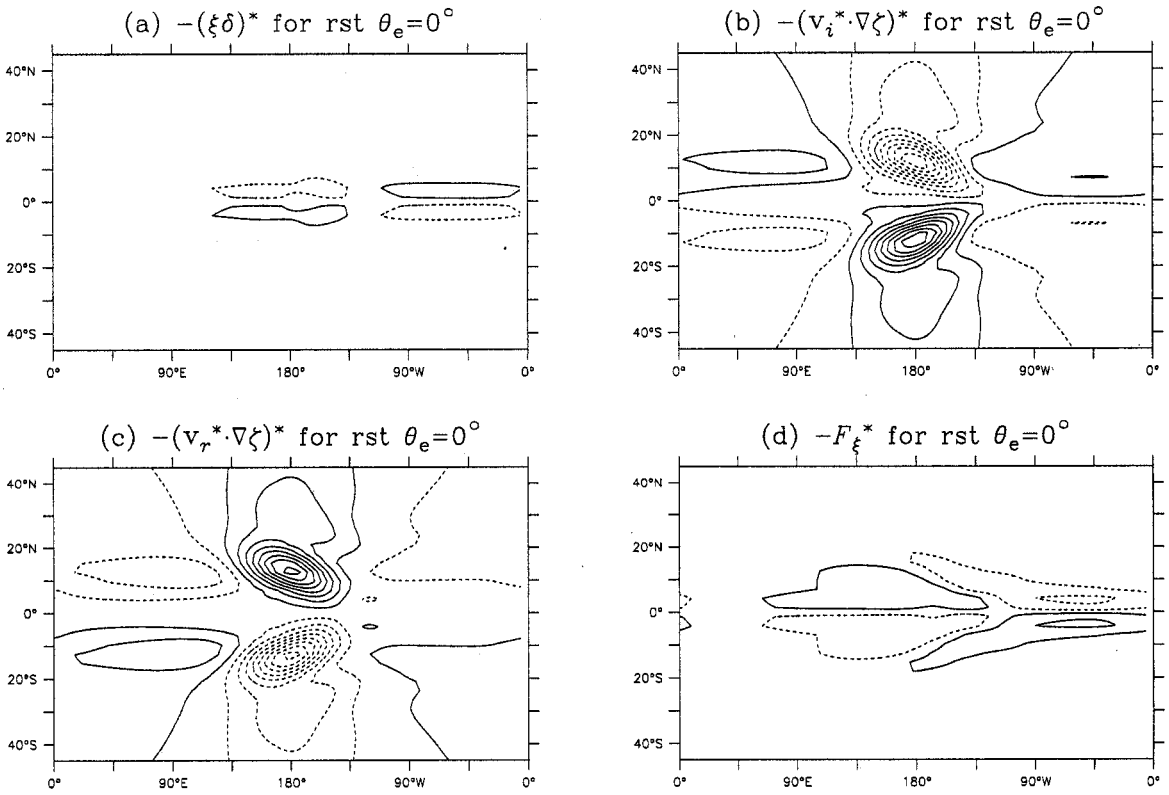

Figure 8. Vorticity balance components (2.12) for the $\theta_e = 0°$ resting basic state experiment, contours every 1.5×10^{-11} s^{-2}.

course of the integration) and divergent advection (which remains relatively stable in amplitude, but changes in shape as the finite vorticity anomalies develop). The balance between rotational and divergent advection explains why the eddy winds are weak away from the equator in the resting basic state, and also why the anticyclonic circulation is centered to the west of the mass source.

Figure 9 shows the vorticity balance for the experiment with eddy forcing centered off the equator in the resting basic state. Comparing Figure 9 with Figure 8, it is clear that the amplification and slight northward shift of the Northern Hemisphere response can be attributed mainly to an increase in the vortex stretching term. The forcing of rotational flow by eddy divergence is stronger when the mass source is moved off the equator because planetary vorticity increases with latitude and because the latitudinal displacement of the mass source moves the divergence anomaly outside the "pool of zero

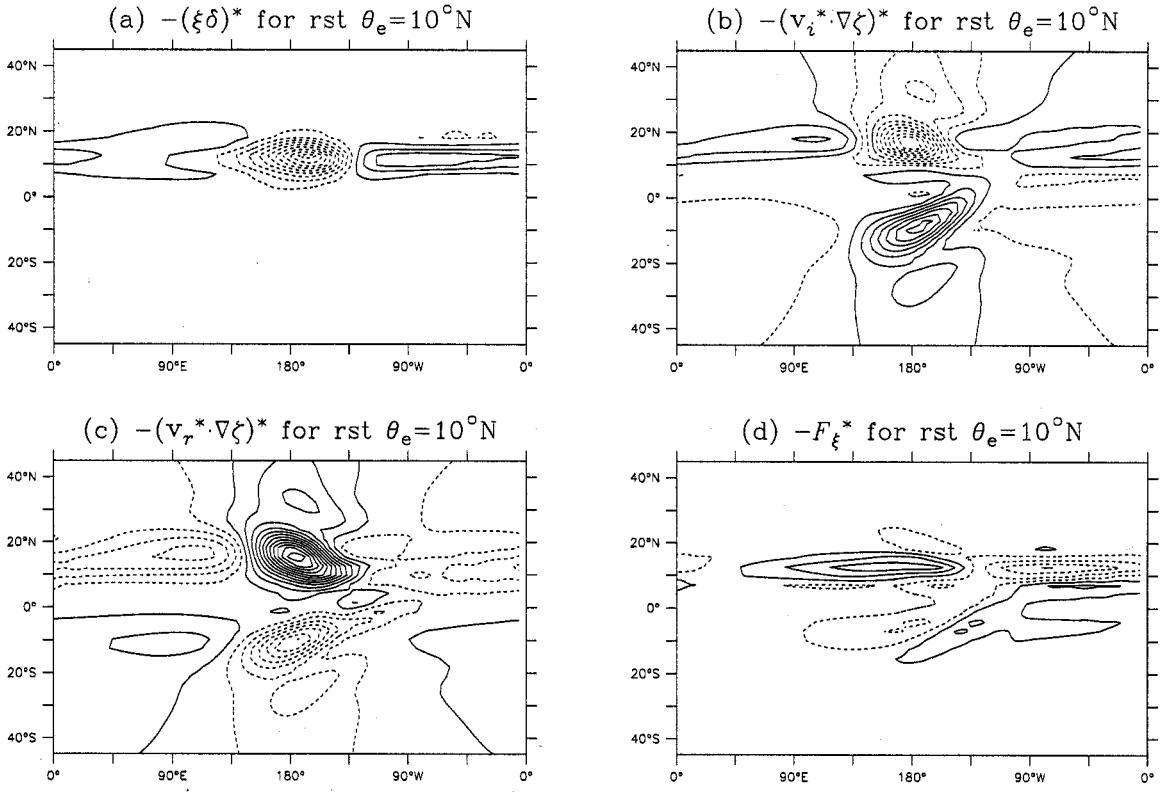

Figure 9. Vorticity balance components (2.12) for the θ_e = 10°N resting basic state experiment, contours every 1.5×10^{-11} s^{-2}.

vorticity" at the equator. The reason why the Southern Hemisphere response only weakens slightly when the eddy forcing is moved north of the equator, on the other hand, is because the eddy divergent winds continue to provide significant anticyclonic vorticity advection on the other side of the equator (Figure 9b) by virtue of their broad meridional scale (compare Figures 6b and 7b) and the concentration of the vorticity gradient at the southern edge of the "pool of zero vorticity". The weak vorticity gradient at the equator also explains why the northerly eddy divergent winds immediately to the south of the mass source do not give rise to a cyclonic response. As in the hemispherically-symmetric case, the rotational forcing by the divergence and divergent winds is balanced mainly by rotational advection (Figure 9c), with frictional damping (Figure 9d) making only a small contribution.

4.3 Linear response to eddy forcing

Figure 10 shows the linear response of the shallow water model to eddy forcing centered at the equator, which is obtained by reducing the amplitude of the eddy forcing anomaly by a factor of 1000 (with the results multiplied by the same factor to facilitate comparison with the nonlinear results). Figure 11 shows the eddy vorticity balance for the same integration. The difference between these plots and the corresponding nonlinear solution in Figures 5a, 6, and 8 provides a direct indication of the role played by nonlinearity in controlling the response to tropical eddy forcing. The most prominent difference between the linear and nonlinear integrations is the strength of the anticyclonic circulation anomalies in the linear case. The eddy vorticity balance (Figure 11) indicates that the increase in anticyclonic vorticity in the linear solution may be attributed to stronger vortex stretching; since the eddy divergence field is similar in the linear and nonlinear integrations, the enhanced vortex stretching may in turn be attributed to the absence of finite-amplitude eddy vorticity anomalies in the total vorticity field (compare Figure 10c with Figure 6b). Phlips and Gill (1986) and Van Tuyl (1986) reached similar conclusions when comparing the linear and nonlinear response to tropical forcing in similar models, and this mechanism is also analogous to the absence of the "pool of zero absolute vorticity" discussed by Hoskins et al (1999).

As in the nonlinear solution, the advection of vorticity by the rotational flow (Figure 11c) balances the advection of vorticity by the divergent flow (Figure 11b), especially on the poleward margins of the mass source, leading to total eddy meridional winds that are generally weak in the full response. However, the enhanced rotational flow around the anticyclonic circulation anomalies on either side of the equator, combined with the absence of finite vorticity anomalies in the warm pool region, leads to anticyclonic vorticity generation by the poleward rotational flow on the western margins of the mass source region. This anticyclonic vorticity advection, along with the stronger

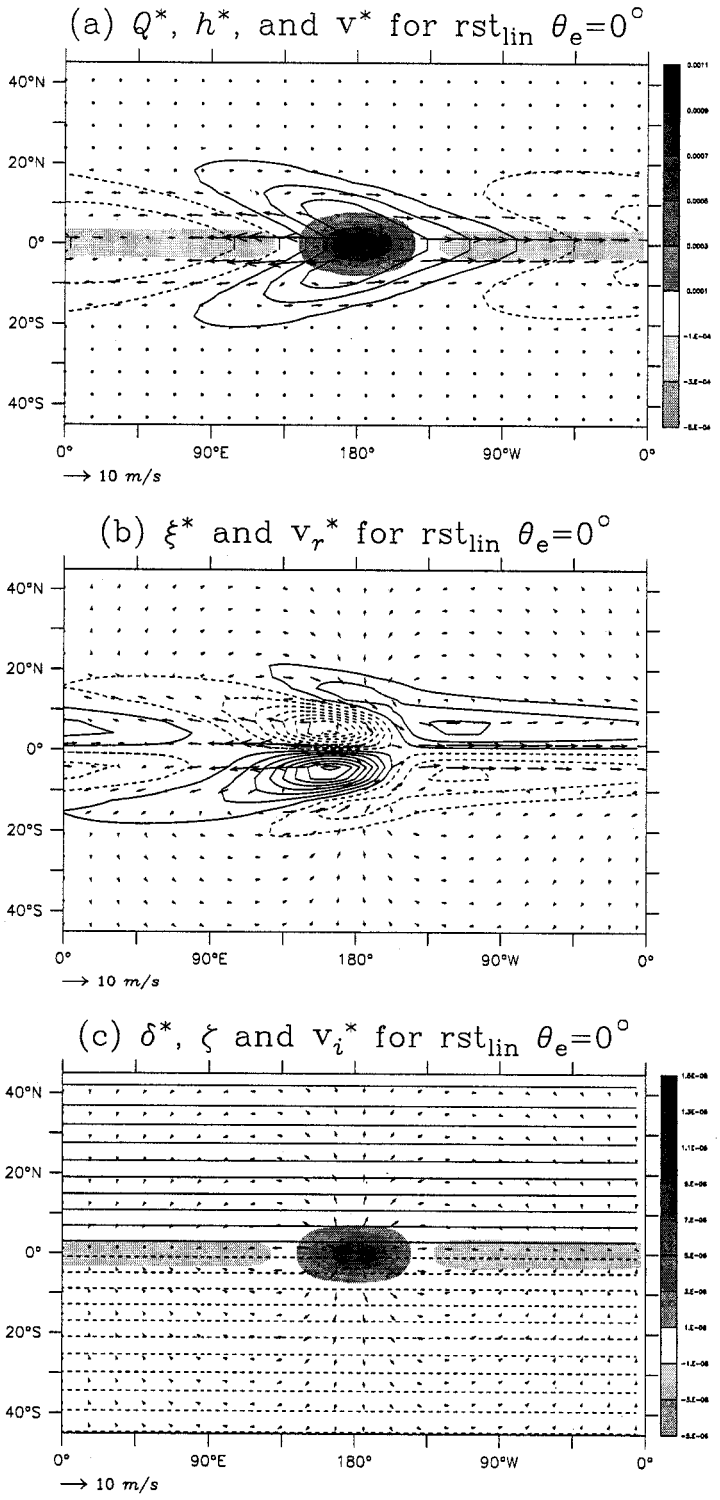

Figure 10. The (a) mass source (shading), eddy height field (contours every 5 m), and eddy winds (vectors); (b) eddy vorticity (contours every 5×10^{-6} s^{-1}) and rotational winds (vectors); and (c) eddy divergence (shading), total vorticity (contours every 1×10^{-5} s^{-1}), and eddy divergent winds (vectors) in the θ_e = 0° linear resting basic state experiment.

vortex stretching term, is balanced mainly by the stronger frictional drag (Figure 6d) associated with the enhanced anticyclonic circulation anomalies in the linear solutions. The increase in the importance of frictional drag suggests that the linear solution could be made to more closely resemble the nonlinear response simply by increasing the strength of the frictional drag. In fact, this is exactly the strategy employed to account for the neglected nonlinearity in linear barotropic and multi-level linear stationary wave models (e.g. Held et al 2001). However, as shown below, the linear and nonlinear responses exhibit much larger structural differences when the eddy forcing is moved off the equator, and that these differences cannot be accounted for by simply increasing the drag term.

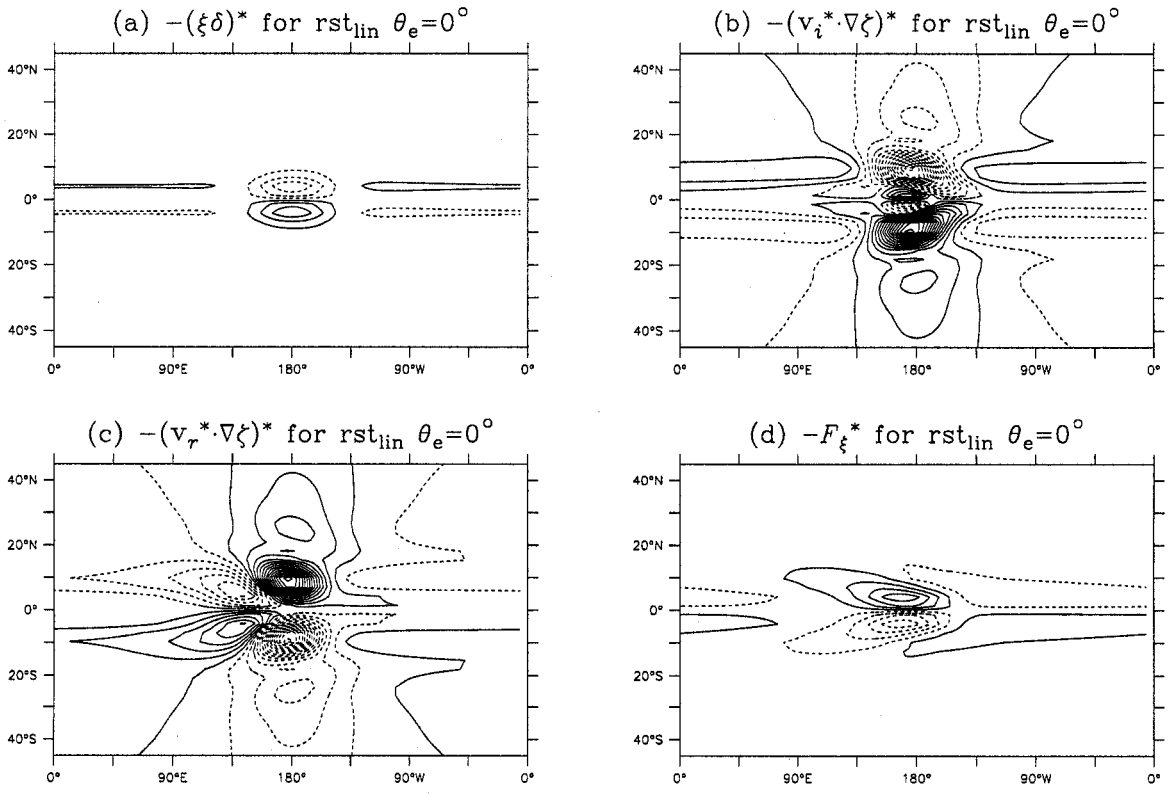

Figure 11. Vorticity balance components (2.12) for the $\theta_e = 0°$ linear resting basic state experiment, contours every 1.5×10^{-11} s^{-2}.

A close inspection of Figures 10a and 5a also reveals some notable differences between the linear and nonlinear eddy responses along the equator. In particular, the trough in the equatorial height field is much weaker and centered farther west in the linear solution than in the nonlinear solution, whereas the easterly eddy zonal winds anomalies along the equator are stronger and more equatorially confined in the linear solution. Hence, the strongest eddy zonal winds are virtually collocated with the trough in the nonlinear solution, while the eddy wind and height anomalies along the equator are essentially in quadrature in the linear experiment. Phlips and Gill (1986) noted similar a difference between the eddy height and wind anomalies in their linear and nonlinear experiments, and attribute it to the Bernoulli effect: the kinetic energy of the finite-amplitude eddy zonal wind anomalies in the nonlinear integration increases the geopotential depression necessary to maintain eddy zonal wind balance along the equator, or conversely, the eddy zonal wind anomalies are somewhat weaker in the nonlinear integration because the kinetic energy of the flow offsets some of the geopotential variations. In both cases, the eddy zonal winds should be nearly zero near the ridge in the height field, which is displaced slightly to the east of the mass source due to the mass transport associated with the convergent meridional flow.

The differences between the linear and nonlinear integrations become much more apparent when the eddy forcing is moved off the equator. The geopotential height and wind anomalies in the linear solution with eddy forcing centered at 10°N, which are shown in Figure 12a, are considerably stronger north of the equator, and somewhat weaker south of the equator, than the corresponding features in the nonlinear case with hemispherically-asymmetric forcing (Figure 5b). The eddy vorticity field in the linear experiment (Figure 12b) shows an intense anticyclone centered just north of the eddy mass source, straddled by cyclonic vorticity anomalies to the north and over the equator,

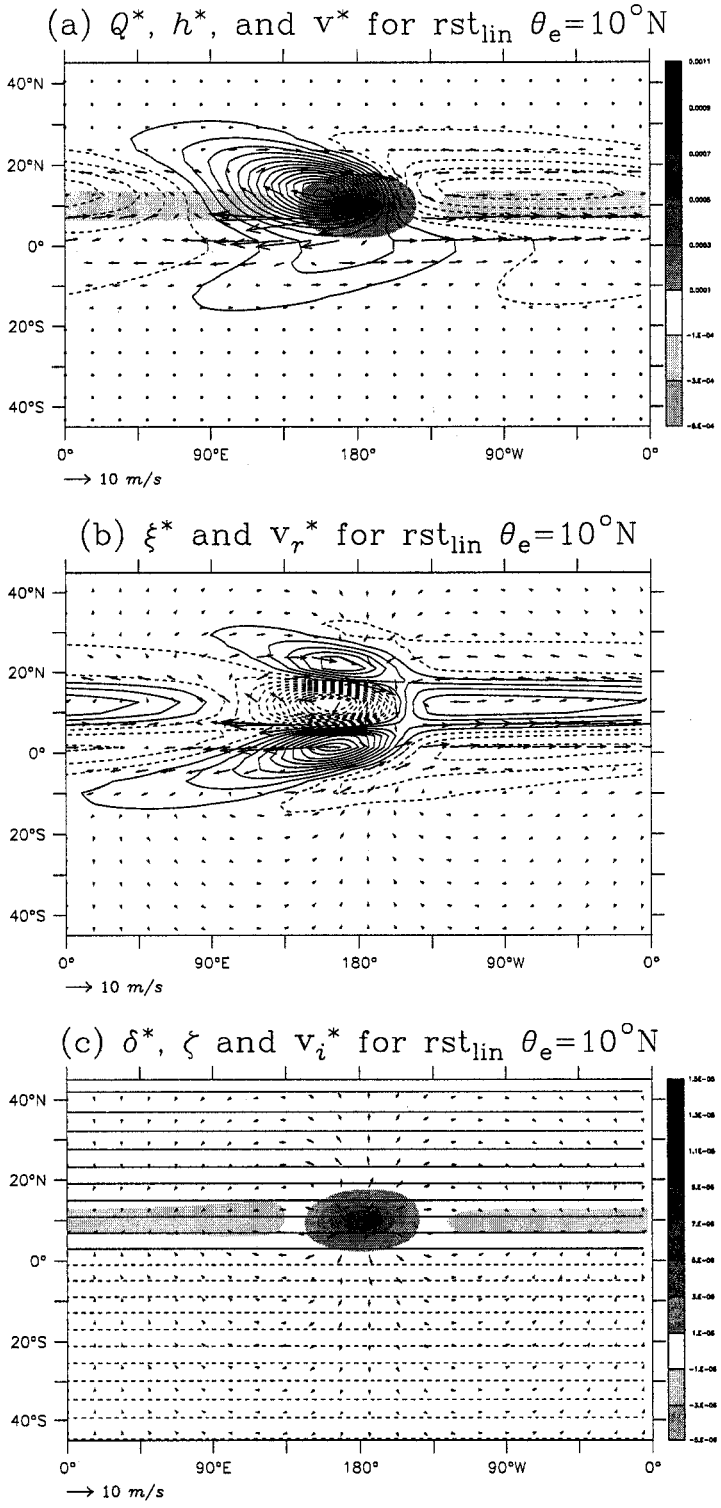

Figure 12. The (a) mass source (shading), eddy height field (contours every 5 m), and eddy winds (vectors); (b) eddy vorticity (contours every 5×10^{-6} s^{-1}) and rotational winds (vectors); and (c) eddy divergence (shading), total vorticity (contours every 1×10^{-5} s^{-1}), and eddy divergent winds (vectors) in the linear θ_e = 10°N resting basic state experiment.

which is considerably different from the slight northward shift in the eddy circulation structures noted in the nonlinear case (Figure 7a). The vorticity balance in the linear solution with off-equatorial forcing, shown in Figure 13, indicates that the stronger vorticity anomalies in the linear solution, relative to the nonlinear case, may again be attributed to the lack of finite-amplitude anticyclonic response in the region with strong eddy divergence (i.e. Figure 12c). The absence of a "zero vorticity pool" also leads to strong vorticity advection over the equator immediately south of the mass source by the eddy divergent flow (Figure 13b), rather than in the opposite hemisphere as in the nonlinear case (Figure 9b). This difference accounts for the strong positive vorticity feature at the equator in Figure 12b.

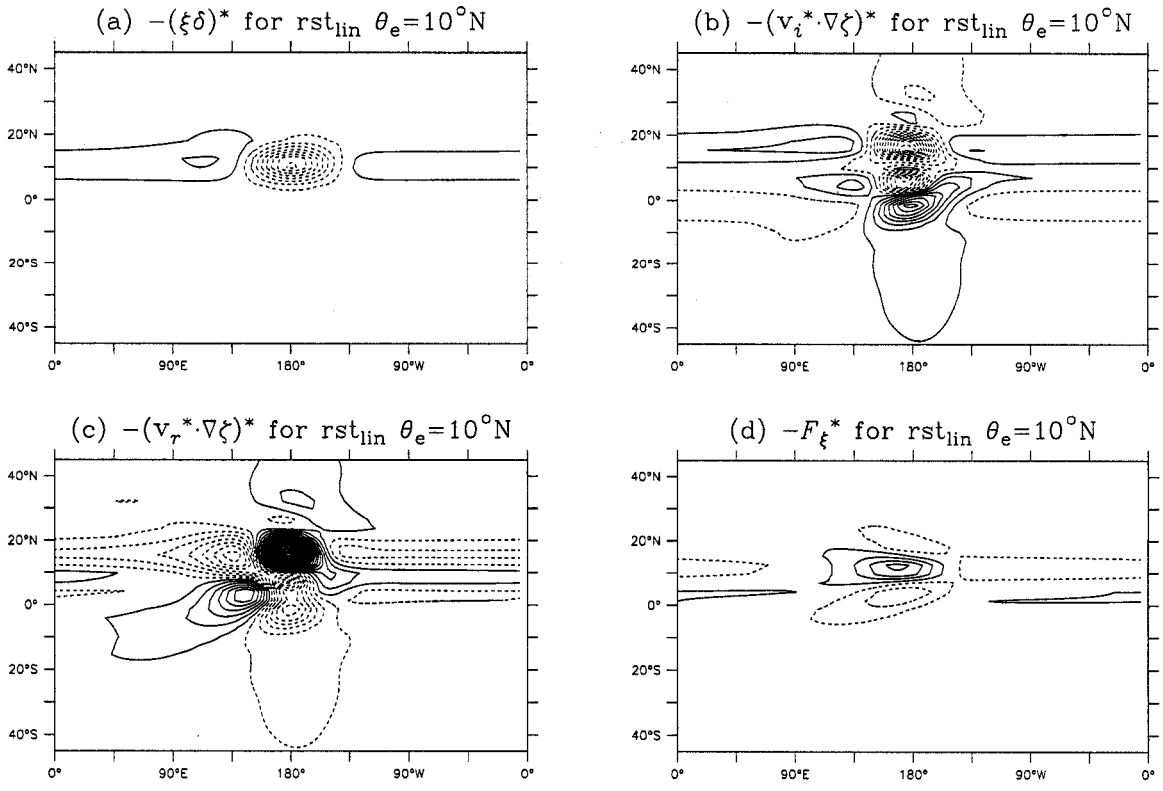

Figure 13. Vorticity balance components (2.12) for the linear θ_e = 10°N resting basic state experiment, contours every 3×10^{-11} s^{-2}.

Advection by the rotational flow (Figure 13c) balances most of the forcing associated with the eddy divergence and divergent winds in the hemispherically-asymmetric linear solution, just as in the nonlinear solution, although the damping (Figure 13d) associated with the large vorticity anomalies in the linear case is also important, especially near the equator. As in the linear solution with hemispherically-symmetric forcing, the strong rotational flow induces anticyclonic vorticity tendencies on the western edge of the forcing region. However, in this case this anticyclonic forcing is balanced by an isolated convergence anomaly to the west of the mass source; this feature is too weak to be seen in the eddy divergence field (Figure 12c), but is evident in Figure 13a, along with a smaller increase in cyclonic vorticity advection by the eddy divergent winds in Figure 13b. A re-examination of the eddy vorticity balance in the nonlinear integration (Figure 9) indicates that analogous, but smaller convergence and divergent wind anomalies are present in the finite-amplitude case. This balancing mechanism is only effective when the eddy forcing is located off the equator, and is stronger in the linear case, because the stretching term requires nonzero total vorticity to generate eddy vorticity anomalies. It will be shown in the next chapter that isolated eddy divergence and convergence anomalies are also more readily induced by poleward rotational flow in Earth-like basic states, which have larger meridional vorticity gradients.

The significant role played by frictional drag in Figure 13d suggests that the neglected nonlinearity in the linear experiments might be crudely approximated by increasing the damping strength. As noted in Chapter 1, this is a strategy commonly employed in linear stationary wave models, usually by imposing stronger frictional drag. Figures 14 and 15 show the responses obtained when the linear forcing experiments are repeated with the strength of frictional drag (k_f) doubled. Although the amplitude of the response in Figure 14 is much closer to the amplitude of the nonlinear solution in Figure

5, the structural differences between the linear and nonlinear responses have actually become somewhat larger. Stronger frictional drag seems to be even less effective at replicating the effects of nonlinearity in the hemispherically-asymmetric solution (compare Figure 15 with Figures 12 and 7).

Linear experiments performed with stronger thermal damping and/or a momentum source corresponding to the mass input to the system (2.10) also fail to make the linear response resemble the nonlinear response, especially when the eddy forcing is

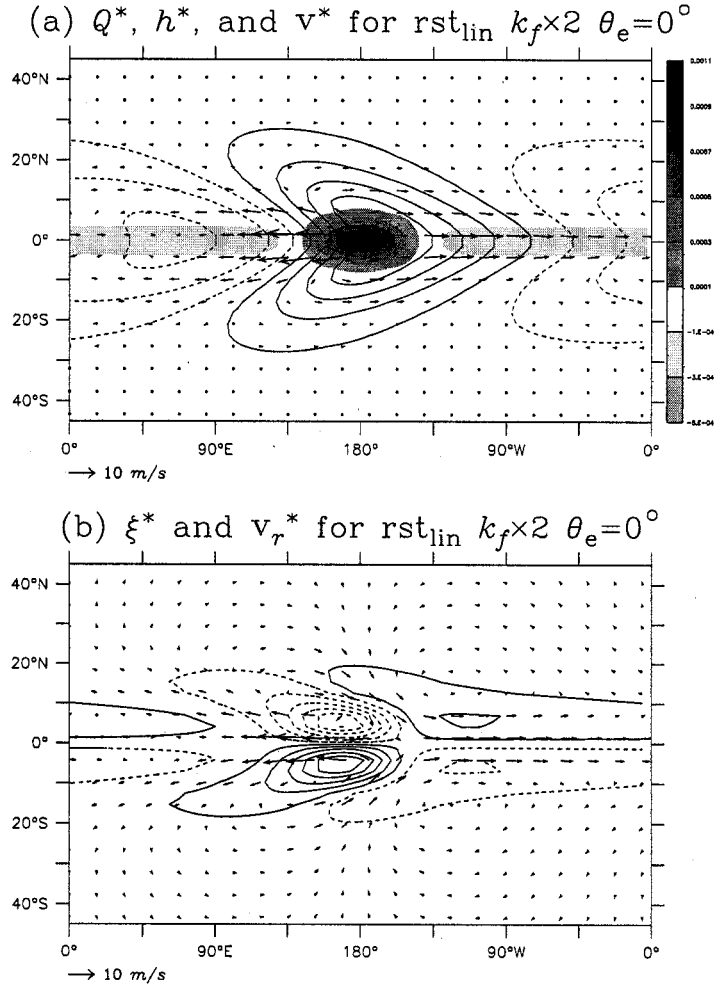

Figure 14. The equilibrium (a) mass source (shading), eddy height field (contours every 5 m), and eddy winds (vectors); and (b) eddy vorticity (contours every 5×10^{-6} s^{-1}) and rotational winds (vectors) in the linear $\theta_e = 0°$ resting basic state experiment with $k_f = (5\,days)^{-1}$.

located at 10°N. Including the forcing term (2.10) suggested by Gent (1993) has little effect on any of the resting basic state solutions because the strongest zonal wind anomalies are located outside the mass source region, and the absence of a basic state means that the total winds are weak and the total amount of fluid added to the system is not very large. Stronger damping can also be imposed by increasing the horizontal scale and/and strength of the numerical diffusion, either with or without increasing the frictional drag, but stronger diffusion also cannot

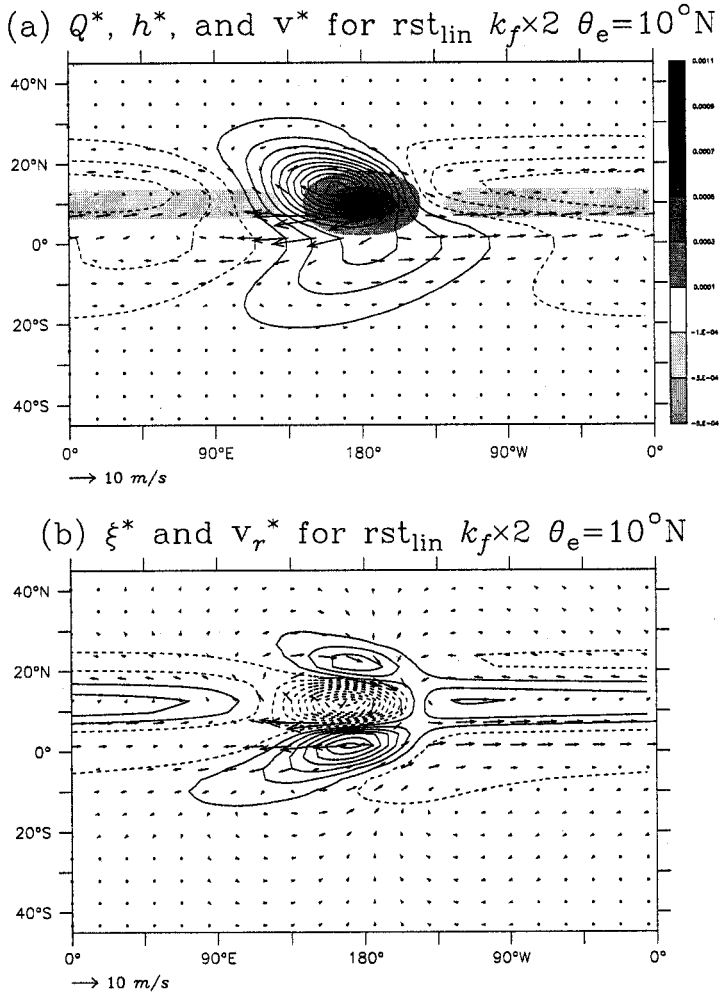

Figure 15. The equilibrium (a) mass source (shading), eddy height field (contours every 5 m), and eddy winds (vectors); and (b) eddy vorticity (contours every 5×10^{-6} s^{-1}) and rotational winds (vectors) in the linear θ_e = 10°N resting basic state experiment with $k_f = (5\,days)^{-1}$.

replicate the changes in the vorticity balance induced by the nonlinear terms in the eddy vorticity equation (2.13), especially the nonlinear stretching term associated with the finite vorticity anomalies in the mass source region. Hence, enhanced damping does not seem to be an effective replacement for nonlinearity, especially when hemispherically-asymmetric forcing is present.

4.4 Chapter summary

- The shallow water model is forced with a mass source-sink distribution centered either at the equator or 10°N in a resting basic state.
- The response of the model to eddy forcing at the equator is similar to that observed in previous studies, with anticyclones straddling the equator to the west of the mass source and easterly (westerly) eddy zonal winds to the west (east).
- The finite-amplitude vorticity anomalies in nonlinear runs reduce the direct generation of vorticity by eddy divergence, especially when the eddy forcing is centered at the equator, and also modifies the advection of vorticity by the eddy divergent winds.
- Moving the eddy forcing off the equator amplifies the response in the forced hemisphere and leads to tilted eddy wind vectors at the equator; however, the amplitude of the response in the opposite hemisphere only decreases slightly because the advection of vorticity by the eddy divergent winds forces a rotational response across a wide range of latitudes
- The linear response is similar to, but slightly stronger than, the nonlinear response when the eddy forcing is centered at the equator. When the eddy forcing is centered off the equator, the linear response is much stronger and significantly distorted, and increasing the frictional damping strength does not improve the correspondence.

5. Tropical stationary waves in Earth-like basic states

Although the response to eddy forcing in a resting basic state has several features in common with the observed stationary waves in the tropical upper troposphere, large discrepancies are also apparent. For instance, the strongest eddy height and circulation anomalies in the tropical upper troposphere tend to be located almost directly poleward of the strongest diabatic forcing (see, e.g., Hendon 1986). The surprising amount of hemispheric symmetry in the observed tropical eddy circulations over the course of the seasonal cycle (Dima et al 2005) also cannot be replicated using a resting basic state. In this chapter, the influence of realistic zonal-mean winds on the structure and amplitude of stationary waves in the tropical upper troposphere is investigated by imposing the same eddy forcing used in Chapter 4 in the zonally-symmetric basic states described in Chapter 3. The results of these experiments indicate that the westerly zonal-mean zonal flow in the subtropical band is responsible for shifting the eddy geopotential height and vorticity anomalies in each hemisphere eastward, so that they are collocated in longitude with the maximum eddy forcing, and that the hemispheric symmetry of the tropical stationary waves may be attributed to the tendency for the maximum eddy forcing and zonal-mean divergence to remain collocated in latitude over the course of the seasonal cycle.

The chapter is organized as follows. Section 4.1 describes the response of the shallow water model to tropical eddy forcing, including forcing centered off the equator, in the equinoctial basic state. In Section 4.2, the solstitial basic state is used to evaluate the influence of hemispherically-asymmetric zonal-mean winds on the steady eddy response. The influence of the Hadley circulation on tropical stationary waves is isolated in Section 4.3 by comparing the results in Sections 4.1 and 4.2 with results obtained using the corresponding no-Hadley basic states. The influence of nonlinearity and damping is discussed in Section 4.4. Section 4.5 lists the principal findings of the chapter.

5.1 Equinoctial response to eddy forcing

Figure 16 shows the equilibrium response of the shallow water model integrated with eddy forcing (4.1) centered on the equator in the equinoctial basic state. The eddy height field (Figure 16a) is dominated by large positive anomalies centered almost directly north and south of the mass source (note that the contour spacing used for height anomalies is twice as large in this chapter), and there is also a corresponding increase in the subtropical eddy winds. The easterly eddy zonal winds along the equator are also slightly stronger, and extend farther into each hemisphere, than their counterparts in the resting basic state, while the westerly wind anomalies are slightly weaker. In addition, the dividing line between easterly and westerly flow and the pattern of height anomalies along the equator have both shifted to the east, so that easterly flow now dominates the mass source region. That all of these features bring the eddy circulation much closer to the observed quasi-stationary wave pattern in the tropical upper troposphere on Earth during spring and autumn (e.g. Dima et al 2005) suggests that the inclusion of a realistic basic state is crucial for accurately simulating the climatological steady eddy circulation in the tropical band.

Most of the differences between Figure 16a and Figure 5a can be attributed to a expansion and eastward shift of the eddy vorticity anomalies and eddy rotational winds associated with the equatorial Rossby wave response (Figure 16b). However, the eddy divergence and divergent winds in the equinoctial θ_e=0° experiment, which are shown in Figure 16c, also exhibit some small changes, including isolated areas of convergence poleward and westward of the subtropical vorticity maxima (there are also isolated divergence anomalies poleward and eastward of the mass source region that are not strong enough to show up in this figure, but can be inferred from Figure 17a below). A close inspection of the eddy divergent winds in Figure 16c reveals that the isolated divergence anomalies induce a slight eastward bias in the eddy divergent wind field in

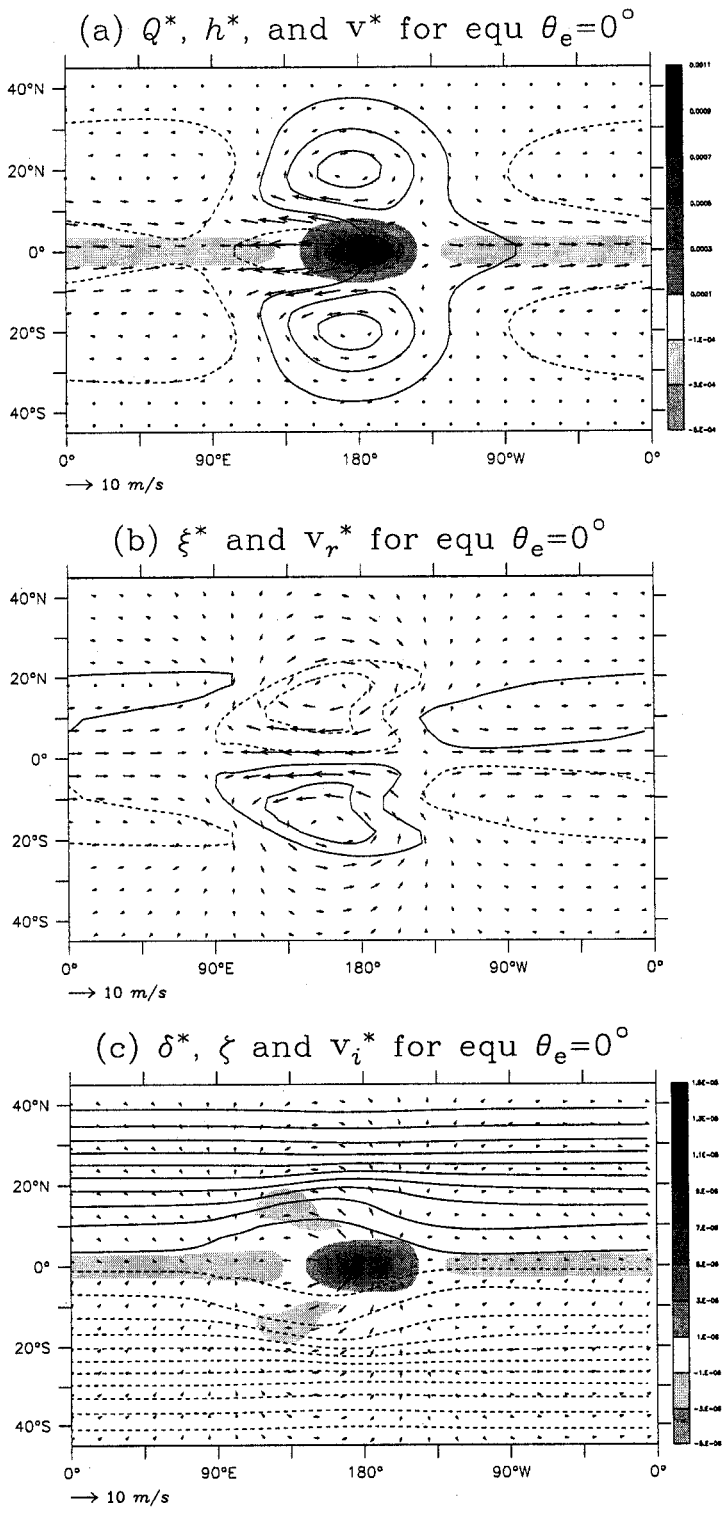

Figure 16. The $\theta_e = 0°$ equinoctial basic state experiment (a) mass source (shading), eddy height field (contours every 10 m), and eddy winds (vectors); (b) eddy vorticity (contours every 5×10^{-6} s^{-1}) and rotational winds (vectors); and (c) eddy divergence (shading), total vorticity (contours every 1×10^{-5} s^{-1}), and eddy divergent winds (vectors).

the mass source region, and also reduce the meridional convergence in the mass sink region, which explains why the cyclonic vorticity anomalies are smaller in this integration. A "pool of zero absolute vorticity" is also apparent in the mass source region, as in the resting basic state, but the pool extends much farther from the equator, and the concentration of vorticity contours in the mass sink region is much less acute (compare Figure 16c with Figure 6b). It should also be noted that the shear associated with the westerly zonal-mean zonal winds increases the vorticity gradient outside of the deep tropics.

The eddy vorticity balance (2.12) in the equinoctial θ_e=0° experiment is shown in Figure 17. As in the resting basic state, the pool of zero vorticity near the equator severely limits the vortex stretching associated with eddy divergence in the mass source region (Figure 17a). The broader scale of the anticyclonic vorticity anomalies in the equinoctial experiment, along with the increase in the meridional vorticity gradient in the subtropics associated with the westerly zonal-mean zonal winds, also leads to a poleward shift and slight reduction in the vorticity advection by the eddy divergent winds north and south of the mass source (Figure 17b). However, this reduction in divergent advection is offset by the vorticity advection by the westerly zonal-mean winds (Figure 17e) and, poleward and eastward of the mass source, by vortex stretching associated with the isolated subtropical divergence anomalies noted in Figure 16c. All of these terms are also associated with cyclonic forcing anomalies to the west of the mass source region, which are discussed below, and their sum is balanced almost exclusively by the advection of vorticity by the rotational flow (Figure 17c), with damping (Figure 17d) and mean meridional advection (Figure 17f) making only small contributions.

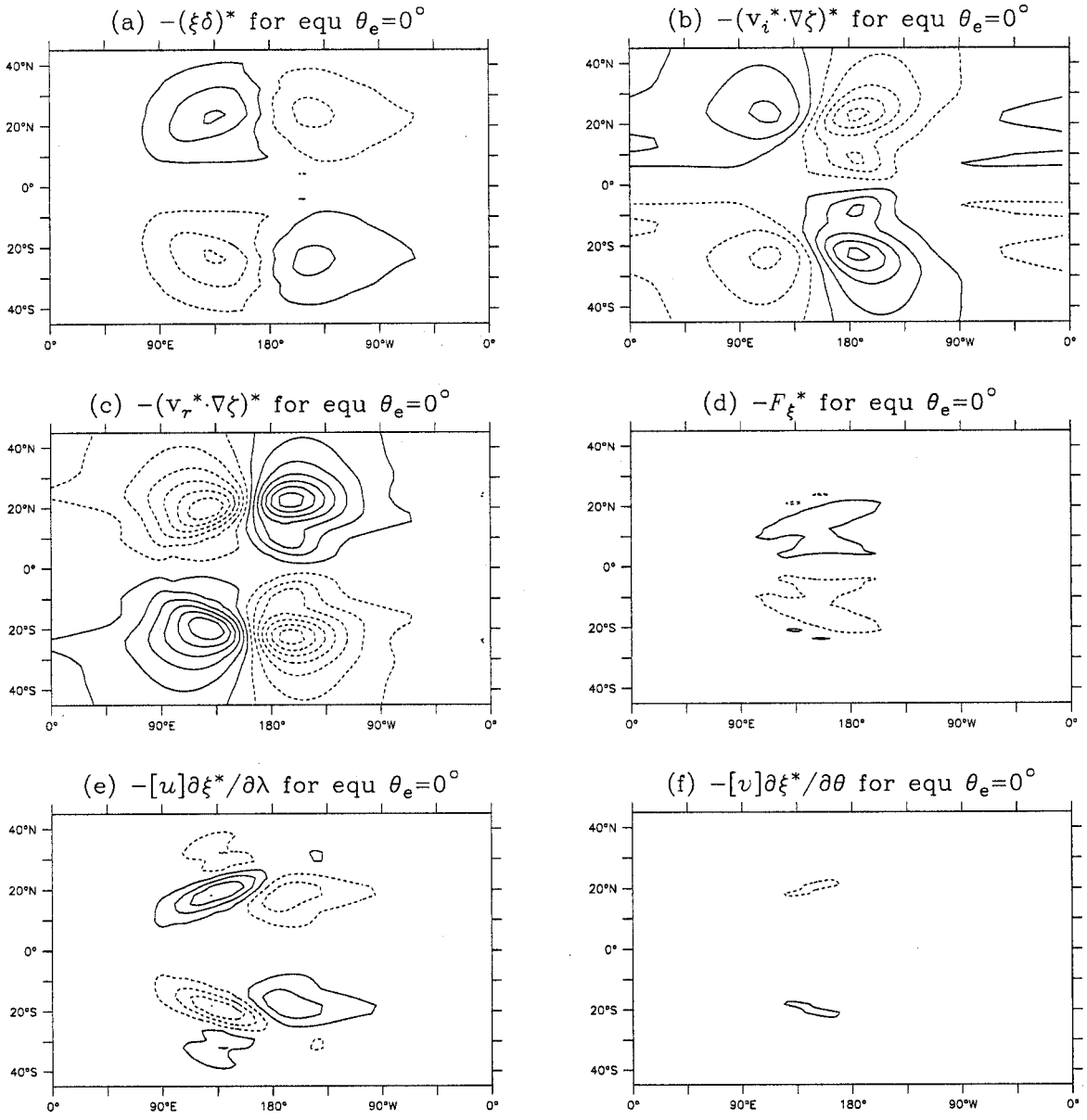

Figure 17. Vorticity balance components (2.12) for the θ_e = 0° equinoctial basic state experiment, contours every 1.5×10^{-11} s^{-2}.

As in the resting basic state, moving the eddy forcing off the equator (Figure 18) amplifies the response in the hemisphere with the forcing and leads to a tilt in the eddy wind vectors along the equator, with only a slight reduction in amplitude in the opposite hemisphere. An examination of the divergent circulation (Figure 18c) confirms that southward divergent flow between the mass source and the equator is responsible for

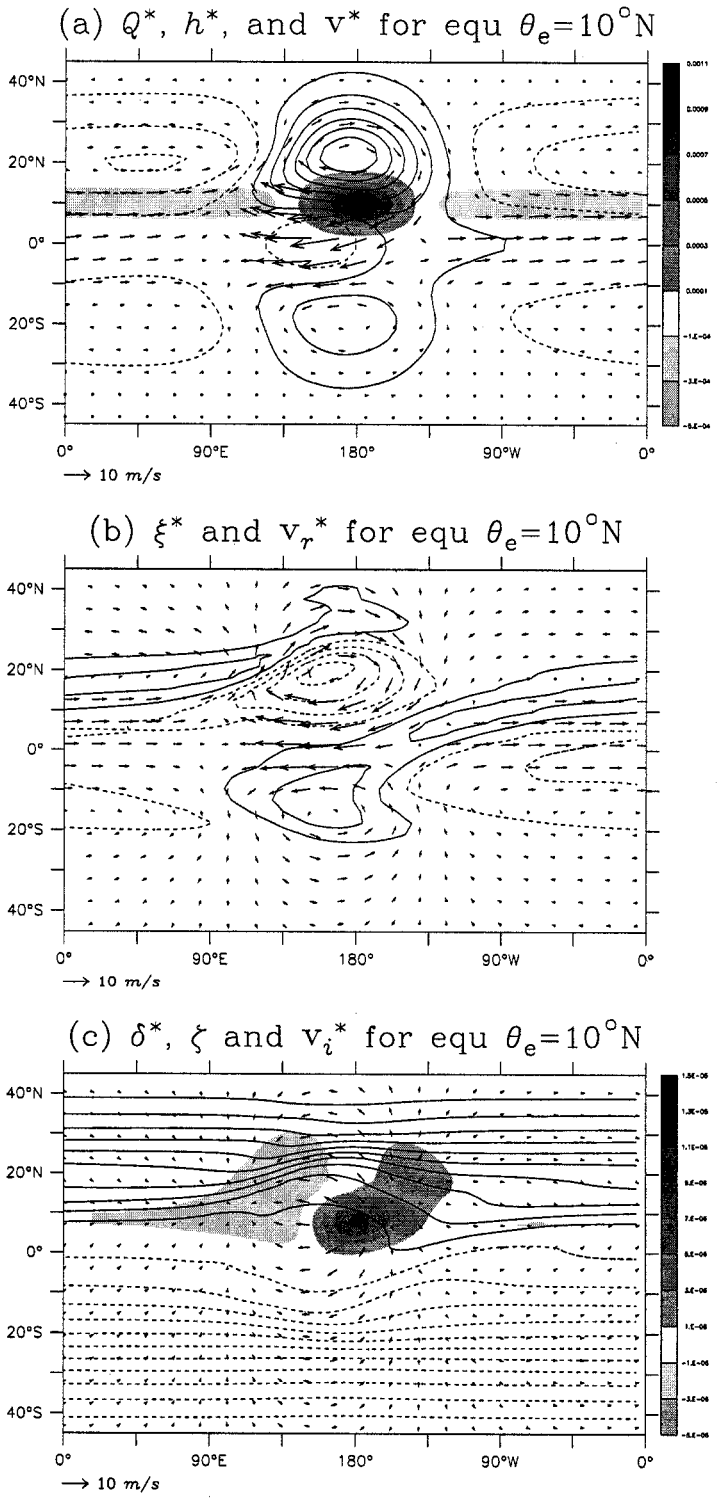

Figure 18. The θ_e = 10°N equinocital basic state experiment (a) mass source (shading), eddy height field (contours every 10 m), and eddy winds (vectors); (b) eddy vorticity (contours every 5×10^{-6} s^{-1}) and rotational winds (vectors); and (c) eddy divergence (shading), total vorticity (contours every 1×10^{-5} s^{-1}), and eddy divergent winds (vectors).

producing the tilted equatorial eddy winds, as in the corresponding resting basic state experiment (Figure 7). The vorticity balance for the equinoctial θ_e = 10°N experiment (Figure 19) likewise confirms that the increase in divergent forcing induced by moving the eddy mass source away from the equator is responsible for the increase in the Northern Hemisphere response, while the persistence of the Southern Hemisphere response can be attributed to the broad meridional scale of the eddy divergent winds. It is also clear that the westerly basic state zonal winds in the equinoctial basic state leads to differences between Figure 19 and Figure 8 that are analogous to the differences between Figure 17 and Figure 6.

The subtropical eddy divergence and convergence anomalies that appear in Figures 16c and 18c play a key role reinforcing the poleward and eastward shift in the eddy vorticity anomalies induced by the zonal-mean zonal winds. Recall that much smaller convergence anomalies were also found to the west of the mass source in the resting basic state experiments with eddy forcing centered off the equator (Figures 7c and 12c). These features arise when the rotational response is unable to configure itself so that the advection of vorticity by the rotational wind (plus the small damping term) exactly cancels the rotational forcing induced by the eddy divergence, eddy divergent winds, and the zonal-mean zonal winds (if present) while simultaneously satisfying the requirements of momentum and mass balance. For example, the convergence anomalies poleward and west of the mass source are induced by the advection of vorticity associated with the rotational flow on the western side of the anticyclonic vorticity anomalies, which has a broader horizontal scale than the associated vorticity anomalies. Note that the isolated subtropical divergence and convergence anomalies are also consistent with the influence of the westerly zonal-mean winds acting on the eddy height field—the westerly mean flow pushes the subtropical height maxima towards the east, and divergence

(convergence) is required to the east (west) of the height maxima in order to maintain an equilibrium state.

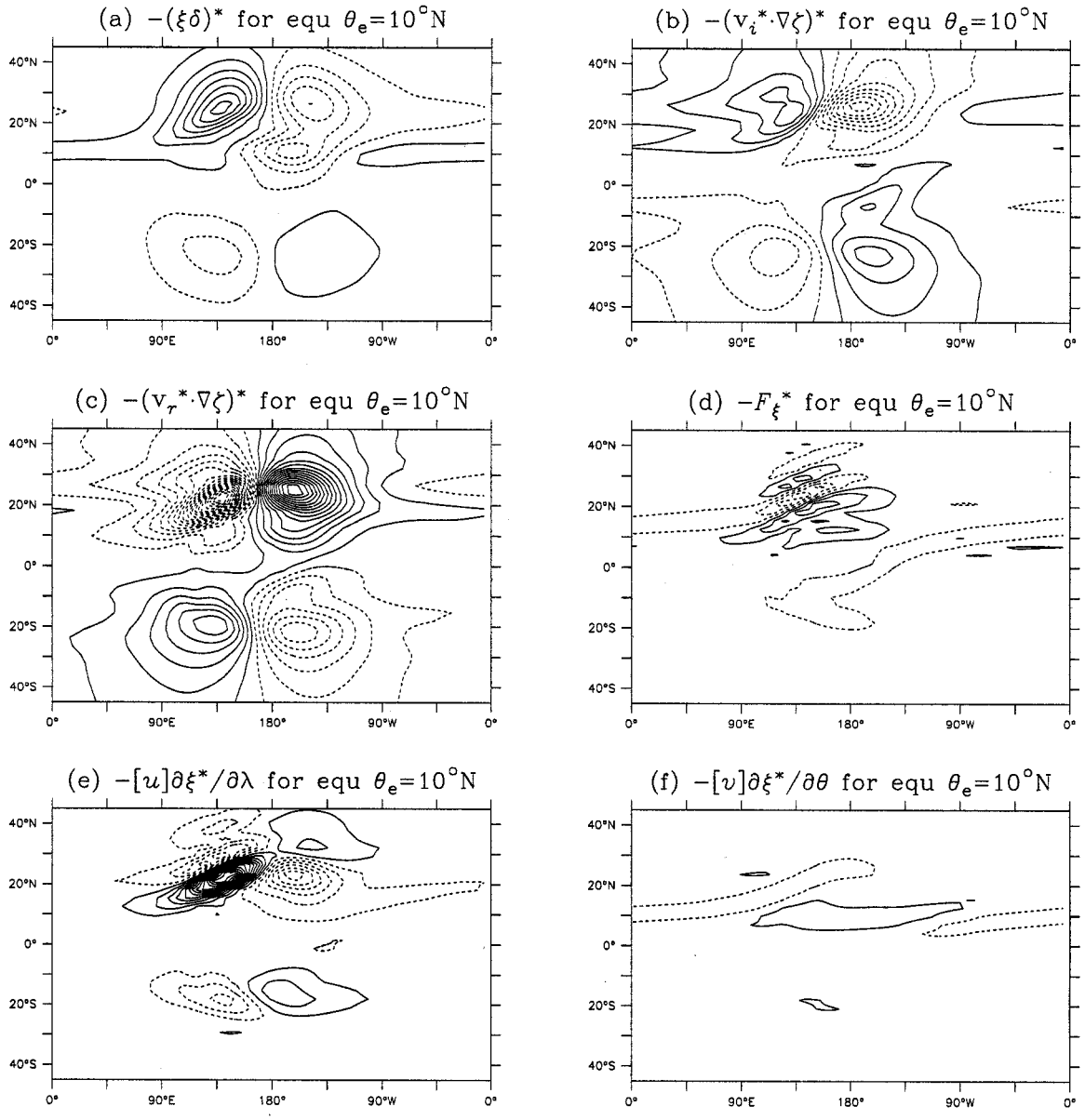

Figure 19. Vorticity balance components (2.12) for the θ_e = 10°N equinoctial basic state experiment, contours every 1.5×10^{-11} s^{-2}.

5.2 Solstitial response to eddy forcing

Figure 20 shows the response of the shallow water model to eddy forcing on the equator in the solstitial basic state. The wind and height variations in the Northern (summer) hemisphere in Figure 20a are much weaker than the corresponding features in the equinoctial basic state (Figure 16a), while the eddy response in the Southern (winter) hemisphere is enhanced. Also note that the strongest eddy winds and the dividing line between clockwise and counter-clockwise rotation (Figure 16b) are both centered slightly south of the equator, while the eddy divergence and divergent winds (Figure 16c) remain collocated with the mass forcing at the equator (although the induced subtropical divergence anomalies are stronger in the Southern Hemisphere). As in the equinoctial run with θ_e=10°N, the latitudinal separation between the rotational and divergent components of the circulation gives rise to a northeast-southwest tilt in the eddy wind vectors near the equator, although in this case the strongest wind anomalies and vector tilts are now found slightly south of the equator.

The vorticity balance in the solstitial θ_e=0° run, which is shown in Figure 21, indicates that most of the differences between the two hemispheres in Figure 20 can be attributed to hemispheric asymmetry of the basic state zonal wind field in the solstitial basic state (Figure 311c). The vortex deformation (Figure 21a), divergent advection (Figure 21b), and rotational advection (Figure 21c) are all enhanced by the stronger mean vorticity gradient south of the equator, while the stronger mean flow increases the strength of the zonal vorticity advection (Figure 21e) and also the height advection implied by the large subtropical eddy divergence anomalies. The weaker zonal-mean zonal winds north of the equator give rise to changes of the opposite sign, although the mean zonal flow apparently remains strong enough to shift the eddy height and vorticity anomalies toward the east, relative to their positions in the resting basic state.

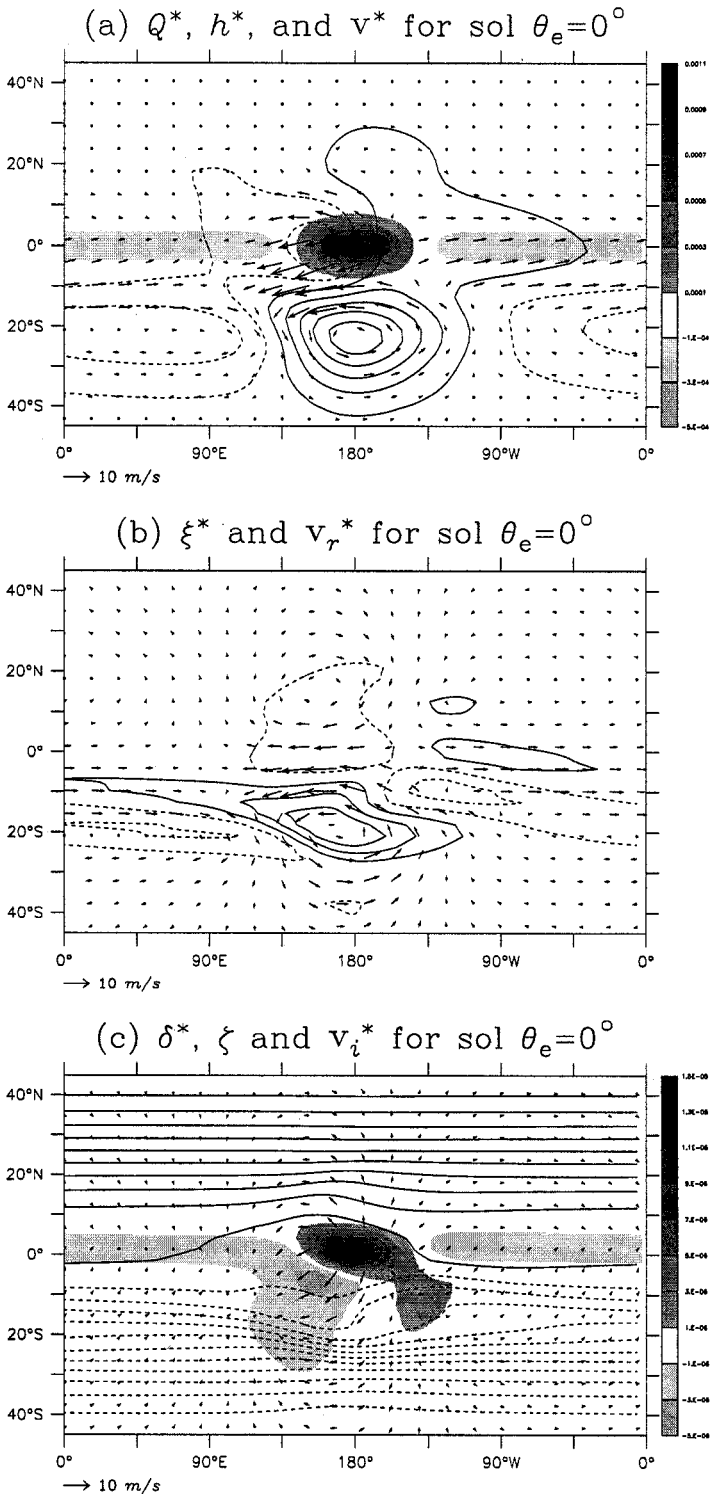

Figure 20. The θ_e = 0°solstitial basic state experiment (a) mass source (shading), eddy height field (contours every 10 m), and eddy winds (vectors); (b) eddy vorticity (contours every 5×10^{-6} s^{-1}) and rotational winds (vectors); and (c) eddy divergence (shading), total vorticity (contours every 1×10^{-5} s^{-1}), and eddy divergent winds (vectors).

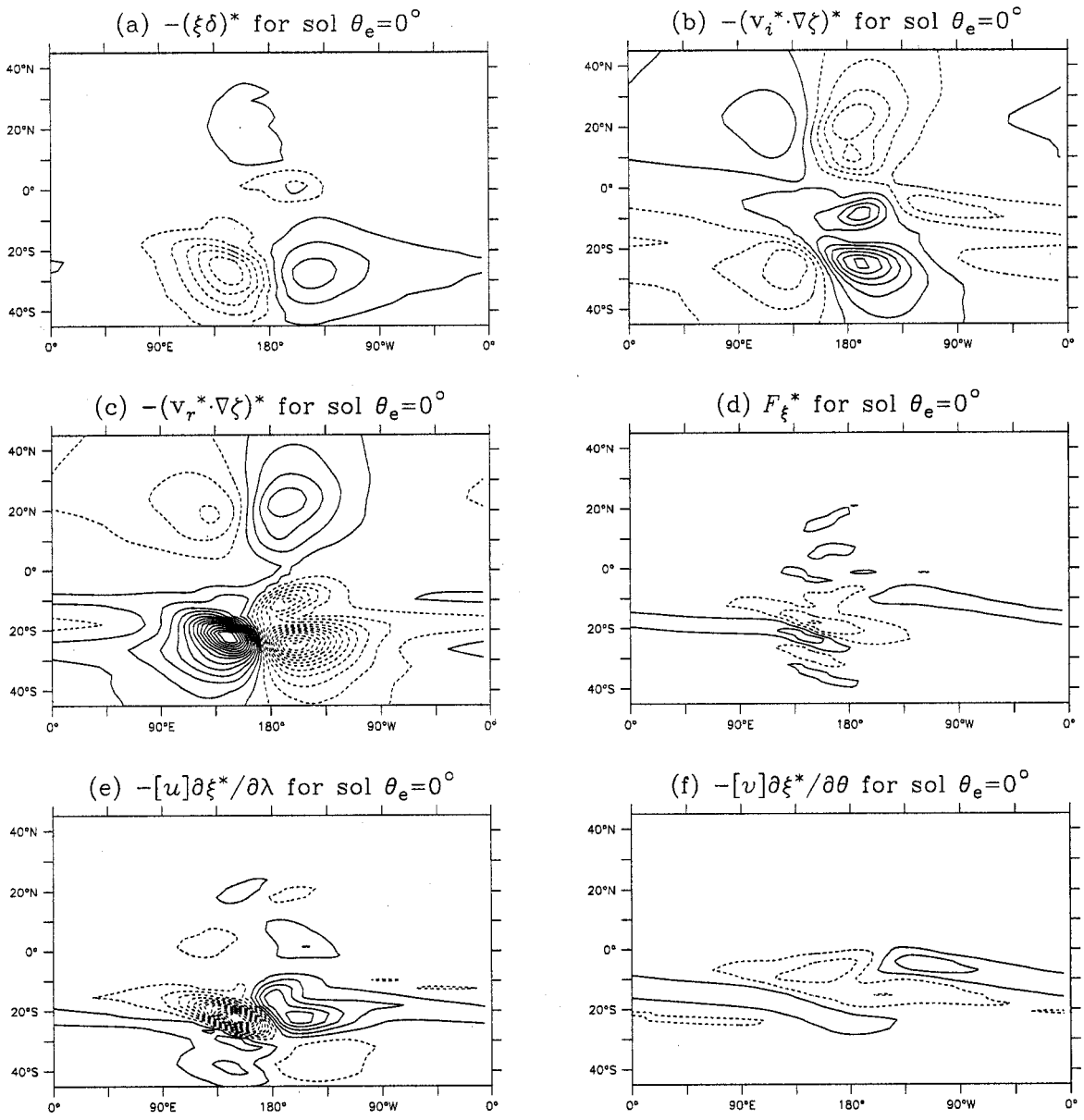

Figure 21. Vorticity balance components (2.12) for the $\theta_e = 0°$ solstitial basic state experiment, contours every 1.5×10^{-11} s^{-2}.

The strong mean meridional winds in the solstitial basic state also give rise to substantial mean meridional vorticity advection (Figure 21f), which appears to be responsible for the southward shift in the dividing line between clockwise and counterclockwise rotation. However, vortex stretching (Figure 21a) reinforces the counter-clockwise motion once the zero vorticity line shifts south of the equator, a feature

not seen in any of the other model integrations. It should also be noted that the zonal-mean divergence associated with the cross-equatorial mean meridional flow tends to reduce the amplitude of the eddy vorticity anomalies in the northern hemisphere, while zonal-mean convergence south of the equator tends to enhance the vorticity anomalies in the Southern Hemisphere, although this effect is responsible for only a small fraction of the hemispheric differences in Figure 21a.

As in the equinoctial and resting basic states, moving the mass forcing north of the equator in the solstitial basic state (Figure 22) enhances the eddy response in the Northern Hemisphere dramatically, with only a slight reduction in the eddy response in the Southern Hemisphere. However, since the Southern Hemisphere response is already quite strong in the solstitial basic state, the eddy height and vorticity anomalies in the solstitial θ_e=10°N experiment exhibit pronounced hemispheric symmetry. The strong response in both hemispheres also leads to stronger eddy zonal winds and height variations along the equator than in any other experiment, and the latitudinal separation between the rotational (Figure 22b) and divergent (Figure 22c) eddy winds once again explains the pronounced northeast-southwest tilt in the equatorial eddy wind vectors. The eddy vorticity balance for the solstitial θ_e=10°N experiment (Figure 23) confirms that the enhanced response north of the equator, relative to the θ_e=0° solution, may once again be attributed to the relocation of the mass source into a region with a stronger vorticity gradient, while the strong response in the Southern Hemisphere can be attributed to both the broad scale of the divergent eddy winds and the strong zonal-mean zonal winds south of the equator in the solstitial basic state.

The eddy height pattern in Figure 22a bears a strong resemblance to the observed tropical stationary wave pattern over the Pacific Ocean during Northern Summer (see, e.g. Dima et al 2005). This result suggests that the surprising hemispheric symmetry of

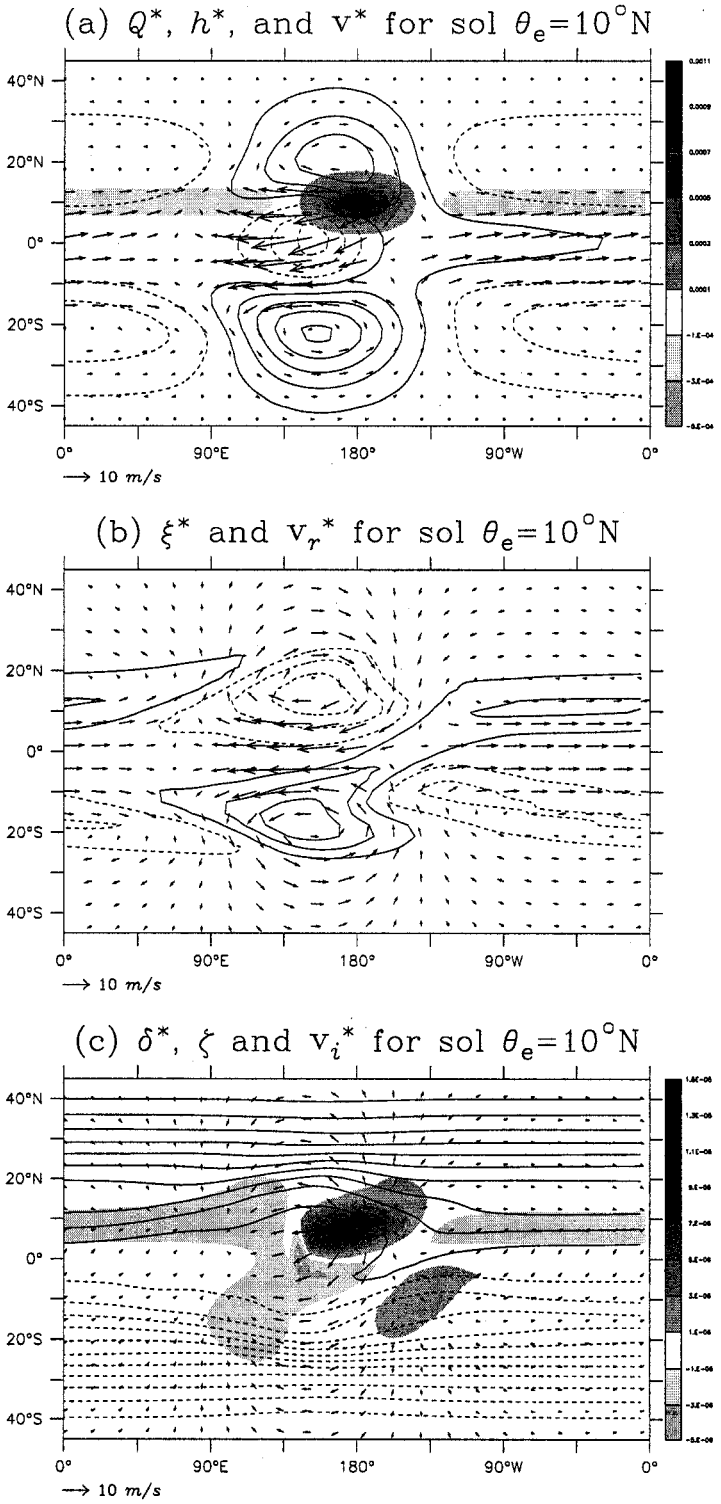

Figure 22. The θ_e = 10°N solstitial basic state experiment (a) mass source (shading), eddy height field (contours every 10 *m*), and eddy winds (vectors); (b) eddy vorticity (contours every 5×10^{-6} s^{-1}) and rotational winds (vectors); and (c) eddy divergence (shading), total vorticity (contours every 1×10^{-5} s^{-1}), and eddy divergent winds (vectors).

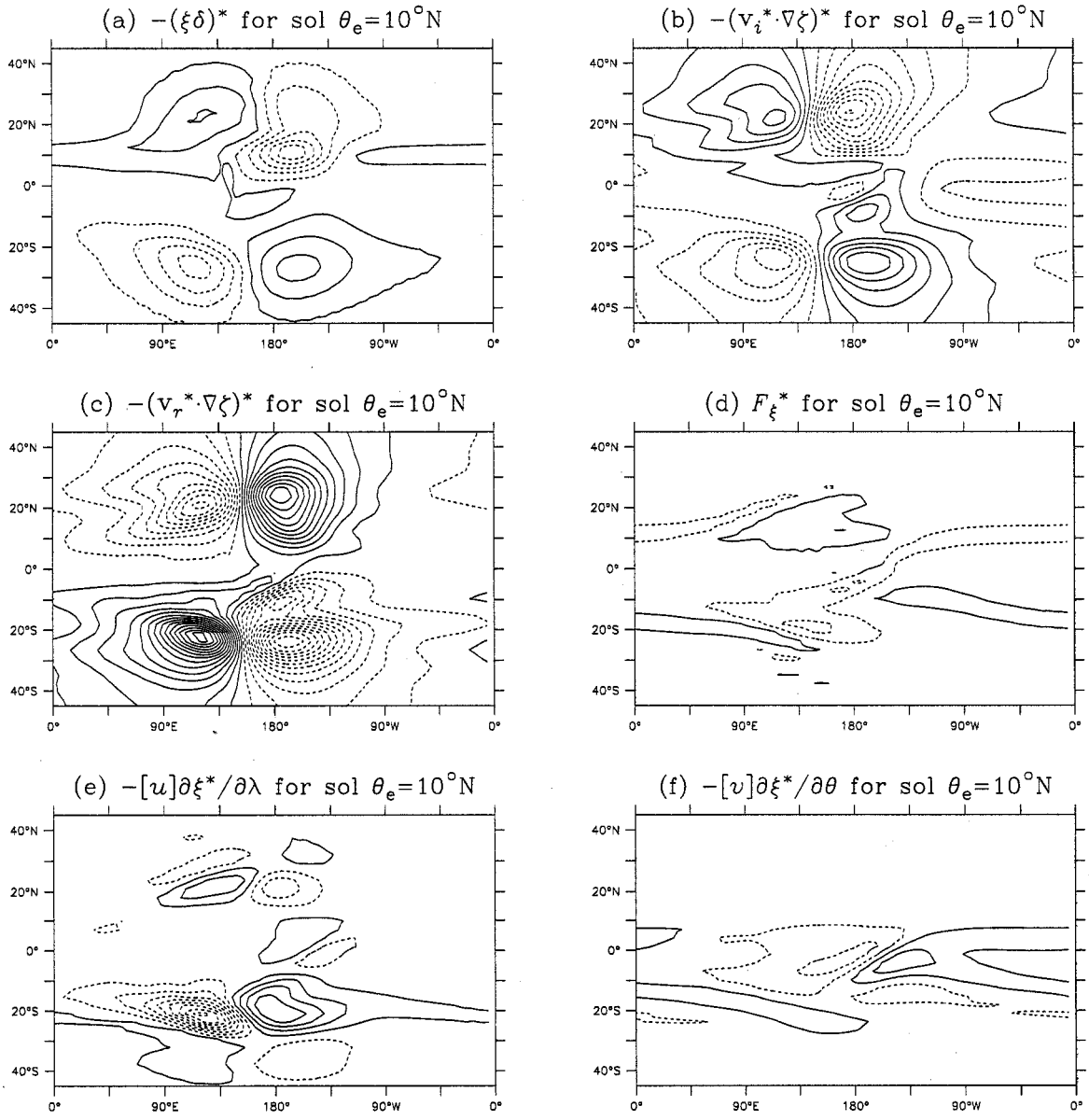

Figure 23. Vorticity balance components (2.12) for the θ_e = 10°N solstitial basic state experiment, contours every 1.5×10^{-11} s^{-2}.

the stationary waves in the tropical upper troposphere during solstitial seasons may be explained by the fact that the strongest eddy forcing tends to reside in the summer hemisphere. However, it should be noted that the solution in Figure 22 is very close to being numerically unstable, because the Froude number approaches unity in the vicinity of the equatorial trough, where the zonal winds are also very strong. The strong

convergence anomaly southwest of the mass source in Figure 22c and the ripples on the contours in Figures 23a&c are both manifestations of this near instability.

5.3 Influence of the Hadley circulation

Watterson and Schneider (1988) determined that cross-equatorial mean meridional winds enhance the propagation of wave activity in the direction of the flow, and reduce wave propagation in the opposite direction. It has also been noted that both advection by the mean meridional flow and the zonal-mean divergence associated with the mean meridional flow play a small but significant role in the eddy vorticity balance, especially in the solstitial basic state. To isolate the influence of the mean meridional winds on the equilibrium response to eddy forcing in the shallow water model, the θ_e=0° and θ_e=10°N eddy forcing experiments were repeated using the no-Hadley basic states described in Chapter 3.

Figure 24 shows the equilibrium eddy height and wind anomalies from the equinoctial no-Hadley experiments with on- and off-equatorial forcing. The subtropical eddy height and circulation anomalies in these two experiments are virtually identical to the corresponding equinoctial solutions in Figures 16a and 18a, which (along with the negligible vorticity advection by the mean meridional flow in Figure 17 and 19) indicates that the Hadley circulation in the equinoctial basic state is simply too weak to have a significant influence on the response to tropical eddy forcing. However, a close inspection of Figure 24 reveals that the subtropical eddy height variations are slightly weaker and the equatorial trough is slightly deeper when the mean meridional flow is removed, which suggests that equinoctial Hadley circulation does slightly enhance the propagation of wave activity away from the equator.

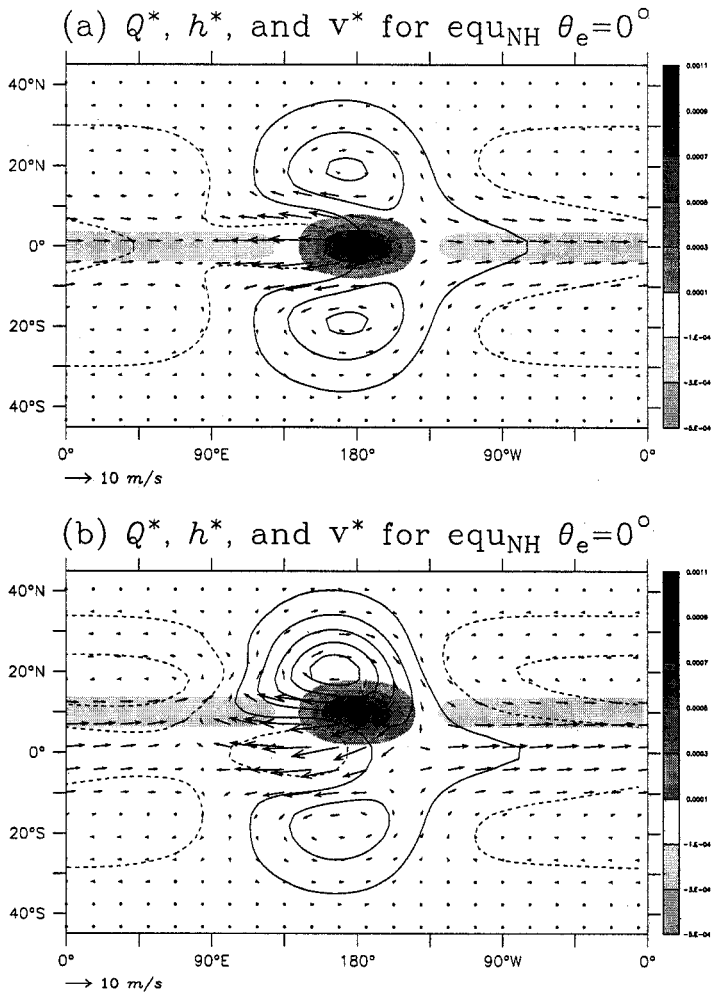

Figure 24. The mass source (shading), eddy height field (contours every 10 *m*), and eddy winds (vectors) in the equinoctial no-Hadley (a) θ_e = 0° and (b) θ_e = 10°N experiments.

The solstitial no-Hadley θ_e=0° experiment, which is shown Figure 25, exhibits a slightly weaker response in the winter hemisphere than the corresponding full solstitial integration (Figure 20), along with a slightly stronger response along the equator. A close inspection of Figure 25b also reveals that the Southern Hemisphere anticyclone and corresponding rotational flow are displaced slightly eastward of their position in Figure 20b, which is consistent with the slightly weaker subtropical eddy divergence and convergence anomalies in Figure 25c, since these anomalies are induced by the poleward rotational flow along the western margin of the anticyclone. The removal of the Hadley

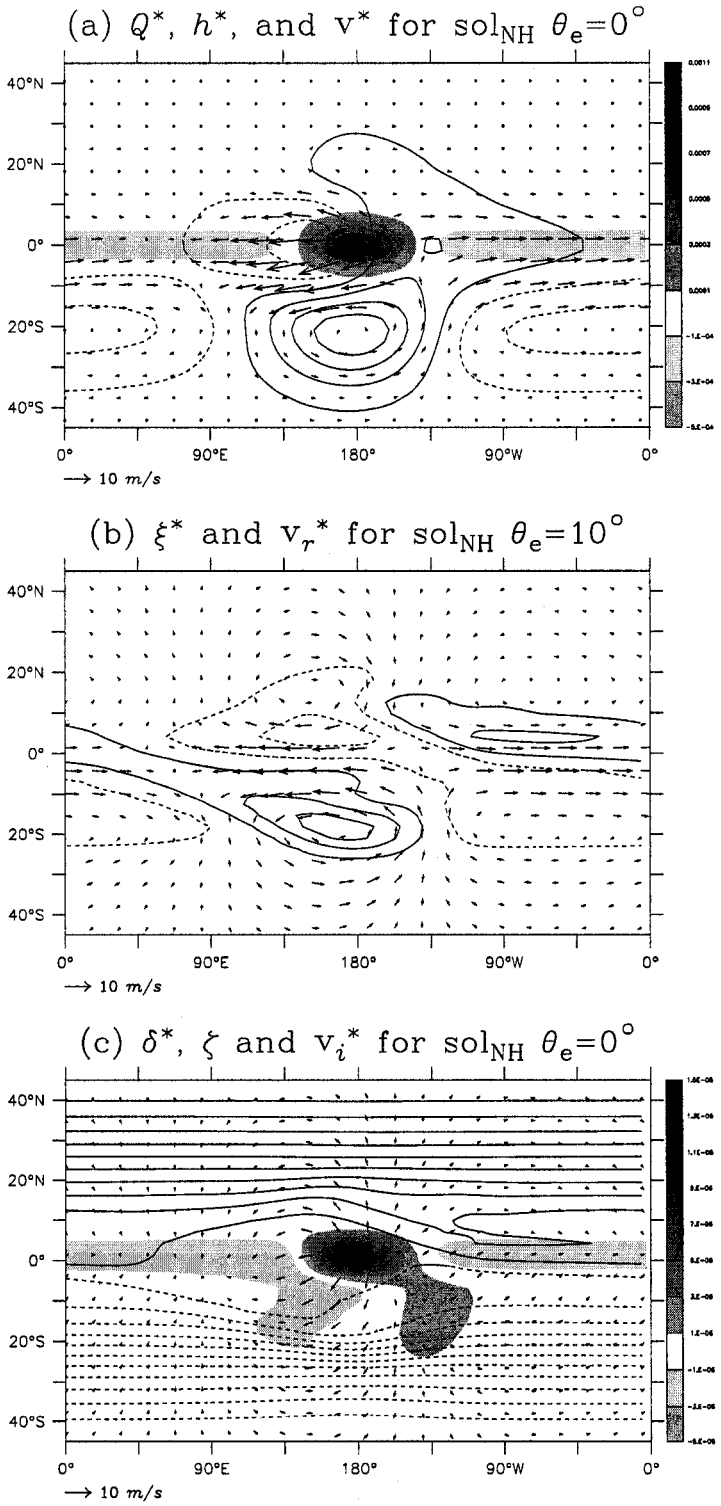

Figure 25. The θ_e = 0°solstitial no-Hadley experiment (a) mass source (shading), eddy height field (contours every 10 *m*), and eddy winds (vectors); (b) eddy vorticity (contours every 5×10^{-6} s^{-1}) and rotational winds (vectors); and (c) eddy divergence (shading), total vorticity (contours every 1×10^{-5} s^{-1}), and eddy divergent winds (vectors).

circulation also appears to reduce the northeast-southwest tilt in the eddy wind vectors along the equator. These results suggest that the Hadley circulation does in fact promote the propagation of stationary waves in the direction of the mean meridional flow in the full solstitial basic state. Apparently, however, this effect is relatively weak when the eddy forcing is at the equator, presumably because the eddy divergence is located fairly close to the sharp vorticity gradient in the winter hemisphere, and the wave energy does not need to traverse a broad region of easterly mean winds.

When the eddy forcing is moved north of the equator in the solstitial no-Hadley basic state (Figure 26), on the other hand, the stationary wave response in the winter hemisphere is dramatically reduced relative to the corresponding full basic state solution (Figure 22a). The vorticity anomalies and induced divergence anomalies south of the equator are both weaker in the absence of strong cross-equatorial flow, and the Southern Hemisphere anticyclone is also shifted slightly toward the west. The eddy vorticity balance (Figure 27) does not offer much insight into the origin of weaker Southern Hemisphere response, especially since the advection of vorticity by the mean meridional flow provides a damping effect south of the equator in the full solstitial integration (Figure 23f), so the removal of this term cannot explain the weaker response in Figure 26 (and the zonal-mean convergence south of the equator acting on the eddy vorticity anomalies only represents a very small component of the vortex stretching in Figure 23a).

As in the solstitial no-Hadley experiment with eddy forcing centered at the equator, the eddy winds along the equator in Figure 26 exhibit considerably less tilt than those in the corresponding full basic state integration. However, in the present case the eddy zonal winds (and, by the Bernoulli effect, the trough under the eddy easterly winds) are also considerably reduced, which indicates that the removal of the Hadley circulation leads to a much smaller cross-equatorial eddy momentum flux. As discussed in more

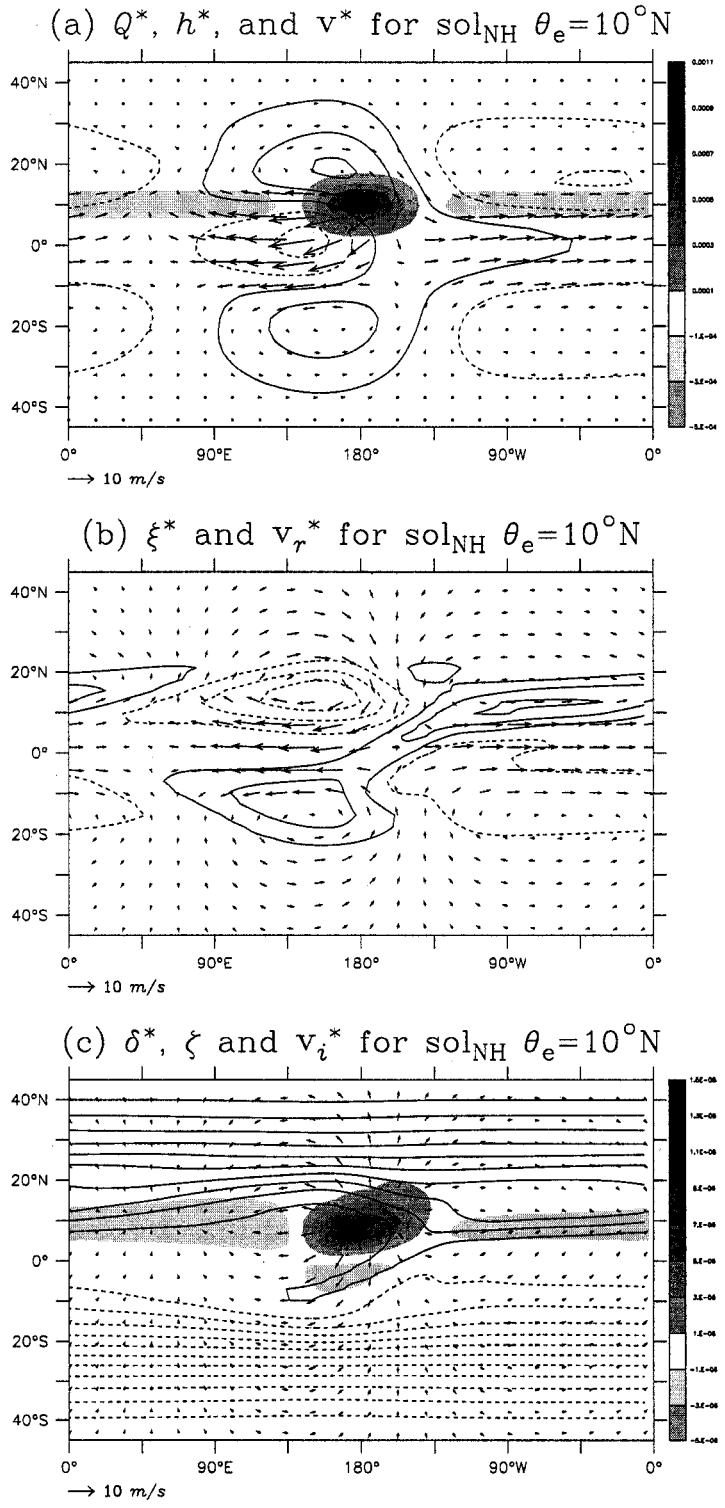

Figure 26. The θ_e = 10°N solstitial no-Hadley experiment (a) mass source (shading), eddy height field (contours every 10 m), and eddy winds (vectors); (b) eddy vorticity (contours every 5×10^{-6} s^{-1}) and rotational winds (vectors); and (c) eddy divergence (shading), total vorticity (contours every 1×10^{-5} s^{-1}), and eddy divergent winds (vectors).

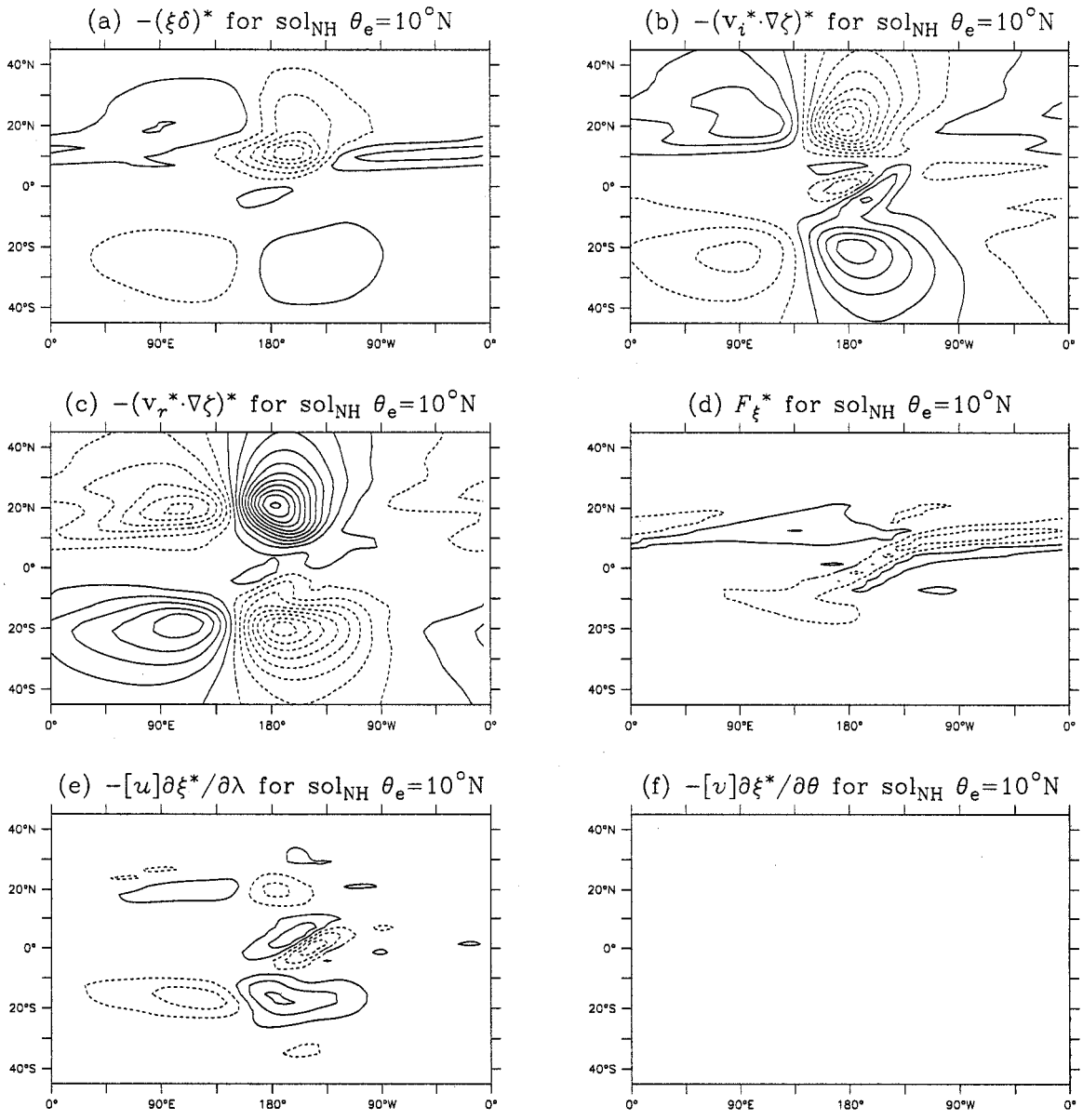

Figure 27. Vorticity balance components (2.12) for the θ_e = 10°N solstitial no-Hadley experiment, contours every 1.5×10^{-11} s^{-2}.

detail in Chapter 6, this eddy momentum flux reduction is consistent with the reduced cross-equatorial propagation of planetary wave activity, which strongly suggests that the cross-equatorial mean flow in the full solstitial basic state enhances the propagation of wave activity across the easterly mean wind region at the equator, as suggested by Watterson and Schneider (1987).

5.4 Influence of nonlinearity and damping

In this section, the experiments in Sections 5.1 and 5.2 are repeated using linear eddy forcing and/or different damping parameters to determine if the results are highly sensitive to these aspects of the model. Figure 28 shows the equilibrium eddy height and winds fields in the equinoctial and solstitial experiments when a momentum source proportional to the mass source (2.10) is included in the model forcing. The assumption that the added fluid should have zero momentum and kinetic energy is not entirely consistent with the identification of the fluid layer with an isentropic layer in the tropical upper troposphere, since the winds at lower levels in the tropics are not at rest. Moreover, vorticity balances calculated from observations of the upper-tropospheric circulation (e.g. Sardeshmukh and Held 1985), along with the realistic eddy circulations produced by GCMs integrated without a cumulus friction parameterization, suggest that vertical momentum exchange has only a weak influence on the large-scale circulation. However, it is still instructive to consider the effect of (2.10) because previous authors (e.g. Rosenlof et al 1986) have argued that "cumulus friction" has a significant influence on the eddy circulations in the tropical upper troposphere, and this formulation would be expected to yield the maximum influence on the eddy response.

The eddy responses in Figure 28 are similar in structure to the responses in the corresponding integrations without the mass source (Figures 16a, 18a, 20a, and 22a). For instance, the solstitial solution with off-equatorial forcing (Figure 28d) still exhibits a roughly symmetric response across the equator and tilted eddy wind vectors at the equator. However, all of the experiments exhibit a noticeable decrease in the amplitude of the eddy circulation, especially along the equator. This is somewhat surprising, given that the changes induced by the same mass source term were relatively small in the zonally-symmetric and resting basic state experiments in Chapters 3 and 4. A momentum source of the form (2.10) induces larger changes when a realistic basic state and eddy forcing

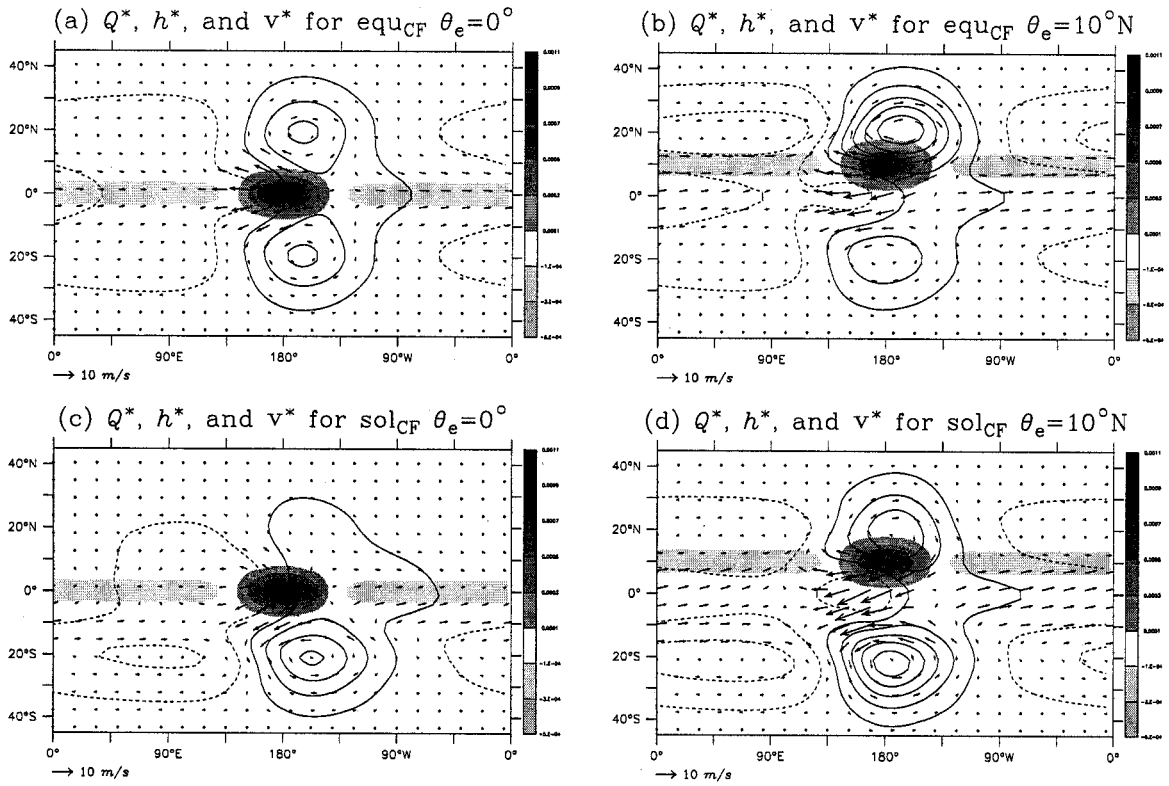

Figure 28. The mass source (shading), eddy height field (contours every 10 *m*), and eddy winds (vectors) in the (a) θ_e = 0° equinoctial (b) θ_e = 10°N equinoctial (c) θ_e = 0° solstitial, and (d) θ_e = 10°N solstitial experiments performed with a momentum source corresponding to the mass source as per (2.10).

are both present because the nonlinear superposition of the zonally-symmetric thermal relaxation with the eddy mass source increases the total mass flux in the mass source region, especially when the eddy forcing and zonal-mean divergence are collocated, as they are in the hemispherically-symmetric experiment and the solstitial experiment with eddy forcing in the summer hemisphere. The superposition of the zonal-mean easterly flow with the easterly eddy wind anomalies along the equator further increases the amplitude of the drag term in the solstitial basic state experiments.

The final experiments performed with the shallow water model are linear integrations in the equinoctial and solstitial basic states. The eddy height and wind fields from these linear experiments are shown in Figure 29, while the eddy vorticity anomalies

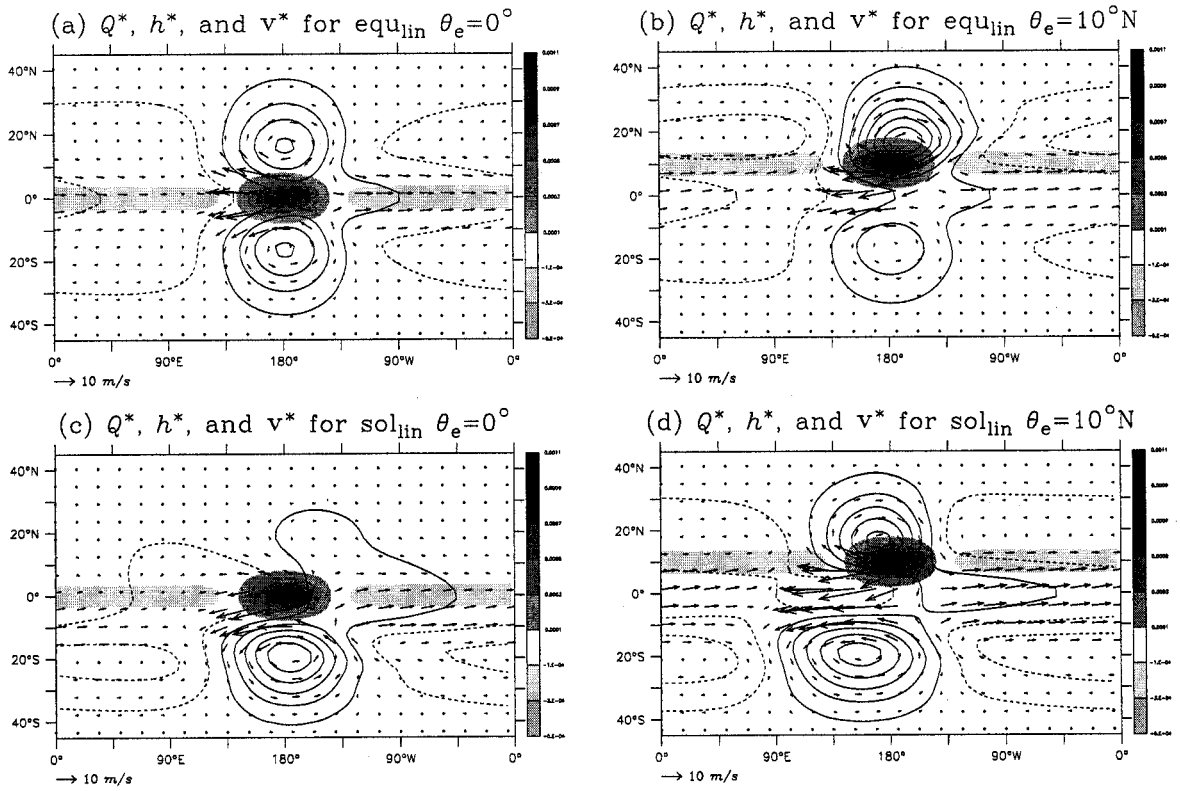

Figure 29. The mass source (shading), eddy height field (contours every 10 *m*), and eddy winds (vectors) in the linear (a) $\theta_e = 0°$ equinoctial (b) $\theta_e = 10°$N equinoctial (c) $\theta_e = 0°$ solstitial, and (d) $\theta_e = 10°$N solstitial experiments.

and rotational winds are shown in Figure 30. Comparing these experiments to the corresponding nonlinear runs (Figures 16, 18, 20, and 22), it can be inferred that the principal effects of nonlinearity in the realistic basic states experiments are the same as the effects of nonlinearity in the resting basic state. That is, to reduce the amplitude of the eddy vorticity anomalies straddling the equator via the formation of finite anticyclonic vorticity anomalies, and to increase the strength of the easterly eddy winds along the equator and depth of the equatorial trough via the Bernoulli effect. The similarity between the subtropical eddy height and circulation anomalies in the linear and nonlinear experiments with realistic basic states, on the other hand, indicate that these features are largely controlled by linear processes, in particular the increase in the subtropical

vorticity gradient and the eastward advection of vorticity and height anomalies by the zonal-mean flow discussed in the preceding section

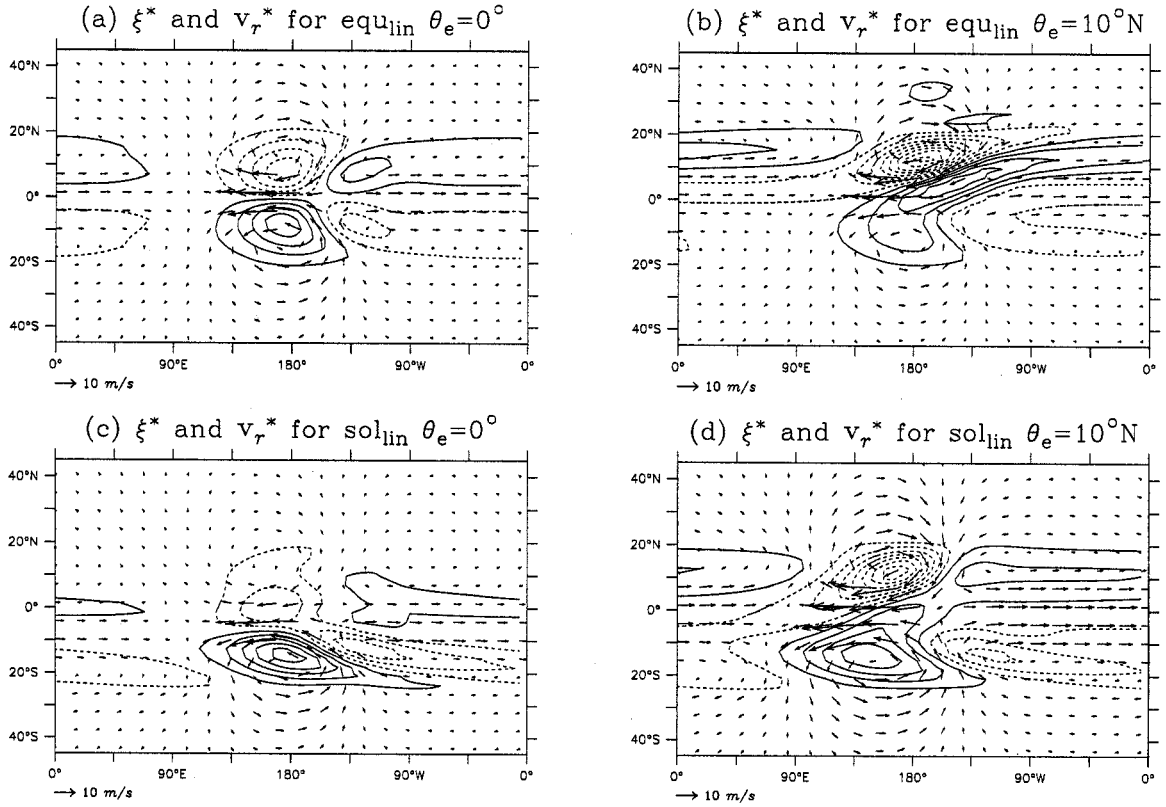

Figure 30. The eddy vorticity (contours every 5×10^{-6} s^{-1}) and rotational winds (vectors) in the linear (a) θ_e = 0° equinoctial (b) θ_e = 10°N equinoctial (c) θ_e = 0° solstitial, and (d) θ_e = 10°N solstitial experiments.

5.5 Chapter summary

- The response to tropical eddy forcing in the nonlinear shallow water model with topographically-forced basic states is similar to the observed eddy circulations at low latitudes and to the response of more complicated models to tropical eddy heating.

- Westerly zonal-mean zonal winds in the subtropics amplify the subtropical response to eddy forcing at the equator by increasing the zonal-mean relative vorticity, and shift the centers of the eddy height and vorticity anomalies poleward and eastward, bringing the response of the model into closer agreement with the observed stationary wave pattern in the tropical upper troposphere.
- The stronger zonal-mean zonal winds in the winter hemisphere of the solstitial basic state amplify the local response to eddy forcing, while the weaker winds in the summer hemisphere lead to a weaker eddy response; the disparity between the rotational response in the two hemispheres also leads to tilted eddy wind vectors along the equator.
- When the eddy forcing is moved into the summer hemisphere of the solstitial basic state, so that the eddy and zonal-mean divergence are collocated in latitude, the eddy response is strong in both hemispheres because the off-equatorial forcing enhances the eddy response in the summer hemisphere, while the eddy divergent winds and mean meridional flow promote a strong response in the winter hemisphere.
- The cross-equatorial mean meridional flow in the solstitial basic state significantly amplifies the response in the winter hemisphere, especially when the eddy forcing is located in the summer hemisphere.
- The symmetry of the response in the solstitial experiment with off-equatorial forcing suggests that the hemispheric symmetry of the observed quasi-stationary waves in the tropical upper troposphere arises due to the tendency for the strongest eddy and zonal-mean diabatic forcing to occur in the same latitude band.

6. Tropical wave-mean flow interaction

In Chapters 4 and 5, it was shown that hemispheric asymmetry in either the basic state or the eddy forcing distribution in the shallow water model leads to tilted eddy zonal wind vectors at the equator, which implies a cross-equatorial flux of eddy momentum. The results of the no-Hadley experiments in Chapter 5 also indicate that the cross-equatorial mean meridional flow in the solstitial basic state enhances the propagation of wave activity across the equator in the direction of the mean flow and increases the tilt in the low-latitude eddy zonal wind vectors. In this chapter, the zonally-averaged flux of westerly momentum from each of the eddy forcing experiments is evaluated, along with the changes in the zonal-mean zonal wind distribution induced by these fluxes. The barotropic vorticity equation is also used to demonstrate the influence of the mean meridional flow on low-latitude eddy momentum fluxes in an even simpler context.

The eddy momentum fluxes from the experiments described in the preceding chapters are presented and discussed in Section 6.1. The zonal-mean zonal wind changes from each experiment are presented and discussed in Section 6.2. Section 6.3 describes a linear barotropic model on an equatorial beta-plane, which is used to show, in the simplest possible context, that nonzero mean meridional winds amplify the flux of momentum in the opposite direction. The final section provides a chapter summary.

6.1 Eddy momentum fluxes

The zonally-averaged eddy momentum fluxes in the resting, equinoctial, equinoctial no-Hadley, solstitial, and solstitial no-Hadley experiments with the default model parameters (i.e. nonlinear forcing amplitude, eddy forcing centered at both the equator and 10°N) are shown in Figure 31. The fluxes in the resting basic state (Figure 31a) are generally weak, which reflects the weak planetary wave response in the absence of realistic basic state winds. However, the experiment with off-equatorial forcing clearly

exhibits stronger fluxes in the forced hemisphere and weaker fluxes in the unforced hemisphere, such that the net flux at the equator is positive, in accordance with the tilted eddy wind vectors along the equator noted in Figure 5b. In both cases, the eddy momentum fluxes reflects the superposition of the eddy divergent and rotational winds, as discussed in Chapter 4, and converge in the latitude band where the eddy forcing is located, which is consistent with the general theory of wave propagation in geophysical fluids. Lau and Lim (1984) noted similar tilts in the eddy circulations forced by isolated mass sources centered farther north (27N and 35N) in a similar model, and interpreted this shift in terms of the meridional dispersion of Rossby wave modes. However, in the present context it is probably more useful to view the changes in eddy momentum flux in terms of the strength of the planetary wave response.

In the presence of a realistic basic state, the eddy momentum fluxes induced by tropical eddy forcing increase dramatically. The fluxes in the equinoctial basic state (Figure 31b) resemble those in the resting basic state, except that the fluxes are much stronger and centered slightly farther from the equator, consistent with the stronger and broader rotational flow noted in Figures 16b and 18b. When the peak of the zonal-mean topography is moved into the Northern Hemisphere (Figure 31c), the eddy momentum fluxes induced by equatorial forcing (solid curve) nearly double in the winter hemisphere, and are reduced to almost zero in the summer hemisphere, which reflects the hemispheric asymmetry of the rotational response in this experiment (Figure 20). When both the eddy forcing and the zonal-mean topography are located north of the equator, however (dashed curve in Figure 31c), the northward eddy momentum flux increases dramatically, reflecting the strong rotational response in each hemisphere combined with the strong southward divergent flow at the equator (Figure 22).

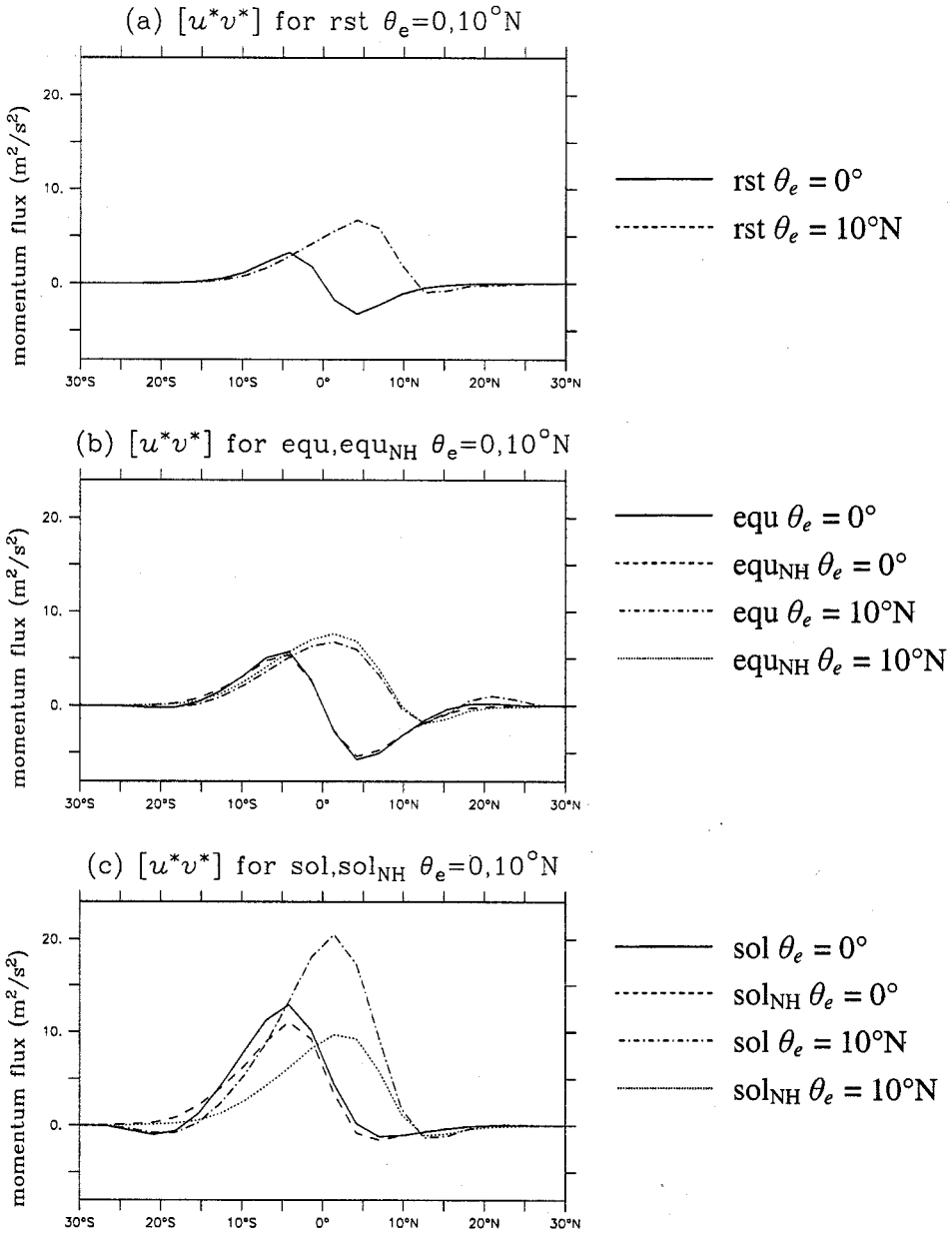

Figure 31. Eddy momentum fluxes in the (a) $\theta_e = 0°$ resting (solid) and $\theta_e = 10°N$ resting (dotted); (b) $\theta_e = 0°$ equinoctial (solid), $\theta_e = 0°$ equinoctial no-Hadley (dashed), $\theta_e = 10°N$ equinoctial (dot-dashed), and $\theta_e = 10°N$ equinoctial no-Hadley (dotted); and (c) $\theta_e = 0°$ solstitial (solid), $\theta_e = 0°$ solstitial no-Hadley (dashed), $\theta_e = 10°N$ solstitial (dot-dashed), and $\theta_e = 10°N$ solstitial no-Hadley (dotted) experiments.

The most striking result in Figure 31 is the sharp reduction in the northward eddy momentum flux when the Hadley circulation is removed from the solstitial basic state experiment with eddy forcing at 10°N (dot-dashed curve in Figure 31c), which reflects

the sharp decrease in the eddy response south of the equator in this experiment (Figure 26). The northward eddy momentum fluxes are also slightly weaker when the mean meridional flow is removed from the solstitial θ_e=0° experiment (dotted curve in 31c) and, to a lesser extent, the two equinoctial experiments (Figure 31b). These results indicate that the mean meridional flow has a much stronger influence on the meridional propagation of wave activity during solstitial months, as originally postulated by Watterson and Schneider, and suggest that this effect is most pronounced when the eddy forcing is located in the summer hemisphere, such that the maximum zonal-mean and eddy divergence are collocated in latitude, presumably because the eddy activity has difficultly propagating across the mean easterly flow near the equator in the solstitial basic state unless cross-equatorial flow is present.

The large difference between the amplitude of the eddy momentum fluxes in the equinoctial θ_e=0° and solstitial θ_e=10°N experiments is also consistent with the seasonal cycle of the eddy momentum fluxes and mean meridional flow in the NCEP Reanalysis noted by Dima et al (2005). In particular, the tropical eddy momentum fluxes are generally much larger during solstitial seasons, when the maximum eddy and zonal-mean diabatic heating are both located on the same side of the equator, than during equinoctial periods, when they are both located closer to zero latitude. Hence, our results indicate that the anti-correlation between the mean meridional winds and eddy momentum fluxes observed in the tropical upper troposphere over the seasonal cycle reflects the tendency for the maximum eddy and zonal-mean diabatic heating to occur at the same latitude.

Figures 32 and 33 show the eddy momentum fluxes in the linear experiments and enhanced damping experiments, respectively, described in Section 5.4. Both figures bear a close resemblance to Figure 31b-c. There are also some small discrepancies between the eddy momentum fluxes in the linear and nonlinear integrations with off-equatorial

eddy forcing, which arise due to the anomalous cyclonic forcing induced by the eddy divergent winds near the equator in the linear integrations (e.g. Figure 12b). However, the sensitivity of the eddy momentum fluxes to hemispheric asymmetry is clearly not strongly affected by the presence of nonlinearity or "cumulus friction".

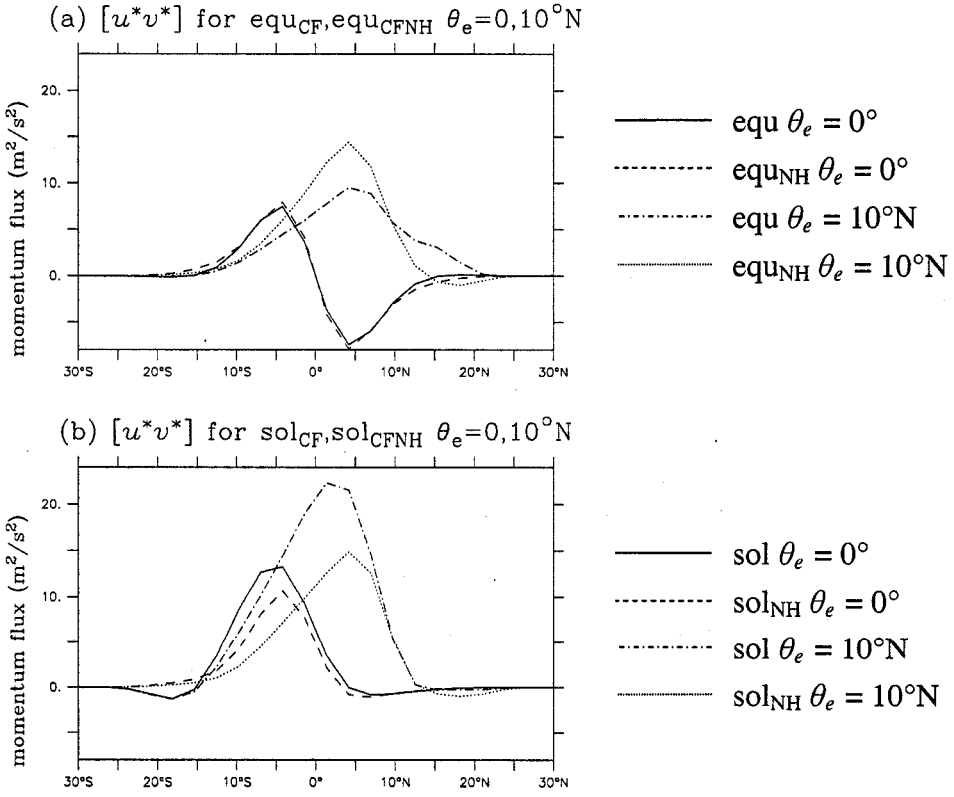

Figure 32. Eddy momentum fluxes in the (a) $\theta_e = 0°$ equinoctial (solid), $\theta_e = 0°$ equinoctial no-Hadley (dashed), $\theta_e = 10°$N equinoctial (dot-dashed), and $\theta_e = 10°$N equinoctial no-Hadley (dotted); and (b) $\theta_e = 0°$ solstitial (solid), $\theta_e = 0°$ solstitial no-Hadley (dashed), $\theta_e = 10°$N solstitial (dot-dashed), and $\theta_e = 10°$N solstitial no-Hadley (dotted) experiments performed with a momentum source corresponding to the mass source as per (2.10).

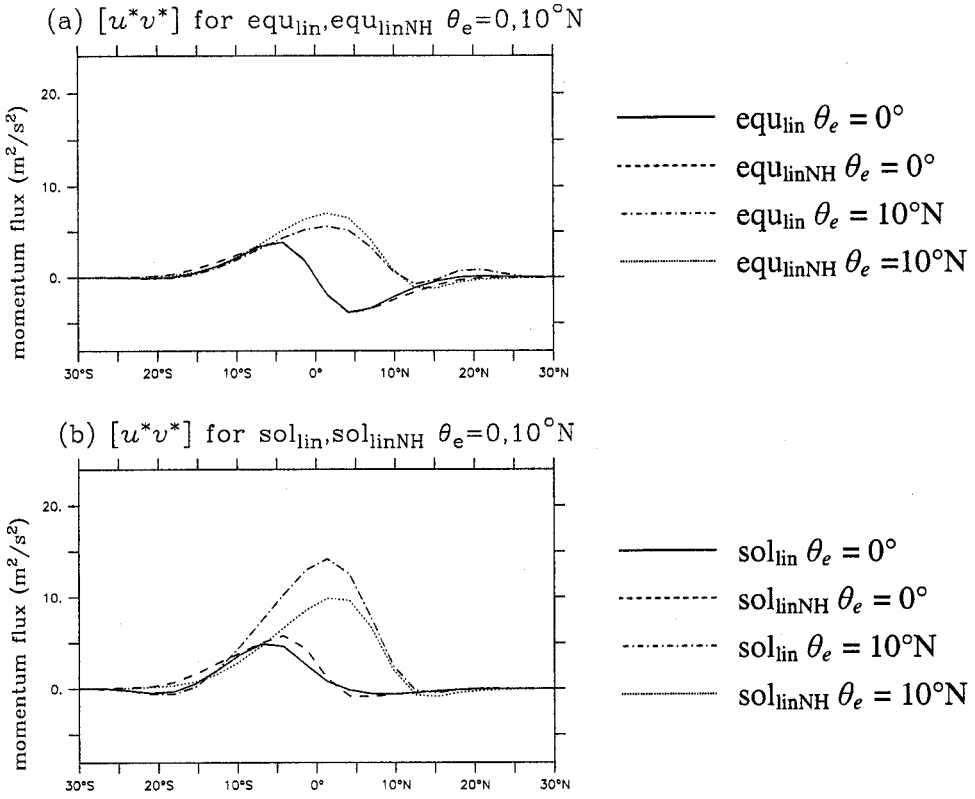

Figure 33. Eddy momentum fluxes in the linear (a) $\theta_e = 0°$ equinoctial (solid), $\theta_e = 0°$ equinoctial no-Hadley (dashed), $\theta_e = 10°$N equinoctial (dot-dashed), and $\theta_e = 10°$N equinoctial no-Hadley (dotted); and (b) $\theta_e = 0°$ solstitial (solid), $\theta_e = 0°$ solstitial no-Hadley (dashed), $\theta_e = 10°$N solstitial (dot-dashed), and $\theta_e = 10°$N solstitial no-Hadley (dotted) experiments.

6.2 Zonal-mean zonal wind balance

Convergent eddy momentum fluxes, such as those associated with the stationary waves in the tropics, represent a westerly torque, which will accelerate the zonal-mean flow unless or until there is a compensating easterly torque (c.f. Kraucunas and Hartmann 2005). The response of the zonal-mean zonal winds in the shallow water model to steady eddy forcing is shown in Figure 34 for the resting, equinoctial, and solstitial basic states. Interestingly, the mean zonal wind changes are relatively small in all of the experiments, and predominantly negative. It is of particularly interest to note that the mean zonal wind change at the equator is nearly zero when the eddy forcing and basic state are both

hemispherically-symmetric, because this is a situation that leads to strong equatorial superrotation in multi-level models.

To see why eddy forcing only gives rise to a weak, predominantly easterly zonal-mean zonal wind response in the shallow water system, consider the following form of the zonal momentum equation (2.1), which has been rewritten using the chain rule and trigonometric identities to simplify the advective terms:

$$\frac{\partial u}{\partial t} = fv - \frac{\partial\left(uv\cos^2\theta\right)}{a\cos^2\theta\,\partial\theta} + u\delta - \frac{g}{a\cos\theta}\frac{\partial H}{\partial\lambda} - F_u \tag{5.1}$$

Considering the equilibrium response, and taking the zonal-mean:

$$\frac{\partial[u]}{\partial t} = f[v] - \frac{\partial\left([u][v]\cos^2\theta\right)}{a\cos^2\theta\,\partial\theta} - \frac{\partial\left(\left[u^*v^*\right]\cos^2\theta\right)}{a\cos^2\theta\,\partial\theta} + [u][v] + \left[u^*\delta^*\right] - [F_u] \approx 0 \tag{5.2}$$

Finally, using the chain rule to simplify the zonal-mean terms, and combining the relative and absolute vorticity terms, we obtain the advective form of the zonal-mean zonal wind balance for the shallow water model:

$$\frac{\partial[u]}{\partial t} = [v]\left(f - \frac{\partial\left([u]\cos\theta\right)}{a\cos\theta\,\partial\theta}\right) - \frac{\partial\left(\left[u^*v^*\right]\cos^2\theta\right)}{a\cos^2\theta\,\partial\theta} + \left[u^*\delta^*\right] - [F_u] \approx 0 \tag{5.3}$$

Equation (5.2) is the shallow water equivalent of the zonal-mean zonal wind balance in three-dimensions discussed by Kraucunas (2001), Kraucunas and Hartmann (2005), and Dima et al (2005). The difference between the three-dimensional and two-dimensional forms is that the vertical momentum flux term has been replaced in (5.3) with the correlation between the eddy zonal winds and eddy divergence anomalies. As discussed in Chapter 3, in the absence of eddy forcing the balance is simply between zonal-mean

advection by the mean meridional flow (i.e. the first term on the RHS of (5.3), which is driven by thermal relaxation) and frictional drag.

Figure 35 shows the changes in the zonal-mean zonal wind balance that lead to the zonal-mean zonal wind changes shown in Figure 34. The horizontal axis has been expanded since the mean zonal wind change is small outside the tropics. In all cases, the convergence of eddy momentum fluxes leads to a westerly acceleration in the eddy forcing region, which as noted above is a standard feature of planetary wave propagation through rotating geophysical fluids. This westerly acceleration is balanced by the easterly acceleration associated with the anticorrelation between the eddy zonal winds and divergence anomalies along the forced latitude band, which arises due to the dominance of easterly flow over the mass source region, and represent the shallow water analogue to the vertical eddy momentum fluxes noted by Kraucunas (2001) and Kraucunas and Hartmann (2005) in a general circulation model forced by tropical eddy heating anomalies. The easterly torque associated with the divergence of the eddy momentum fluxes in the surrounding latitudes is also compensated by the eddy divergence-eddy zonal wind correlation term in the realistic basic states; if one examines any of the horizontal response plots in Chapter 5, it is clear that this term is positive in these regions because the isolated convergence anomalies induced by the rotational flow on the western margins of the mass source region occur in a region with easterly eddy zonal winds.

The cancellation between the eddy momentum flux convergence and the eddy zonal wind-eddy divergence term is analogous to the cancellation between the horizontal and vertical eddy momentum fluxes in three-dimensional models (e.g. Kraucunas 2001). Apparently the eddy zonal wind-eddy divergence term in the shallow water system provides a more efficient easterly torque than the vertical eddy momentum fluxes in three dimensional models, because superrotation is not observed in any of the shallow water

model integrations. The absence of a strong zonal-mean response also simplifies the analysis of the nonlinear stationary wave response to tropical eddy forcing in the shallow water system, because we do not have to account for complex wave-mean flow feedbacks. However, it means that the shallow water system is not a useful analogue for probing the influence of eddy momentum fluxes on the zonal-mean flow.

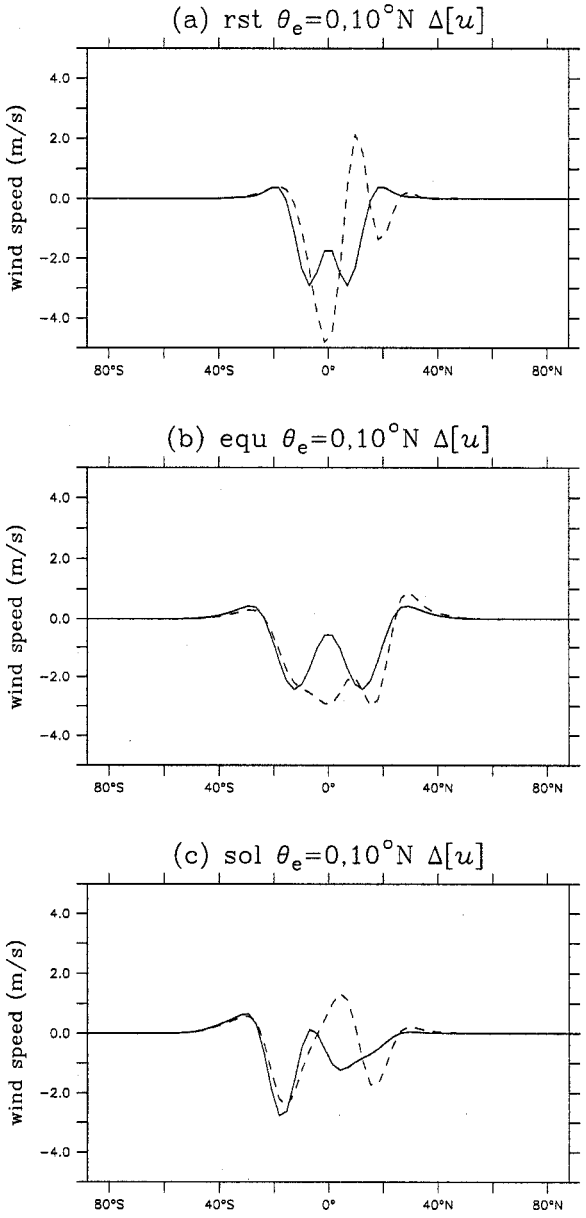

Figure 34. Zonal-mean zonal wind change due to the presence of eddies in the (a) resting, (b) equinoctial, and (c) solstitial basic states with θ_e = 0° (solid) and θ_e = 10°N (dashed).

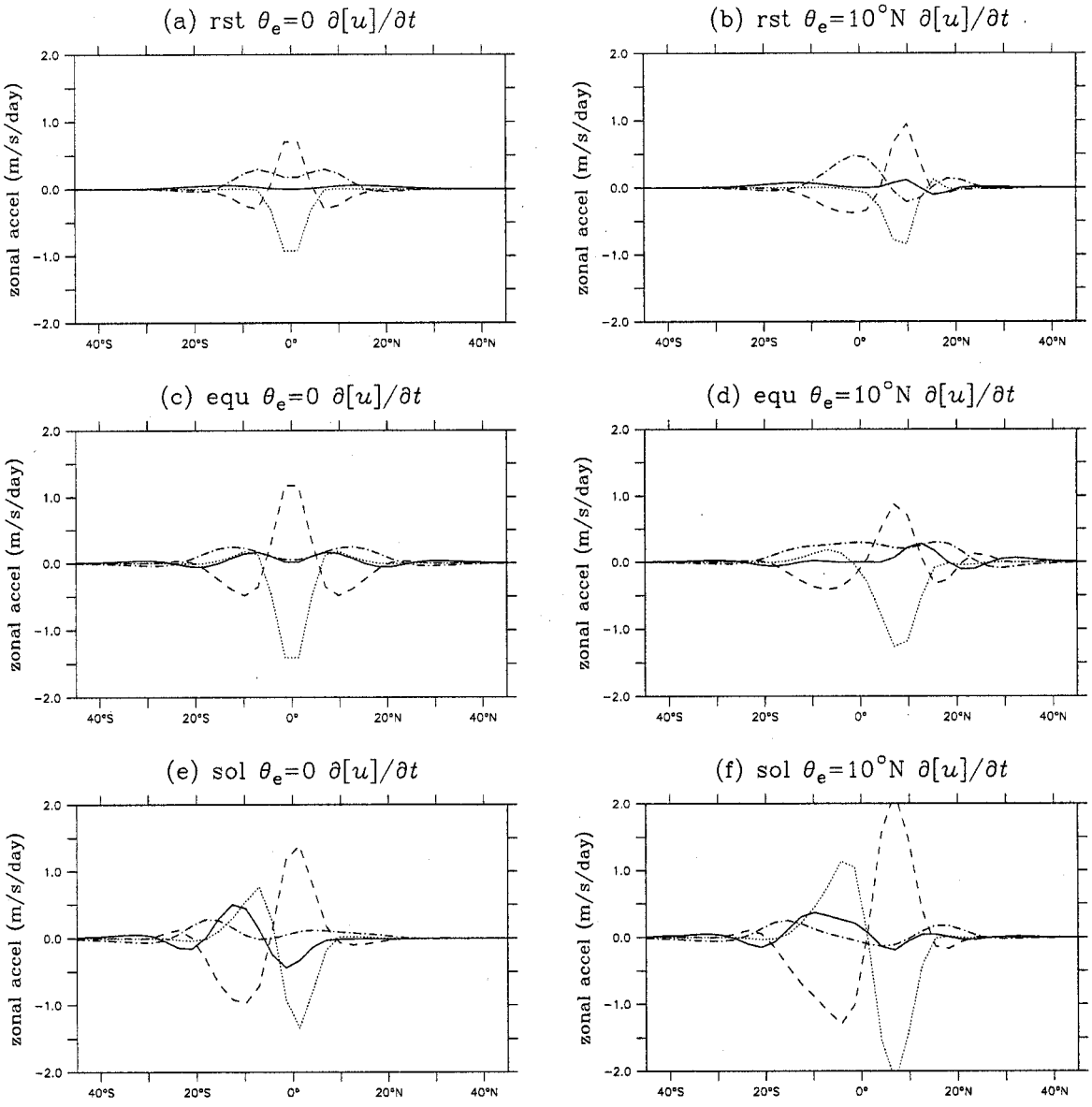

Figure 35. Zonal-mean zonal wind balance components (5.3) in the (a) θ_e = 0° resting, (b) θ_e = 10°N resting, (c) θ_e = 0° equinoctial (d) θ_e = 10°N equinoctial, (e) θ_e = 0°solstitial, and (f) θ_e = 10°N solstitial experiments.

6.3 A simple barotropic model

The amplification of the eddy momentum fluxes near the equator by strong cross-equatorial mean meridional winds can actually be reproduced in an even simpler model. Consider the steady-state barotropic vorticity equation on an equatorial beta-plane, linearized about horizontally-uniform zonal and meridional winds U and V, and forced with a fixed vorticity source F:

$$U\frac{\partial \xi^*}{\partial x}+V\frac{\partial \xi^*}{\partial y}+\beta_o v^* = F - k\xi^* \tag{5.4}$$

Here β_o is the planetary vorticity gradient at the equator, k is the linear damping strength, and x and y represent distance in the zonal and meridional directions, respectively.

Consider simple wavelike to (5.4) of the form $\psi^* = Ae^{(imx+iny)}$, where ψ is the horizontal streamfunction, so $u^* = -\partial\psi^*/\partial y = -in\psi^*$, $v^* = \partial\psi^*/\partial x = im\psi^*$, and $\xi^* = \nabla^2\psi^* = -(m^2+n^2)\psi^*$. To further simplify the problem, consider only plane waves with a single positive zonal wavenumber $m=2\pi M/a$ (where M is an integer) and a single meridional wavenumber $n = 2\pi / \alpha_y$ (where α_y is the meridional scale of the wave in radians), which can be either positive or negative, corresponding to northward and southward moving waves, respectively. Substituting this form into (5.4) yields:

$$\psi^* = F/\left[im\beta-(imU-inV+k)(m^2+n^2)\right] \tag{5.5}$$

Since the forced waves and basic state are identical at all latitudes, the zonally-averaged eddy momentum flux is the same as the globally-averaged eddy momentum flux, and is equal to:

$$\left[u^*v^*\right] = -mn\left|\psi^*\psi^{*\dagger}\right| = \frac{-mnF^2}{\left\{m\beta-(m^2+n^2)(mU+nV)\right\}^2+\left\{k(m^2+n^2)\right\}^2} \tag{5.6}$$

Since m is always positive, (5.6) exhibits the familiar property that waves with positive n (i.e. northward moving waves) are associated with negative (southward) fluxes of momentum, and vice versa. Also note that when V is zero, the flux for positive n will be equal and opposite to the flux for negative n, i.e. the fluxes associated with northward-moving waves and southward-moving waves will be equal and opposite, and the total flux will be zero.

Figure 36 shows the value of (5.6) for two different mean zonal wind speeds and a range of mean meridional wind speeds with $k = (10 \text{ days})^{-1}$, $F = 1.5 \times 10^{-11} \text{ s}^{-2}$, $\alpha_y = 45°$, and $M = 1$. These parameters have been chosen to correspond as closely as possible with the steady eddy circulations in the shallow water model, but the results are relatively insensitive to the scale of the waves or the ratio of the forcing to damping. As expected, when the mean meridional flow is zero, the negative (southward) eddy momentum fluxes associated with the northward-moving wave ($n>0$, solid line) and positive (northward) eddy momentum fluxes associated with the southward-moving wave ($n<0$, dashed line) are equal and opposite, with stronger fluxes when the mean zonal winds are westerly because the generation of Rossby waves is more efficient in westerly flow.

The relative amplitude of the northward and southward momentum fluxes in Figure 36 changes dramatically when the mean meridional flow is changed; northward V induces a large increase in the southward fluxes and a small decrease in the northward fluxes, and southward V induces the opposite changes. Hence, the total flux associated with both northward-moving and southward-moving waves (dotted line) is directed opposite the prevailing mean meridional flow, and generally increases with increasing meridional wind speed, which is exactly the relationship observed in the tropical upper troposphere on Earth over the course of the seasonal cycle (Dima et al 2005). The eddy momentum fluxes are somewhat less sensitive to the mean meridional flow in westerly

zonal-mean winds than easterly zonal-mean winds, which is consistent with the interpretation of Watterson and Schneider (1987), who argue that cross-equatorial mean meridional flow promotes the propagation of wave activity in the direction of the flow, especially across regions with mean easterly flow.

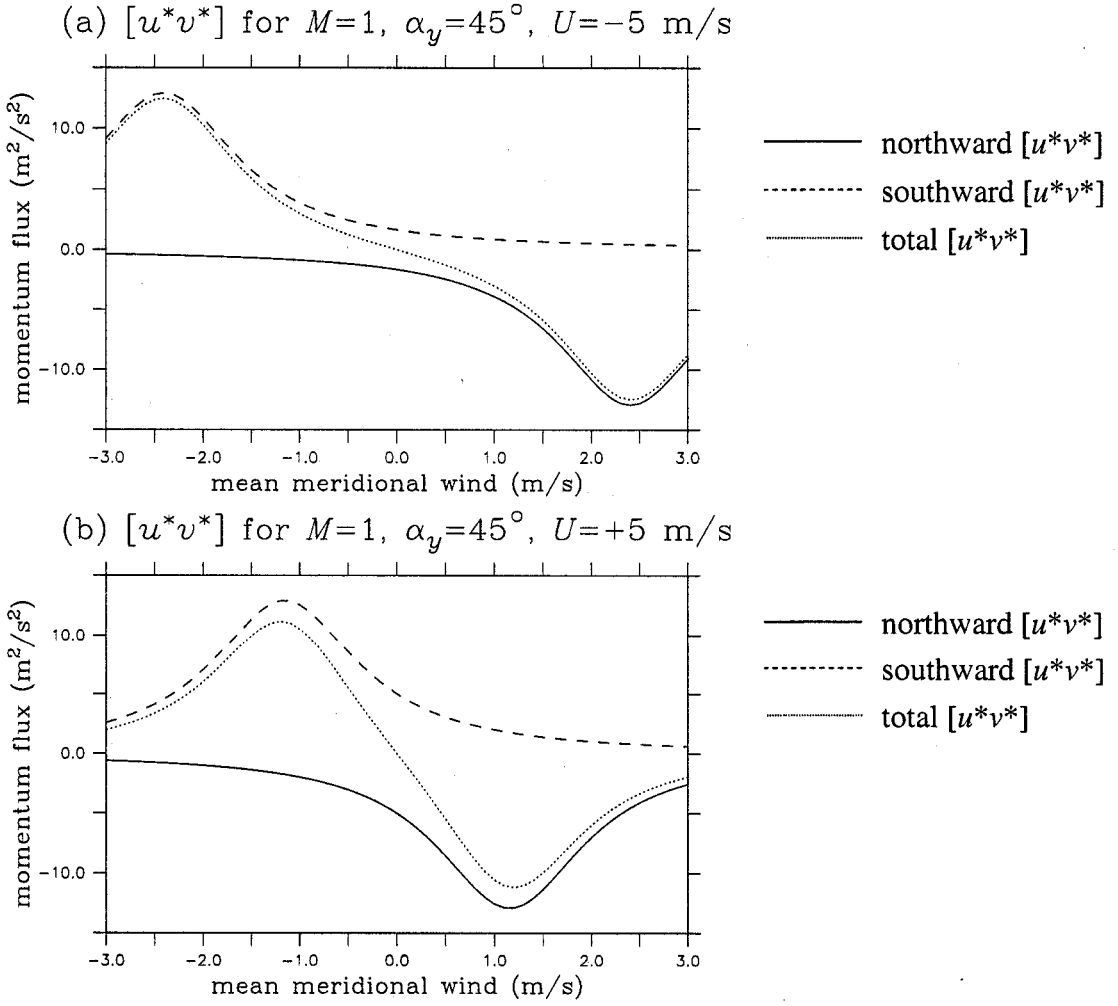

Figure 36. Northward (solid), southward (dashed), and total (dotted) eddy momentum flux calculated using the linear barotropic model (5.6) with a mean zonal wind speed of -5 *m/s* and eddy forcing at zonal wavenumber one with a meridional scale of 45 degrees, plotted as a function of mean meridional wind speed.

6.4 Chapter summary

- Hemispheric asymmetry in either the eddy forcing or the basic state leads to cross-equatorial eddy momentum fluxes.
- In contrast to multi-level models, the zonal-mean zonal winds in the shallow water model do not exhibit a large acceleration when eddy forcing is present at low latitudes because the convergence of eddy momentum fluxes near the equator is offset by a term that involves the longitudinal correlation between the eddy zonal winds and eddy height anomalies.
- Cross-equatorial mean meridional winds enhance the flux of eddy momentum in the opposite direction by promoting the propagation of wave energy in the direction of the flow; this relationship can also be demonstrated in an idealized barotropic framework.

7. Summary and conclusions

This dissertation introduces a novel technique for imposing realistic basic states in the shallow water system: a zonally-symmetric topography distribution that decreases smoothly from the tropics to the poles is placed underneath a thin fluid layer, and the layer depth is relaxed towards its global-mean value. This configuration yields realistic basic state zonal and meridional winds without artificially enhancing tropical wave speeds or neglecting nonlinear terms, thus providing a consistent and versatile framework for studying the influence of different basic states on the steady eddy circulations at low latitudes. Previous attempts to simulate tropical stationary waves using the shallow water system have used horizontally-homogenous basic states, linearization, or large fluid depths at the equator, limiting their ability to accurately simulate tropical wave dynamics.

The response of the model to steady eddy forcing, which is imposed by introducing a fixed pattern of mass sources and sinks along or near the equator, is analyzed under several different basic states. These experiments shed light on the influence of hemispheric asymmetry on the tropical climate system, and also explain several poorly understood aspects of the seasonally-varying large-scale eddy circulations in the tropical upper troposphere. In this study, Emphasis is placed on the hemispheric symmetry and horizontal position of the equilibrium stationary wave structures obtained using different basic states and eddy forcing positions, and on the eddy momentum fluxes associated with the stationary wave response. The influence of the Hadley circulation is isolated by constructing basic states with zero mean meridional flow using the nonlinear balance relationship. Linear experiments and experiments with different damping parameters are also performed to determine the influence of nonlinear processes and damping strength on the equilibrium response to tropical eddy forcing.

One of the most important findings of this dissertation is that the subtropical eddy height and circulation anomalies that arise in response to tropical eddy forcing exhibit similar amplitudes and horizontal patterns in both hemispheres when the eddy forcing and zonal-mean divergence are both located on the equator or in the same hemisphere. This result suggests that the surprising hemispheric symmetry observed in the seasonally-varying tropical stationary waves in the NCEP Reanalysis (Dima et al 2005) arises because the maximum eddy and zonal-mean diabatic heating tend to covary in latitude over the course of the seasonal cycle. It is also notable that the amplitude of the stationary wave response is much larger when the eddy forcing and zonal-mean divergence are both located on the same side of the equator than when they are both hemispherically-symmetric, in agreement with the observed seasonal cycle in stationary wave amplitudes reported by Dima et al (2005).

The strength and symmetry of the response to off-equatorial eddy forcing in the solstitial basic state can be explained as follows. The amplification of the eddy response in the summer hemisphere arises because the eddy mass source, and hence the eddy divergence anomaly, is moved into a region that has a stronger zonal-mean vorticity and vorticity gradient, which enhances the generation of vorticity by vortex stretching. The amplification of the winter hemisphere response, on the other hand, can be attributed to three different factors: the advection of vorticity by the eddy divergent wind field, which forces rotational flow across a much broader latitudinal range than the eddy divergence anomaly itself, the stronger zonal-mean zonal winds in the winter hemisphere, which provide a stronger mean vorticity gradient for the horizontal winds to act on, and the cross-equatorial mean meridional flow, which enhances the propagation of wave activity in the direction of the flow, a phenomenon originally discussed by Watterson and Schneider (1987).

The relatively weak stationary wave response obtained when both the eddy forcing and the basic state are hemispherically-symmetric, on the other hand, can be attributed to the large anticyclonic vorticity anomalies that form on either side of the equator, which reduce the effective vorticity and vorticity gradient in the vicinity of the mass source. Were it not for the advection of vorticity by the eddy divergent winds, which operate over a much broader latitudinal scale than the vortex stretching associated with the eddy divergence anomaly, the response to eddy forcing centered on the equator would be very small. Sardesmukh and Hoskins (1988) reached a similar conclusion regarding the global stationary wave response to a fixed tropical eddy divergence anomaly in a barotropic model.

The seasonal variations in the low-latitude eddy momentum fluxes reported by Dima et al (2005) can also be attributed to the tendency for the maximum zonal-mean and eddy forcing to occur in the same latitude band. Hemispheric asymmetry in either the mean meridional flow or tropical eddy forcing produces steady eddy momentum fluxes that are directed across the equator. The momentum flux is strongest near the equator because the flow is less constrained by planetary rotation, and because the weaker vorticity gradient allows stronger eddy meridional winds, especially when finite amplitude anticyclonic vorticity anomalies are present. The momentum fluxes are enhanced when the eddy forcing and zonal-mean divergence are located in the same hemisphere because the cross-equatorial mean meridional flow helps planetary waves propagate across the equator. Hence, the eddy momentum fluxes associated with the tropical stationary wave response are anti-correlated with the mean meridional flow and strongest when the basic state and eddy forcing are both hemispherically-asymmetric, which mirrors the relationship between the observed seasonally-varying large-scale waves and mean meridional flow in the equatorial upper troposphere.

The response of the zonally-averaged climate of the shallow water model to tropical eddy forcing is fundamentally different from the zonal-mean response to eddy forcing in three-dimensional models. Kraucunas (2001) and Kraucunas and Hartmann (2005) demonstrated that convergent eddy momentum fluxes associated with tropical stationary wave forcing will rapidly induce equatorial superrotation in an idealized general circulation model with a hemispherically-symmetric basic state, but not in a solstitial basic state that includes a strong cross-equatorial mean meridional wind. In the shallow water model, the zonal-mean zonal wind tendency equation includes a term representing the longitudinal correlation between the eddy divergence and eddy zonal wind anomalies; this term offsets virtually all of the zonal wind tendency associated with the eddy momentum flux convergence induced by the tropical stationary waves, leading to a very small mean zonal wind response. Although the lack of a large zonal-mean response makes the shallow water system useful for isolating the influence of the basic state flow on stationary wave structures at low latitudes, it means that more complicated models are required to study tropical wave-mean flow interactions.

Another important conclusion arising from the shallow water model experiments described in the preceding chapters is that westerly zonal-mean winds in the subtropics shifts the centers of subtropical vorticity and height anomalies eastward, relative to their positions in a resting basic state, by advecting the anticyclonic circulation and height anomalies induced by the tropical mass source eastward. Divergence and convergence anomalies induced by the strong rotational flow on either side of the mass source also play an important role in controlling the size and shape of the eddy response in realistic basics states; this feedback would not be resolved in a barotropic model or a model with fixed eddy divergence anomalies. All of these features are reproduced in a linearized version of the model. Hence, Hendon's (1986) argument that nonlinearity is responsible

for the eastward displacement of the subtropical anticyclones forced by tropical eddy heating appears to be wrong. However, it should be noted that the centers of rotational flow are still centered slightly to the west of the mass source in the shallow water experiments, whereas the observed subtropical anticyclones seem to be situated directly north of south of the strongest eddy forcing. The results of Ting and Held (1990) suggest that transient eddy fluxes could be responsible for this remaining discrepancy.

In general, the differences between linear and nonlinear experiments are consistent with the effects of nonlinearity discussed by Van Tuyl (1986), Gill and Phlips (1987), Sardesmukh and Hoskins (1988), and Hoskins et al (1999). The finite vorticity anomalies in, and to the west of, the mass source region reduce the absolute vorticity gradient in the nonlinear experiments, limiting the generation of anticyclonic vorticity by the eddy divergence and divergent winds. Hence, the linear experiments exhibit stronger rotational flow than in their nonlinear counterparts because vorticity generation must be balanced by linear advection and damping alone. The easterly eddy zonal winds and negative height anomalies along the equator, on the other hand, are stronger in the nonlinear solutions because of the Bernoulli effect, which increases the zonal height gradient required to maintain the eddy wind field. The differences between the linear and nonlinear solutions are more pronounced when the eddy forcing is located off the equator because the effective forcing is stronger, but are less pronounced in Earth-like basic states because linear advection is more effective.

Future work with shallow water models like the one described in this study might prove useful for studying the influence of different horizontal eddy forcing patterns on the low-latitude circulation under different basic state configurations. The transient response to tropical eddy forcing is another potential application. Finally, the results of previous shallow water experiments could be revisited with realistic basic states.

LIST OF REFERENCES

Branstator, G., and S. E. Haupt (1998): An empirical model of barotropic atmospheric dynamics and its response to tropical forcing. *J. Clim.*, 11, 2645-2667.

Bretherton, C. S., and A. H. Sobel (2003): The Gill model and the weak temperature gradient approximation. *J. Atmos. Sci.*, 60, 451-460.

Chang, H.-R., and P. J. Webster (1990): Energy accumulation and emanation at low latitudes. Part II: Nonlinear response to strong episodic equatorial forcing. *J. Atmos. Sci.*, 47, 2624-2644.

Chen, P. (2001): Thermally forced stationary waves in a quasigeostrophic system. *J. Atmos. Sci.*, 58, 1585-1594.

Chen, P., M. P. Hoerling, and R. M. Dole (2001): The origin of the subtropical anticyclones. *J. Atmos. Sci.*, 58, 1827-1835.

Dima, I., J. M. Wallace, and I. Kraucunas, 2005: Tropical angular momentum balance in the NCEP Reanalysis, *J. Atmos. Sci.*, 62, 2499-2513.

Esler, J. G., L. M. Polvani, and R. A. Plumb (2000): The effect of a Hadley circulation on the propagation and reflection of planetary waves in a simple one-level model. *J. Atmos. Sci.*, 57, 1536-1556.

Farrell, B., and I. Watterson (1985): Rossby waves in opposing currents. *J. Atmos. Sci.*, 42, 1746-1756.

Gent, P. R. (1993): The energetically consistent shallow-water equations. *J. Atmos. Sci.*, 50, 1323-1325.

Geophysical Fluid Dynamics Laboratory (2005): The Flexible Modeling System. http://www.gfdl.noaa.gov/~fms/

Gill, A. E. (1980): Some simple solutions for heat-induced tropical circulation. *Quart. J. Roy. Meteor. Soc.*, 106, 447-462.

Gill, A. E. and P. J. Phlips (1986): Nonlinear effects on the heat-induced circulations of the tropical atmosphere. *Quart. J. Roy. Meteor. Soc.*, 112, 69-91.

Held, I. M., and P. J. Phillips (1990): A barotropic model of the interaction between the Hadley cell and a Rossby wave. *J. Atmos. Sci.*, 47, 856-869.

Held, I. M., M. Ting, and H. Wang (2002): Northern winter stationary waves: theory and modeling. *J. Clim.*, Vol 15, 2125-2144.

Hendon, H. H. (1986): The time-mean flow and variability in a nonlinear model of the atmosphere with tropical diabatic forcing. *J. Atmos. Sci.*, 43, 72-88.

Hoskins, B. J., and D. J. Karoly (1981): The steady linear response of a spherical atmosphere to thermal and orographic forcing. *J. Atmos. Sci.*, 38, 1179-1196.

Hoskins, B. J., and F. Jin (1991): The initial value problem for tropical perturbations to a baroclinic atmosphere. *Quart. J. Roy. Meteor. Soc.*, 117, 299-317.

Hoskins, B. J., and M. J. Rodwell (1995): A model of the Asian summer monsoon. Part I: The global scale. *J. Atmos. Sci.*, 52, 1329-1340.

Jin, F., and B. J. Hoskins (1995): The direct response to tropical heating in a baroclinic atmosphere. *J. Atmos. Sci.*, 52, 307-319.

Kang, I.-S., and I. M. Held (1986): Linear and nonlinear diagnostic models of stationary eddies in the upper troposphere during Northern summer. *J. Atmos. Sci.*, 43, 3045-3057.

Kasahara, A., and P. L. Silva Dias (1986): Response of planetary waves to stationary tropical heating in a global atmosphere with meridional and vertical shear. *J. Atmos. Sci.*, 43, 1893-1911.

Kraucunas, I. (2001): *Equatorial superrotation: the response to tropical eddy heating in a multi-level general circulation model*, M.S. thesis, U. of Washington, 187 pp.

Kraucunas, I. and D. L. Hartmann (2005): Equatorial superrotation and the factors controlling the zonal-mean zonal winds in the tropical upper troposphere, *J. Atmos. Sci.*, 62, 371-389.

Lau, K.-M., and H. Lim (1982): Thermally driven motions in an equatorial β–plane: Hadley and Walker circulations during the winter monsoon. *Mon. Wea. Rev.*, 110, 336-353.

Lau, K.-M., and H. Lim (1984): On the dynamics of equatorial forcing of climate teleconnections. *J. Atmos. Sci.*, 41, 161-176.

Lim, H., and C.-P. Chang (1983): Dynamics of teleconnections and Walker circulations forced by equatorial heating. *J. Atmos. Sci.*, 40, 1897-1915.

Matsuno, T. (1966): Quasi-geostrophic motions in the equatorial area. *J. Meteor. Soc. Japan*, 44, 25-42.

Murakami, T., and B. Wang (1993): Annual cycle of equatorial east-west circulation over the Indian and Pacific Oceans. *J. Clim.*, 6, 932-952.

Nieto Ferreira, R., and W. H. Schubert (1999): The role of tropical cyclones in the formation of tropical upper-troposphere troughs. *J. Atmos. Sci.*, 56, 2891-2907.

Nigam, S., I. M. Held, and S. W. Lyons (1986): Linear simulation of the stationary eddies in a general circulation model. Part I: The no-mountain model. *J. Atmos. Sci.*, 43, 2944-2961.

Nigam, S., I. M. Held, and S. W. Lyons (1988): Linear simulation of the stationary eddies in a GCM. Part II: The "mountain" model. *J. Atmos. Sci.*, 45, 1433-1452.

Phlips, P. J., and A. E. Gill (1987): An analytic model of the heat-induced tropical circulation in the presence of a mean wind. *Quart. J. Roy. Meteor. Soc.*, 113, 213-236.

Rodwell, M. J., and B. J. Hoskins (1996): Monsoons and the dynamics of deserts. *Quart. J. Roy. Meteor. Soc.*, 122, 1385-1404.

Rosenlof, K. H., D. E. Stevens, J. R. Anderson, and P. E. Ciesielski (1986): The Walker circulation with observed zonal winds, a mean Hadley cell, and cumulus friction. *J. Atmos. Sci.*, 43, 449-467..

Sardeshmukh, P. D., and I. M. Held (1984): The vorticity balance in the tropical upper troposphere of a general circulation model. *J. Atmos. Sci.*, 41, 768-778.

Sardeshmukh, P. D., and B. J. Hoskins (1985): Vorticity balances in the tropics during the 1982-1983 El Niño-Southern Oscillation event. *Quart. J. Roy. Meteor. Soc.*, 111, 261-278.

Sardeshmukh, P. D., and B. J. Hoskins (1987): The generation of global rotational flow by steady idealized tropical divergence. *J. Atmos. Sci.*, 45, 1228-1251.

Seager, R., R. Murtugudde, N. Naik, A. Clement, N. Gordon, and J. Miller (2003): Air-sea interaction and the seasonal cycle of the subtropical anticyclones. *J. Clim.*, 16, 1948-1966.

Schneider, E. K., and I. G. Watterson (1984): Stationary Rossby wave propagation through easterly layers. *J. Atmos. Sci.*, 41, 2069-2083.

Schneider, E. K. (1987): A simplified model of the modified Hadley circulation. *J. Atmos. Sci.*, 44, 3311-3329.

Schumacher, C., R. A. Houze, and I. Kraucunas, 2004: The tropical dynamical response to latent heating estimates derived from the TRMM Precipitation Radar. *J. Atmos. Sci.*, 61, 1341-1358.

Shell, K. M., and I. M. Held (2004): Abrupt transition to strong superrotation in an axisymmetric model of the upper troposphere. *J. Atmos. Sci.*, 61, 2928-2935.

Ting, M., and I. M. Held (1990): The stationary wave response to a tropical SST anomaly in an idealized GCM. *J. Atmos. Sci.*, 47, 2546-2566.

Ting, M., and P. D. Sardeshmukh (1993): Factors determining the extratropical response to equatorial diabatic heating anomalies. *J. Atmos. Sci.*, 50, 907-918.

Ting, M. (1994): Maintenance of Northern summer stationary waves in a GCM. *J. Atmos. Sci.*, 51, 3286-3308.

Ting, M., H. Wang, and L. Yu (2001): Nonlinear stationary wave maintenance and seasonal cycle in the GFDL R30 GCM. *J. Atmos. Sci.*, 58, 2331-2354.

Ting, M., and L. Yu (1998): Steady response to tropical heating in wavy linear and nonlinear baroclinic models. *J. Atmos. Sci.*, 55, 3565-3582.

Valdez, P. J., and B. J. Hoskins (1989): Linear stationary wave simulations of the time-mean climatological flow. *J. Atmos. Sci.*, 46, 2509-2527.

Van Tuyl, A. H. (1986): Advective influences on forced tropical motions. *J. Atmos. Sci.*, 43, 141-161.

Wang, H., and M. Ting (1999): Seasonal cycle of the climatological stationary waves in the NCEP-NCAR reanalysis. *J. Atmos. Sci.*, 56, 3892-3919.

Watterson, I. G., and E. K. Schneider (1987): The effect of the Hadley circulation on the meridional propagation of stationary waves. *Quart. J. Roy. Meteor. Soc.*, 113, 779-813.

Webster, P. J. (1981): Mechanisms determining the atmospheric response to sea surface temperature anomalies. *J. Atmos. Sci.*, 38, 554-571.

Webster, P. J., and J. R. Holton (1982): Cross-equatorial response to middle-latitude forcing in a zonally-varying basic state. *J. Atmos. Sci.*, 39, 722-733.

Webster, P. J., and H.-R. Chang (1988): Energy accumulation and emanation regions at low latitudes: Impacts of a zonally varying basic state. *J. Atmos. Sci.*, 45, 803-829.

Wu, Z., E. S. Sarachik, and D. S. Battisti (2000): Vertical structure of convective heating and the three-dimensional structure of the forced circulation on an equatorial beta-plane. *J. Atmos. Sci.*, 57, 2169-2187.

Wu, Z., E. S. Sarachik, and D. S. Battisti (2001): Thermally driven tropical circulations under Rayleigh friction and Newtonian cooling: Analytic solutions. *J. Atmos. Sci.*, 58, 724-741.

Zhang, C., and P. J. Webster (1989): Effects of zonal flows on equatorially trapped waves. *J. Atmos. Sci.*, 46, 3632-3651.

VITA

Ian Kraucunas was born in New South Wales, Australia in September 1975. His family moved to Tolland, Connecticut in 1977, then to Fairfax, Virginia in 1986, where he graduated from Robinson Secondary School in 1993. Ian attended the University of Virginia for the next four years, where he majored in Physics and Environmental Science, and completed a thesis project that included a climatological assessment of North American anticyclone activity. He entered graduate school at the University of Washington in 1997 and completed a Master's degree in Atmospheric Sciences in 2001. Ian has also completed the requirements for the Environmental Management Certificate Program. After graduation he will be working for the Board on Atmospheric Sciences and Climate the National Academy of Sciences in Washington, D.C.